Transmission Expansion Planning for Large Power Systems

by

Hui Zhang

A Dissertation Presented in Partial Fulfillment
of the Requirements for the Degree
Doctor of Philosophy

Approved July 2013 by the
Graduate Supervisory Committee:

Vijay Vittal, Co-Chair
Gerald T. Heydt, Co-Chair
Hans D. Mittelmann
Kory W. Hedman

ARIZONA STATE UNIVERSITY

December 2013

ABSTRACT

Transmission expansion planning (TEP) is a complex decision making process that requires comprehensive analysis to determine the time, location, and number of electric power transmission facilities that are needed in the future power grid. This dissertation investigates the topic of solving TEP problems for large power systems.

The dissertation can be divided into two parts. The first part of this dissertation focuses on developing a more accurate network model for TEP study. First, a mixed-integer linear programming (MILP) based TEP model is proposed for solving multi-stage TEP problems. Compared with previous work, the proposed approach reduces the number of variables and constraints needed and improves the computational efficiency significantly. Second, the AC power flow model is applied to TEP models. Relaxations and reformulations are proposed to make the AC model based TEP problem solvable. Third, a convexified AC network model is proposed for TEP studies with reactive power and off-nominal bus voltage magnitudes included in the model. A MILP-based loss model and its relaxations are also investigated.

The second part of this dissertation investigates the uncertainty modeling issues in the TEP problem. A two-stage stochastic TEP model is proposed and decomposition algorithms based on the *L*-shaped method and progressive hedging (PH) are developed to solve the stochastic model. Results indicate that the stochastic TEP model can give a more accurate estimation of the annual operating cost as compared to the deterministic TEP model which focuses only on the peak load.

ACKNOWLEDGMENTS

First, I would like to express my deepest gratitude to my advisors, Dr. Vijay Vittal and Dr. Gerald T. Heydt. It has been a great fortune and pleasure to work with them during the past three years. Their guidance, support and encouragement throughout my research have significantly influenced my Ph.D. career.

I am very grateful to Dr. Hans D. Mittelmann and Dr. Kory W. Hedman for serving on my Ph.D. Committee. Dr. Mittelmann has generously provided me with many of his computational resources, which significantly facilitated my Ph.D. research. Dr. Hedman's insightful comments and constructive criticisms at different stages of my research were thought provoking and helped hold a high standard of this dissertation.

This work is supported in part by the U.S. Department of Energy under a subcontract from contract DOE-FOA0000068 assigned to the Western Electricity Coordinating Council (WECC). I would like to thank Mr. Bradley Nickell and Mr. Keegan Moyer for providing financial support throughout my Ph.D. research and the internship opportunities with WECC. It was a great pleasure and wonderful experience to work with the transmission planning team at WECC. My special acknowledgment goes to Mr. Michael Bailey for his kind guidance and mentoring during my internship.

In addition, I am also very thankful to Dr. Jaime Quintero and Dr. Yacine Chakhchoukh for their valuable comments and suggestions on my research. Finally, I would like to thank my friends Fan Miao, Xing Liu, Dexinghui Kong, Xuan Wu, Iknoor Singh, Parag Mitra and Nitin Prakash at Arizona State University power engineering group for the joyful days we spent together.

TABLE OF CONTENTS

Page

LIST OF TABLES

Tables Page

LIST OF FIGURES

Figures Page

NOMENCLATURE

Acronyms:

ACOPF	Optimal power flow using the AC model
ACTEP	Transmission expansion planning using the AC model
AMPL	Algebraic mathematical programming language
BA	Balance authority
DCOPF	Optimal power flow using the DC model
ISOs	Independent system operators
KKT	Karush–Kuhn–Tucker
LACTEP	Transmission expansion planning using the linearized AC model
LMP	Locational marginal price
LP	Linear programming
MILP	Mixed-integer linear programming
MINLP	Mixed-integer non-linear programming
NERC	North American Electric Reliability Corporation
NLP	Non-linear programming
OPF	Optimal power flow
PDF	Probability density function
PPF	Probabilistic power flow
PV	Photovoltaic
QP	Quadratic programming
RPS	Renewable portfolio standard
RLT	Reformulation relaxation technique
SDP	Semi-definite programming
TEP	Transmission expansion planning
WECC	Western Electricity Coordinating Council

Symbols:

a_g	Quadratic cost coefficient of generator g
b_g	Linear cost coefficient of generator g
b_k	Series admittance of line k, a negative value
b_{k0}	Charging admittance of line k
c_g	Fixed cost coefficient of generator g
c_k	Investment cost of the line k
C_{loss}^{inv}	Investment cost obtained from the lossy TEP model
$C_{lossless}^{inv}$	Investment cost obtained from the lossless TEP model
C_{loss}^{opr}	Operating cost obtained from the lossy TEP model
$C_{lossless}^{opr}$	Operating cost obtained from the lossless TEP model
CF_{gt}	Capacity factor of generator g in year t
CG_{gt}	Hourly energy cost of generator g in year t
d	Discount factor
e_i	Real part of the complex bus voltage V_i
f_i	Imaginary part of the complex bus voltage V_i
g_k	Conductance of line k, a positive value
$k(l)$	The slope of the l^{th} piecewise linear block
$j \in i$	Element j connect to element i
M	Disjunctive factor, a large positive number
ng	Total number of generators
nl	Total number of lines, including potential lines
P_k	Active power flow on line k
$\Delta P_k(l)$	The l^{th} linear block of active power flow on line k
PD_d	Active power demand of load d
PG_g	Active power generated by generator g
$PG_g^{\max}$	Maximum active power output of generator g
$PG_g^{\min}$	Minimum active power output of generator g
PL_k	Active power loss on line k

Q_k	Reactive power flow on line k
QD_d	Reactive power demand of load d
QG_g	Reactive power generated by generator g
$QG_g^{\max}$	Maximum reactive power output of generator g
$QG_g^{\min}$	Minimum reactive power output of generator g
QL_k	Reactive power loss on line k
r_k	Series resistance of line k
$\mathbf{R}_+$	Set of positive real numbers
$S_k^{\max}$	MVA rating of line k
SD_d	MVA of load d
t_k	In-phase transformer off-nominal turns ratio
TO	Operating horizon
TP	Planning horizon
V_i	Bus voltage magnitude in p.u. at bus i
ΔV_i	Voltage magnitude deviation from 1.0 p.u. at bus i
$\Delta V^{\max}$	Upper bound on the voltage magnitude deviation
$\Delta V^{\min}$	Lower bound on the voltage magnitude deviation
x_L, y_L	Lower bound of x, y
x_U, y_U	Upper bound of x, y
x_k	Series reactance of line k
y_k	Series admittance of line k
y_{k0}	Charging admittance of line k
z_k	Binary decision variable for a prospective line k
Z_k	Series impedance of line k
$u_k(l)$	Binary variable for the l^{th} linear block
δ_k	Binary variable for modeling $\lvert\theta_k\rvert$
θ_k	Phase angle difference across line k
$\theta^{\max}$	Maximum angle difference across a line
θ_k^+, θ_k^-	Nonnegative slack variables used to replace θ_k

$\Delta\theta_k(l)$	The l^{th} linear block of angle difference across line k
Ω_g	Set of generators
Ω_k	Set of existing lines
Ω_k^+	Set of prospective lines

Chapter 1

RESEARCH BACKGROUND AND LITERATURE REVIEW

1.1 Motivation and Research Objectives

The national push for a smart grid and the increasing penetration of renewable energy resources today has significantly influenced the operations and planning of the traditional power system. The future power grid is expected to be a smarter network that is flexible and robust enough to withstand various uncertainties and disturbances. According to the 10-year planning summary [1] prepared by the Western Electricity Coordinating Council (WECC), loads are projected to increase 14% from 2009 to 2020, which is a 1.2 percent compound annual growth rate. From the generation side, the future generation mix is expected to have a significant departure from the past because the addition of new generation to replace the retired units is dominated by renewables to fulfill state-mandated renewable portfolio standards (RPSs). By the year 2020, a total amount of 15 GW in nameplate generation is going to retire and 59 GW of additional generation will be added in the U.S. Western Interconnection. Among the cited 59 GW, over 50% is composed of wind and solar PV. In addition, the U.S. Western Interconnection is projected to generate 17% of its energy from non-hydro renewable sources in 2020.

With these contemporary changes, some problems are expected in the future power system. First, the load increase may change the power flow in the existing grid and may result in potential overloads and stability issues. These issues may violate reliability criteria. Second, the renewable resources are usually located in remote areas and are not

readily connected to the main power grid. In order to address these problems, additional transmission capacity is needed [1].

The objective of this research is to develop new algorithms and tools to facilitate the regional transmission expansion planning (TEP) process for the U.S. Western Interconnection in the coming decade with the expected load increase and high renewable penetration. It is expected that such a TEP process could be extended without loss of generality to any system and venue. Based on the existing research, the work presented in this dissertation focuses on the following two areas:

1. Develop new TEP models with a better approximation of the AC power flow model.
2. Develop decomposition algorithms to solve TEP problem with uncertainties and evaluate the long-term regional transmission capacity needs under a comprehensive set of load and generation scenarios.

The TEP models and algorithms presented in this dissertation can be used for developing interregional level transmission plans for the future U.S. Western Interconnection. The planning results can provide guidance for decision-makers and facilitate the development of needed transmission infrastructure.

1.2 Transmission Expansion Planning: A Literature Review

Transmission expansion planning is an important research area in power systems and has been studied extensively during the past several decades. The TEP exercise normally focused on improving the reliability and security of the power system when economic impacts were not the primary concern. In contemporary power systems however, the increasing complexity of the network structure and the deregulated market

environment have made the TEP problem a complicated decision-making process that requires comprehensive analysis to determine the time, location, and number of transmission facilities that are needed in the future power grid. Building the correct set of transmission lines will not only relieve congestions in the existing network, but will also enhance the overall system reliability and market efficiency. The state-of-the-art of the TEP studies is reviewed and summarized in the following.

1.2.1 TEP Modeling and Solution Techniques

Various TEP models have been developed during the past several decades. Among these models, mathematical programming and heuristic methods are two major classes of solution approaches. Mathematical programming methods guarantee the optimality of the solution in most cases, but often have stricter requirements on the model to be optimized. In order to obtain the global optimal solution efficiently, the problem or at least the continuous relaxation of the problem should have a convex formulation. Heuristic methods, on the other hand, are usually not sensitive to the model to be optimized and can potentially examine a large number of candidate solutions. The main criticism of heuristic methods, however, is that most of such methods do not guarantee an optimal solution, and provide few clues regarding the quality of the solution. Reference [2] presents a comprehensive review and classification of the available TEP models.

Due to the complexity of the TEP problem, the DC power flow model has been extensively used for developing TEP models [3]-[9]. One of the early works, [3] presents a linear programming (LP) approach to solve TEP problems. A mixed integer linear programming (MILP) based disjunctive model in [4] eliminates the nonlinearity caused by the binary decision variables. In [6], the behavior of the demand was modeled through

demand side bidding. A bilevel programming model appears in [7] where the solution to the problem is the Stackelberg equilibrium between two players. A transmission switching coordinated expansion planning model was presented in [8] where the planning problem and the transmission switching problem are solved alternately.

In terms of security constraints, the North American Electric Reliability Corporation (NERC) planning criteria state that power systems must survive an $N - 1$ contingency [10]. For the linearized model, this criterion simply indicates that there should be no thermal limit violation with the outage of a single transmission or generation facility. The modeling of security constraints can be found in [11]-[13], where an MILP based disjunctive method is proposed for transmission line switching studies.

The active power losses are usually neglected in the linearized power flow model. However, the losses may shift the generation economic dispatch solution and therefore influence the optimal transmission plan. Two loss models are presented in [5] and [11] respectively, where the proposed models use piecewise linear approximations to represent the quadratic loss term.

Application of the AC power flow model to TEP problems (ACTEP) is rarely discussed in the literature. The advantage of formulating TEP problems using the AC model is that the AC model represents the electric power network accurately. Nevertheless, the nonlinear and non-convex nature of the ACTEP model can make the problem very difficult to solve and to obtain a desirable solution. Reference [14] presented a mixed-integer nonlinear programming (MINLP) approach for solving TEP problems using the AC network model. The interior point method and a constructive heuristic algorithm were employed to solve the relaxed nonlinear programming problem

and obtain a good solution. It is reported in [15] that by relaxing binary variables, the NLP-based ACTEP model can solve a small-scale TEP problem within an acceptable time range and obtain a local optimal solution. However, solving a MINLP-based ACTEP problem is still extremely challenging at this moment.

Heuristic approaches are an alternative to mathematical programming for solving optimization problems. Heuristic approaches usually refer to the algorithms that mimic some behavior found in nature, e.g., the principle of evolution through selection and mutation (genetic algorithms). For problems that have significant computational complexity in finding an optimal solution, heuristic methods can usually give a solution with relatively smaller computational effort, though the obtained solution may not be optimal. In recent years, heuristic methods have been introduced to solve TEP problems in power systems [16]-[21]. In many of these instances, the heuristic method is not used on a stand-alone basis. In order to obtain better computational performance, heuristic methods are frequently used in conjunction with mathematical methods when solving practical TEP problems.

1.2.2 Treatment of Uncertainty

The electric power system is not a deterministic system. Uncertain events such as load demand variation and line contingencies can occur at any time. Moreover, some renewable generation resources such as wind and solar PV are highly unpredictable. These renewable generation sources, if massively integrated, could greatly affect the power system operations and undermine the grid reliability. The traditional TEP models are based on a deterministic framework where loads are treated as known fixed parameters. The deterministic model certainly simplifies the problem, but fails to capture

the stochastic nature of the real power system and may generate unrealistic transmission plans. In recent years, modeling of uncertainties in the TEP model has drawn increasing attention [22]-[29]. Stochastic programming, chance constrained programming and scenario-based analysis are three approaches that are frequently used.

Two-stage stochastic programming is a widely used stochastic formulation that optimizes the *mathematical expectation* of the weighed future scenarios. A two-stage stochastic programming-based TEP model is proposed in [22] to coordinate the generation and transmission planning. In [23], a scenario-based multi-objective TEP model is presented to address the uncertainties and risks in the planning process. Due to the computational burden, decomposition methods are usually used to solve the above stochastic TEP models [24]. In terms of the resource uncertainties, a probabilistic power flow (PPF)-based planning model is proposed in [25]. That reference evaluates a statistical range of the possible power flows instead of a single solution. Recently, a chance-constrained model is presented in [26] to address the uncertainties of loads and wind farms. It should be noticed that the PPF-based planning model and the chance-constrained planning model are both risk-based games in which the planners need to decide the confidence level at a specified risk.

In terms of reliability assessment, the probabilistic approach can also be applied [27]-[28]. The traditional deterministic planning approaches are not able to capture the probabilistic characteristics in power system. In reality, this may lead to either overinvestment or potential reliability violations [27]. A method for choosing the optimal expansion plan considering a probabilistic reliability criterion is proposed in [28]. The probabilistic planning concept is applied to liberalized electricity markets in [29].

1.2.3 Planning Horizon

Compared to the static planning model where lines are planned for a single target year, the multi-stage planning model considers the continuing growth in demand and determines *when* to carry out the transmission expansion as well [30]-[33]. The major obstacle in the development of multi-stage planning models is still the computational burden. Heuristic algorithms are usually used to solve multi-stage planning problems. A genetic algorithm is presented in [30] to solve the problem of multistage and coordinated TEP problem. A multi-criteria formulation for multiyear dynamic TEP problems is presented in [31] and is subsequently solved by a simulated annealing algorithm with the objective to find the optimal balance of investment costs, operation costs, as well as the expected unsupplied energy. Ordinal optimization is used in [32] for solving a multi-year TEP problem. The ordinal optimization algorithm uses crude models and rough estimates to derive a small set of optimal plans in each sub-planning period for which simulations are necessary and worthwhile to find acceptable solutions. In [33], a multiyear security constrained generation-transmission planning model is presented and a constructive heuristic algorithm is developed to solve the problem.

1.3 Dissertation Outline

The rest of this dissertation is organized as follows. Chapter 2 gives an overview of the power systems background that will be used in this dissertation. Some important concepts including power flow, optimal power flow (OPF) and $N-1$ reliability criteria are revisited in this chapter. Chapter 3 presents a multi-stage TEP model based on the DC power flow model. Active power losses and the $N-1$ reliability criteria are included in this model. Chapter 4 explores the possibility to formulate TEP models using the AC

power flow model. In Chapter 5, a better approximation of the AC model is derived and a convexified ACOPF model is proposed in which reactive power and off-nominal bus voltage magnitudes are integrated. A MILP-based loss model and its relaxations are investigated. The OPF model developed in Chapter 5 is then extended to formulate a TEP model in Chapter 6. TEP under uncertainty environment and algorithms for solving the stochastic TEP models are developed in Chapter 7. The conclusions and possible future work are in Chapter 8. Several of the test beds used, and a sample MATLAB script used in this research are described in three appendices.

1.4 Main Contributions

The main contributions of the work are summarized as follows:

1. In Chapter 3, a new approach for modeling the active power losses in the network is presented. Compared with the previous work, the proposed approach reduces the number of variables and constraints needed and improves the computational efficiency significantly.
2. In Chapter 4, the TEP models based on the AC power flow formulation are investigated. Two nonlinear programming (NLP)-based TEP models are presented.
3. In Chapter 5, a relaxed OPF model is proposed based on a Taylor series, in which the reactive power, off-nominal bus voltage magnitudes as well as network losses are retained. A MILP-based loss model is developed to eliminate the fictitious losses. Relaxations of the MILP model are investigated. The mathematical proofs of the conditions under which the relaxations are exact are given.

4. In Chapter 6, a novel TEP model is proposed based on the network model developed in Chapter 5. An iterative approach to incorporate the $N - 1$ contingency criterion efficiently in the TEP model is also presented.
5. In Chapter 7, decomposition and heuristic methods are developed for solving TEP problems with uncertain loads. The proposed algorithm is applied to a 569-bus reduced WECC system.

Chapter 2

POWER SYSTEMS ESSENTIALS

2.1 Chapter Overview

Power system modeling plays an important role in TEP studies. A solid understanding of the basic power system concepts will not only facilitate the development of a good TEP model, but will also lead to a better decision in the planning process. This chapter reviews the essential power systems background that will be used later in the dissertation.

2.2 Modeling of Network Components

In this section, the mathematical models of the common power system components for steady state analysis are reviewed.

2.2.1 Transmission Lines

In steady state power system analysis, the lumped parameter π-equivalent model as shown in Fig. 2.1 is often used to model an AC transmission line.

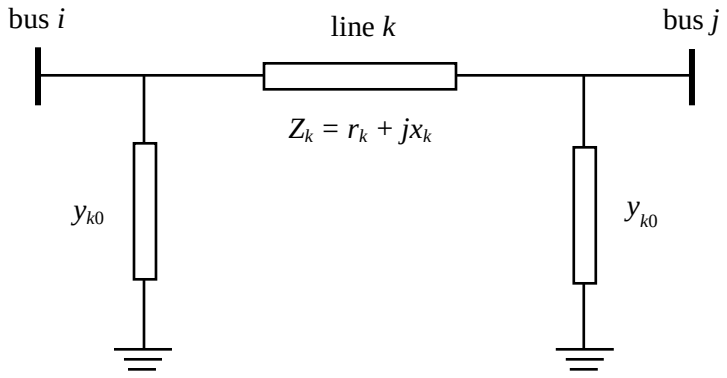

Fig. 2.1. The lumped parameter π-equivalent model of an AC transmission line

In Fig. 2.1, Z_k is the series impedance of the line and can be written as,

$$Z_k = r_k + jx_k \tag{2.1}$$

where r_k and x_k are referred to as the resistance and reactance of the line, respectively. When formulating the network equations, the series admittance is needed. The series admittance of the line is defined as the reciprocal of the series impedance and takes the following form

$$y_k = z_k^{-1} = \frac{r_k}{r_k^2 + x_k^2} + j\frac{-x_k}{r_k^2 + x_k^2} = g_k + jb_k \tag{2.2}$$

where g_k and b_k are referred to as the conductance and susceptance of the line, respectively. It should be noticed that in the power system, g_k is always positive while b_k is usually negative. In the π equivalent model, the total line charging admittance is divided by half and connected at the two terminals of the line denoted by y_{k0} in Fig. 2.2. In the power system, the real part of y_{k0} is usually zero (g_{k0} = 0) and only the shunt susceptance (b_{k0}) is considered.

In AC power systems, the complex power flow in a line is denoted by

$$S_k = P_k + jQ_k \tag{2.3}$$

where P_k and Q_k are the active and reactive power flows respectively. Separating the real and imaginary parts in (2.3) and defining *i* and *j* as the two terminal buses of the line, the active and reactive power flows from bus *i* to *j* is calculated by the following equations,

$$P_k^{(ij)} = V_i^2 g_k - V_i V_j \left(g_k \cos\theta_k + b_k \sin\theta_k \right) \tag{2.4}$$

$$Q_k^{(ij)} = -V_i^2 \left(b_k + b_{k0} \right) + V_i V_j \left(b_k \cos\theta_k - g_k \sin\theta_k \right) \tag{2.5}$$

where θ_k is the phase angle difference between bus *i* and bus *j*, *i.e.*, ($\theta_i - \theta_j$). The active and reactive power flows in the same line but metered from the opposite direction can be obtained in a similar way,

$$P_k^{(ji)} = V_j^2 g_k - V_i V_j \left(g_k \cos\theta_k - b_k \sin\theta_k \right) \tag{2.6}$$

$$Q_k^{(ji)} = -V_j^2 \left(b_k + b_{k0} \right) + V_i V_j \left(b_k \cos\theta_k + g_k \sin\theta_k \right). \tag{2.7}$$

In power systems, the active power loss of a line is the active power consumed by the series resistance of the line. Using (2.4) and (2.6), the active power loss of the line is obtained as

$$PL_k = P_k^{(ij)} + P_k^{(ji)} = g_k \left(V_i^2 + V_i^2 - 2V_i V_j \cos\theta_k \right). \tag{2.8}$$

Similarly, summing (2.5) and (2.7) gives

$$QL_k = Q_k^{(ij)} + Q_k^{(ji)} = -b_{k0} \left(V_i^2 + V_i^2 \right) - b_k \left(V_i^2 + V_i^2 - 2V_i V_j \cos\theta_k \right). \tag{2.9}$$

The definition of reactive power loss on a line can be tricky, because the reactive power is both consumed and generated along the line. The first term in (2.9) is the reactive power generated by the charging (capacitive) susceptance in the π-equivalent model, while the second term represents the reactive power consumed by the line (inductive) reactance.

2.2.2 Transformers

There are many types of tranformers in contemporary power systems and the detailed modeling of these transformers can be very complicated. In this section, only the ideal transformer with real number turns ratio is discussed and balanced three-phase operation is assumed throughout. For transformers of this kind, the π-equivalent model used for modeling transmision lines can be used with some modifications. As shown in Fig. 2.2, the impedance of the transformer is at the tap side with the turns ratio equals to a real number t_k, the π-equivalent model for this transformer is illustrated in Fig. 2.3.

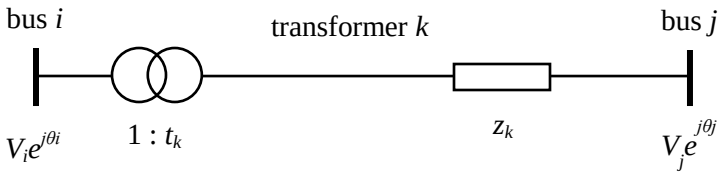

Fig. 2.2. The in-phase transformer model

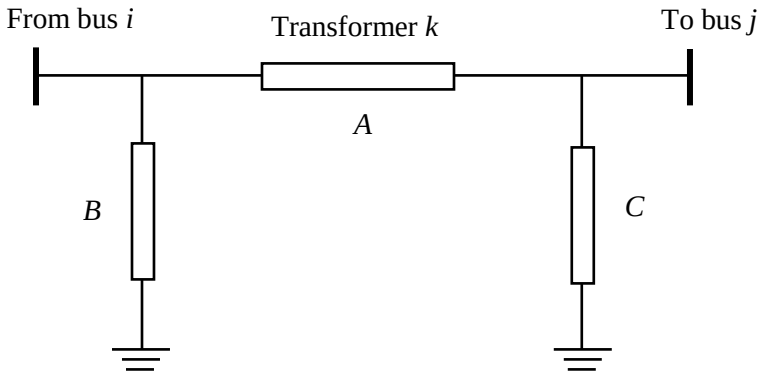

Fig. 2.3. The π-equivalent model of the in-phase transformer

Using two-port network theory, the A, B and C parameters can be identified as follows,

$$A = t_k y_k \tag{2.10}$$

$$B = t_k (t_k - 1) y_k \tag{2.11}$$

$$C = (1 - t_k) y_k \,. \tag{2.12}$$

Hence, the real and reactive power flow equations for the transformer with real turns ratio t_k are obtained as,

$$P_k^{(ij)} = \left(t_k V_i\right)^2 g_k - t_k V_i V_j \left(g_k \cos\theta_k + b_k \sin\theta_k\right) \tag{2.13}$$

$$Q_k^{(ij)} = -\left(t_k V_i\right)^2 \left(b_k + b_{k0}\right) + t_k V_i V_j \left(b_k \cos\theta_k - g_k \sin\theta_k\right) \tag{2.14}$$

Notice that if the turns ratio of a transformer is equal to the ratio of the nominal rated voltages of its associated network sections, then $t_k = 1$. In this case, (2.13) and (2.14) have the same form as (2.4) and (2.5).

2.2.3 Loads and Shunts

Loads are important components in the power system and various sophisticated load models have been developed to capture the dynamic behavior of the loads more accurately during the transient period. For steady state power flow analysis, the constant MVA model is usually used. In the constant MVA model, the load is simply modeled as a sink of constant active and reactive power and is independent of the change in bus voltage magnitude,

$$SD_d = PD_d + jQD_d \tag{2.15}$$

where PD_d and QD_d are the active and reactive part of the load respectively and are both constants.

In power systems, the term “shunts” means “phase to ground” is usually referred to the reactive power compensation devices connected at buses. By switching in and out the shunt devices, a wider range of control of the bus voltage magnitude can be achieved. The modeling of shunts is similar to the modeling of loads. The only difference in modeling is that the reactive power a shunt device can provide or consume is voltage dependent. In data files, the shunt data are usually denoted in the form of reactive power at the nominal voltage. The actual reactive power a shunt device can provide or consume is

$$SD_i = jQD_iV_i^2 . \tag{2.16}$$

2.2.4 Generators

In power flow studies, the generator is modeled as the source of active power and reactive power. The generator bus is also known as a "*P*-*V*" bus, for which the active power dispatch is pre-determined based on economic dispatch. The voltage magnitude of a generator bus can be regulated freely as long as the reactive power needed for the voltage regulation is within the generator reactive power capability and the generator maximum voltage is not exceeded.

2.3 Steady State Power System Analysis

2.3.1 Power Flow

The power flow problem is referred to as a problem to obtain the voltage magnitude and angle information at each bus for a specific load condition with the active power output and voltage level of each generator and real and reactive power at all loads specified. With this information, active and reactive power flows in each line as well as generator reactive power outputs can be analytically determined. The AC power flow model uses the exact expressions of the power flow equations as derived above, while the DC power flow model is an approximated model, which aims to provide a fast power flow solution based on a good initial condition.

Mathematically, the AC power flow problem finds a feasible solution to a set of nonlinear equations, *i.e.*, nodal balance equations. The polar form of the nodal balance equations are as follows,

$$0 = PG_i - PD_i - V_i \sum_{j \in i} V_j \left(g_k \cos\theta_k + b_k \sin\theta_k \right) \tag{2.17}$$

$$0 = QG_i - QD_i - V_i \sum_{j \in i} V_j \left(g_k \sin\theta_k - b_k \cos\theta_k \right). \tag{2.18}$$

For load buses (*P*-*Q* bus), both (2.17) and (2.18) are needed. For generator buses (*P*-*V* bus) that are not on VAr limits, only (2.17) is needed because the generator reactive power dispatch is determined after all other variables are solved, including (2.18) will introduce additional variables. The generators that are on VAr limits are treated the same as the load bus with the reactive power being fixed at the limits. No equations are needed for the swing bus (*V*-θ bus). As the reference of the system, the phase angle of the swing bus is generally set to zero. Another form of the nodal balance equations is known as the rectangular form. Using Euler's formula, the complex bus voltage can be decomposed as

$$\mathbf{V}_i = V_i \cos\theta_i + jV_i \sin\theta_i = e_i + jf_i . \tag{2.19}$$

where $e_i = V_i\cos\theta_i$ and $f_i = V_i\sin\theta_i$ are the real and imaginary part of the complex bus voltage V_i. Substituting (2.19) into (2.17) and (2.18), the nodal balance equations in the rectangular form are obtained as,

$$0 = PG_i - PD_i - \sum_{j\in i}\left[g_k \left(e_i e_j + f_i f_j\right) + b_k \left(e_j f_i - e_i f_j\right)\right] \tag{2.20}$$

$$0 = QG_i - QD_i - \sum_{j\in i}\left[b_k \left(e_i e_j + f_i f_j\right) - g_k \left(e_j f_i - e_i f_j\right)\right]. \tag{2.21}$$

Notice that no matter which form is used, the AC power flow model requires to solve a set of nonlinear equations. Iterative methods such as the Newton-Raphson method are usually used to solve such problems and find a numerical solution.

The DC power flow model is a linearized version of the AC power flow model. The key assumptions made in the DC power flow model are the following:

- The series resistance of the line r_k is negligible, *i.e.*, $P_k^{(ij)} = -P_k^{(ji)}$.
- The reactive power flow in the line is negligible, *i.e.*, $Q_k = 0$.
- The voltage phase angle difference is small so that $\sin\theta_k \approx \theta_k$.

- The bus voltage magnitudes are close to 1.0 p.u.

Based on the above assumptions, the line active power flow in the DC model can be simplified as,

$$P_k = -b_k \theta_k . \tag{2.22}$$

The nodal balance equation for the DC power flow model is written as

$$0 = PG_i - PD_i - \sum_{j \in i} \left(b_k \theta_k \right). \tag{2.23}$$

As observed from (2.23), the DC power flow problem finds the solution to a set of linear equations. Therefore, the DC power flow problem can be solved directly without using the iterative method. It should be pointed out that the model presented above is the most commonly used DC model and is often referred to as the lossless DC model. In reality, the DC power flow model has many variations, *e.g.*, the voltage magnitudes in the DC model can be fixed to the previous AC power flow solution, rather than 1.0 p.u. and the active power losses can be included in the model as well. Some of these variations are investigated in the later chapters.

2.3.2 The N – 1 Reliability Criterion

In order to maintain the reliability of the transmission system, NERC has published a series of standards with which all the balancing authorities within North American interconnection are required to comply [10]. The $N - 1$ reliability criterion states that with the loss of a single element, *e.g.*, a transmission line, a transformer or a generator, due to a fault, the system must remain stable with the thermal and voltage limits within their emergency ratings. There must be no loss of load or curtailed firm transfers if the fault is cleared in the normal clearing time. However, for bus faults and

other faults with delayed clearing, the loss of demand or curtailed firm transfers is acceptable under a planned or controlled manner. In the DC power flow model, the $N-1$ criterion simply indicates that there should be no thermal limit violations with the outage of a single transmission or generation element. Notice that the NERC standards only set the minimum requirement, power utilities and independent system operators (ISOs) may have reliability criteria that are more stringent.

2.4 Economic Dispatch

2.4.1 Optimal Power Flow

In power systems, the term *economic dispatch* is almost used interchangeably with the term *optimal power flow* (OPF), which has been implemented extensively in power system operations and planning since it was first introduced by Carpentier [35]. The goal of the OPF problem is generally to minimize the total energy cost in the power grid subject to the system and resource constraints. These constraints include line flows, bus voltages magnitudes, angles as well as generator capacities. The general mathematical formulation of the OPF problem takes the following form:

$$\min \ f(\mathbf{x}) \tag{2.24}$$

subject to

$$\mathbf{h}(\mathbf{x}) = \mathbf{c} \tag{2.25}$$

$$\mathbf{g}(\mathbf{x}) \le \mathbf{b} \tag{2.26}$$

$$\mathbf{x}^{\min} \le \mathbf{x} \le \mathbf{x}^{\max} \tag{2.27}$$

where **bold face** refers to vectors. In the above general OPF formulation, the total energy cost is usually used in (2.24) as the objective function. The equality constraints (2.25) represent the power flow equations and the inequality constraints (2.26) represent the line

power flow limits. The remaining constraints (2.27) represent the bounds on voltage magnitudes, angles as well as the generator capacity limits.

The AC formulation of the OPF problem (ACOPF) uses the AC power flow equations in the constraints, while the DC formulation of the OPF problem (DCOPF) uses the linearized power flow equations. Most of the ACOPF solution techniques are based on Karush-Kuhn-Tucker (KKT) conditions [36]. Among these solution techniques, Newton's method, due to its fast convergence near the solution, was widely adopted in early literature [36]-[37]. However, Newton's method has difficulties in handling inequality constraints, and the performance of Newton's method depends largely on the initial starting point. As algorithms developed, the interior point algorithms have become the mainstream algorithms for solving the ACOPF problem [38]-[40].

Despite the development of nonlinear algorithms, obtaining a robust solution for large-scale ACOPF problems efficiently still remains a challenge. Therefore, for problems such as real time economic dispatch where the speed is a primary concern, the DCOPF model is often used. The DCOPF model is a linearized version of the ACOPF model [41]. The DCOPF assumes fixed bus voltage magnitudes as well as negligible reactive power and network losses. Thus, the original nonconvex ACOPF model can be reduced to a quadratic programming (QP) model (assuming that generators have quadratic cost curves), which is convex and much easier to solve.

The standard ACOPF formulation is reviewed in this section, the objective function is to minimize the total energy cost,

$$\min \sum_{g\in\Omega_g} \left(c_2 PG_g^2 + c_1 PG_g + c_0 \right) \tag{2.28}$$

$$\sum_{g\in i} PG_g + \sum_{k\in i} P_k = \sum_{d\in i} PD_d \tag{2.29}$$

$$\sum_{g\in i} QG_g + \sum_{k\in i} Q_k = \sum_{d\in i} QD_d \tag{2.30}$$

$$\left\| P_k^2 + Q_k^2 \right\| \le S_k^{\max} \tag{2.31}$$

$$PG_g^{\min} \le PG_g \le PG_g^{\max} \tag{2.32}$$

$$QG_g^{\min} \le QG_g \le QG_g^{\max} \tag{2.33}$$

$$V^{\min} \le V_i \le V^{\max} \tag{2.34}$$

$$-\theta^{\max} \le \theta_k \le \theta^{\max}. \tag{2.35}$$

where P_k and Q_k are given by:

$$P_k = V_i^2 g_k - V_i V_j \left(g_k \cos\theta_k + b_k \sin\theta_k \right)$$

$$Q_k = -V_i^2 \left(b_k + b_{k0} \right) + V_i V_j \left(b_k \cos\theta_k - g_k \sin\theta_k \right).$$

In the above ACOPF model, (2.29) and (2.30) represent the power balance constraints at each bus. The apparent power flow in the line is limited by (2.31) and there is no separate limit for active and reactive power flows in a line. The active and reactive power generation is limited by (2.32) and (2.33) respectively. The unit commitment problem is not considered in the ACOPF, which means that the on and off status of the generator does not change. The voltage magnitude and angle constraints are shown in (2.34) and (2.35), respectively. In the steady state, the phase angle difference across a line is often kept small for security purposes.

The classic DCOPF model is a linearized version of the ACOPF model, in which reactive power and network losses are neglected. The classic DCOPF model is formulated as a linear programming problem which takes the following form,

$$\min \sum_{g \in \Omega_g} c_1 PG_g \tag{2.36}$$

$$\sum_{g \in i} PG_g + \sum_{k \in i} P_k = \sum_{d \in i} PD_d \tag{2.37}$$

$$P_k + b_k \theta_k = 0$$

$$0 \le P_k \le S_k^{\max}$$

$$PG_g^{\min} \le PG_g \le PG_g^{\max}$$

$$-\theta^{\max} \le \theta_k \le \theta^{\max} .$$

where P_k is given by:

$$P_k = V_i^2 g_k - V_i V_j \left(g_k \cos\theta_k + b_k \sin\theta_k \right).$$

Notice that in (2.36), the calculation of the energy cost is further simplified by only considering the linear term in the original quadratic cost function. Compared with the ACOPF model, the DCOPF model is convex and can be solved up to 60 times faster [42]. The variations of the DCOPF model and the TEP models that are built based on the DCOPF model are investigated in the later chapters.

2.4.2 Locational Marginal Price

Locational marginal price (LMP) is a pricing mechanism that is commonly used in contemporary electricity markets. LMP is defined as the least marginal cost to serve the next increment of demand at a specific location in the electric power grid [44]. In reality, LMP can either be used to represent the price at a specific node or a load hub that

involves an aggregation of nodes. From a mathematical point of view, LMP can be envisioned as the local sensitivity with respect to a perturbation in the right hand side of the active power nodal balance constraints. For constrained optimization problems, the local sensitivity is given by the Lagrange multiplier associated with the constraint. Therefore, in the ACOPF model, the LMP at bus i is simply the Lagrange multiplier associated with the active power balance constraint for the bus, while in the DCOPF model, the LMP is the dual variable associated with (2.37).

Chapter 3

TRANSMISSION EXPANSION PLANNING USING THE DC MODEL

3.1 Chapter Overview

From the modeling perspective, the TEP problem shares some common ground with the OPF problem in the sense that they are both constrained optimization problems. However, compared with the OPF problem that optimizes the generator dispatch on a fixed network topology, the TEP problem can be viewed as an extension of the OPF problem because it essentially solves a series of OPF problems with different network topologies as illustrated in Fig. 3.1.

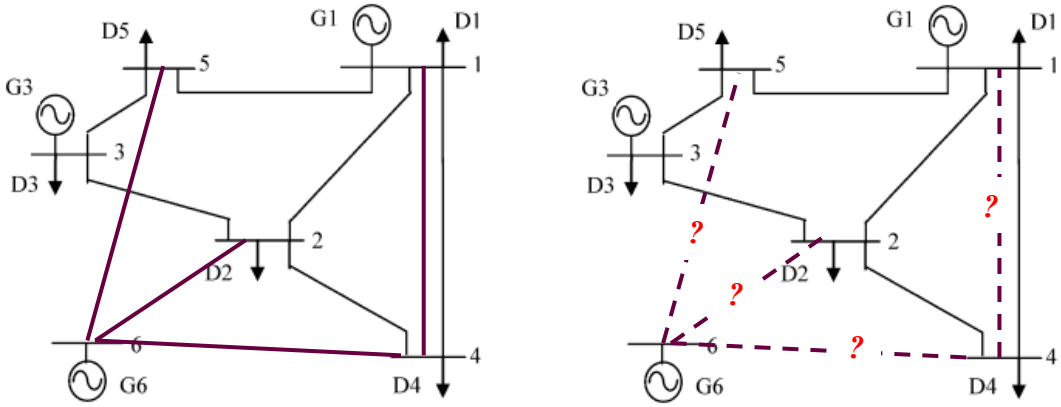

Fig. 3.1. Comparison of OPF and TEP problem

Due to the complexity of the problem, the DC power flow model is widely used in the TEP models. An main assumption in the traditional DC model is that the network losses are negligible. However, this assumption can be problematic when applied to TEP studies because neglecting losses may shift the cost from line investment to operations and influence the efficiency of the transmission expansion plan. In terms of reliability, the NERC planning criterion indicates that there should be no thermal limit violations

with the outage of a single transmission or generation element. This chapter presents a MILP-based TEP model that considers the active power losses and the $N - 1$ criterion. Simulation results show that the proposed TEP model is efficient and has the potential to be applied to solve large-scale power system planning problems.

The remainder of the chapter is organized as follows: Section 3.2 presents a basic TEP model using the lossless DC model. Section 3.3 derives a LP-based piecewise linear model to include network losses in the DC model. The complete mathematical formulation of the TEP model is developed in Section 3.4 and simulation results are demonstrated in Section 3.5. The concluding remarks are indicated in Section 3.6.

3.2 TEP Model Based on the Lossless DC Model

This section presents a TEP model based on the lossless DC model introduced in Section 2.4.2. The model is shown as follows,

$$\min \; c_k z_k \tag{3.1}$$

$$\sum_{k\in\Omega_k^i} P_k + \sum_{g\in\Omega_g^i} PG_g = \sum_{d\in\Omega_d^i} PD_d \quad \forall i \in \Omega_b \tag{3.2}$$

$$P_k = -b_k \theta_k \quad \forall k \in \Omega_k \tag{3.3}$$

$$-(1-z_k)\cdot M_k \le (P_k + b_k\theta_k) \le (1-z_k)\cdot M_k \quad \forall k \in \Omega_k^+ \tag{3.4}$$

$$-P_k^{\max} \le P_k \le P_k^{\max} \quad \forall k \in \Omega_k \tag{3.5}$$

$$-z_k P_k^{\max} \le P_k \le z_k P_k^{\max} \quad \forall k \in \Omega_k^+ \tag{3.6}$$

$$0 \le PG_g \le PG_g^{\max} \quad \forall g \in \Omega_g . \tag{3.7}$$

In the above TEP model, the objective function (3.1) is to minimize the total investment cost. The nodal balance equation is shown in (3.2), where the net power injection at a bus

is equal to the total loads connected to the bus. As shown in (3.3) and (3.4) respectively, the active power flows for existing lines are determined by the product of the line susceptance b_k and the voltage phase angle difference θ_k, while for prospective lines, the big-*M* method needs to be applied to avoid the presence of nonlinear terms. If a perspective line is selected, i.e., z_k is 1, then (3.4) is forced to be an equality constraint as (3.3), otherwise, z_k is 0, the positive number M_k guarantees that (3.4) is not binding. Constraints (3.5) and (3.6) limit the active power on existing lines and prospective lines respectively. If a prospective line is selected, then (3.6) is the same as (3.5), otherwise, the power flow is forced to be zero. The generator output limit is enforced by (3.7).

The difficulty with the Big-*M* method is the choice of a proper *M*. In practice, an arbitrary large *M* will result in numerical difficulties in the solution by dominating the calculations, however, if *M* is not large enough, then the true optimal solution will be excluded from the feasible region which causes the branch-and-bound process terminates at only a suboptimal or even with an infeasible solution. As shown in (3.4), in the TEP model, the choice of M_k depends on the parameters of the existing network topology. In order to calculate a proper value of M_k, two situations are discussed: the simple situation is when a candidate line is in an existing transmission corridor. In this case, if the candidate line is not selected, then according to (3.6), $P_k = 0$. As a result, (3.4) can be rewritten as,

$$-M_k \le b_k \theta_k \le M_k . \tag{3.8}$$

Considering there are *m* existing lines in the transmission corridor, then the value of M_k can be calculated as,

$$M_k = \min\left(P_{k'}^{\max} / b_{k'}\right) b_k \tag{3.9}$$

where $k' = 1, 2, \ldots, m$, represents all the existing lines in the transmission corridor. When a candidate line creates a new transmission corridor, the problem becomes difficult. According to [4], the shortest path between two terminals of the candidate line needs to be calculated and the computation can be burdensome. In fact, it is not practical to calculate the exact M value for each candidate line that creates a new transmissions corridor, instead, an heuristic upper bound, $2\pi b_k$, is used throughout this paper.

The above TEP model is tested on Garver's 6-bus system. As shown in Fig. 3.2, the system has 6 existing lines, 5 loads and 3 generators [3]. Initially, the generator at bus 6 is to be connected to the main system. The data of the system are provided in Table 3.1 and 3.2. It is assumed that at most 3 lines are allowed in each transmission corridor. The total number of candidate lines is 39.

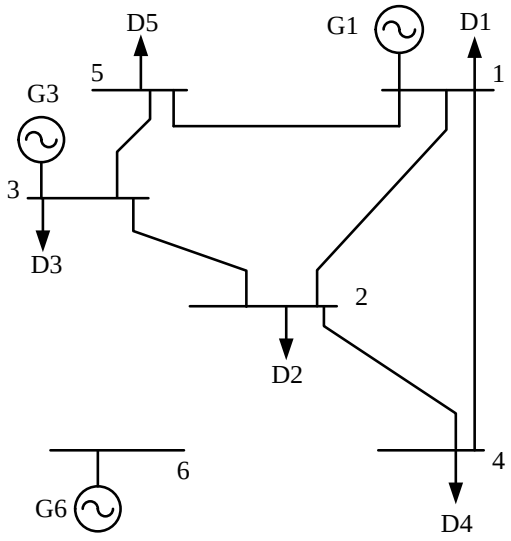

Fig. 3.2. One line diagram of the original Garver's 6-bus system

Table 3.1. Bus data for Garver's 6-bus system

Bus	PG^{min} (MW)	PG^{max} (MW)	Load (MW)
1	0	400	80
2	0	/	240
3	0	400	40
4	0	/	160
5	0	/	240
6	0	600	/

Table 3.2. Branch data for Garver's 6-bus system

Branch	Resistance (p.u.)*	Reactance (p.u.)	Cost (10^6 \$)	Capacity (MW)
1-2	0.10	0.40	40	100
1-3	0.09	0.38	38	100
1-4	0.15	0.60	60	80
1-5	0.05	0.20	20	100
1-6	0.17	0.68	68	70
2-3	0.05	0.20	20	100
2-4	0.10	0.40	40	100
2-5	0.08	0.31	31	100
2-6	0.08	0.30	30	100
3-4	0.15	0.59	59	82
3-5	0.05	0.20	20	100
3-6	0.12	0.48	48	100
4-5	0.16	0.63	63	75
4-6	0.08	0.30	30	100
5-6	0.15	0.61	61	78

*100 MWA base

In Fig. 3.3, the dashed lines represent new lines to be added. In order to connect bus 6 to the main system and serve the existing loads, four additional lines need to be added. The total investment cost is 110 million dollars (M$).

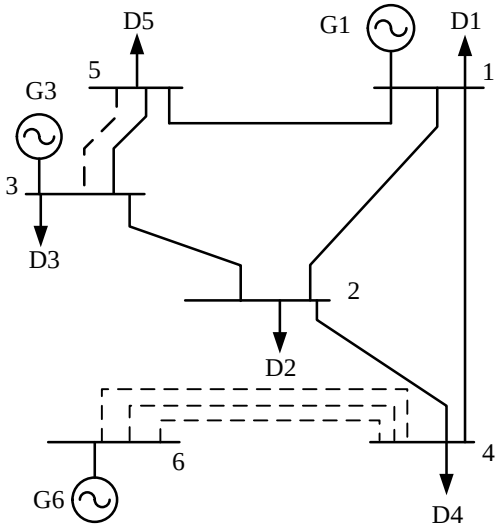

Fig. 3.3. The expanded Garver's 6-bus system

3.3 Modeling Network Losses – An LP Model

The goal of this section is to obtain a linearized loss model that can be incorporated into the TEP model. There are many approaches to include losses in the DC model [5] and [11]. In this section, a non-iterative piecewise linear formulation is presented. It should be noted that the loss model presented in this section is a LP-based approximation, which may be inexact in some cases. A more rigorous MILP-based loss model and its exact relaxations are investigated in Chapter 5. As derived in Section 2.3.1, in the AC power system, the active power loss on a line can be obtained by summing up the power flows metered at the two terminals of the line. Suppose all turns ratios of the transformers are set to one and define bus *i* and bus *j* to be the "from" bus and the "to" bus of line *k*, then the active power losses on line *k* can be calculated as,

$$PL_k = P_k^{(ij)} + P_k^{(ji)} = g_{km}\left(V_i^2 + V_j^2 - 2V_iV_j\cos\theta_k\right) \tag{3.10}$$

Assuming all bus voltage magnitudes are close to 1.0 p.u. and the voltage phase angle across a line is small enough, the following approximations can be applied,

$$V_i \approx 1.0 \tag{3.11}$$

$$\cos\theta_k = 1 - 2\sin^2\left(\theta_k/2\right) \approx 1 - \theta_k^2/2 . \tag{3.12}$$

The angles in these expressions are expressed in radians. Substituting (3.11) and (3.12) into (3.10), the expression of the active power losses on line *k* is approximated as,

$$PL_k \approx g_k \theta_k^2 . \tag{3.13}$$

Recall that in the DC model, the active power on a line is calculated by,

$$P_k = -b_k \theta_k . \tag{3.14}$$

Substituting (3.14) into (3.13), the relationship between the line losses and the active power flows on the line in the DC model can be set as follows,

$$PL_k = \left(g_k / b_k^2\right) P_k^2 . \tag{3.15}$$

Notice that the quadratic equality constraint (3.15) is still non-convex and needs to be further linearized. As indicated in Fig. 3.4, the value of a quadratic function $y = ax^2$, $x \geq 0$ can always be approximated by the summation of a series of linear blocks,

$$y = ax^2 \approx a\sum_{l=1}^{L} k(l)\Delta x \tag{3.16}$$

where the variable *x* is divided into *L* blocks and each block is denoted by Δx. In the summation, the slope $k(l)$ can be calculated as,

$$k(l) = \frac{\left(l\Delta x\right)^2 - \left(l\Delta x - \Delta x\right)^2}{\Delta x} = (2l-1)\Delta x . \tag{3.17}$$

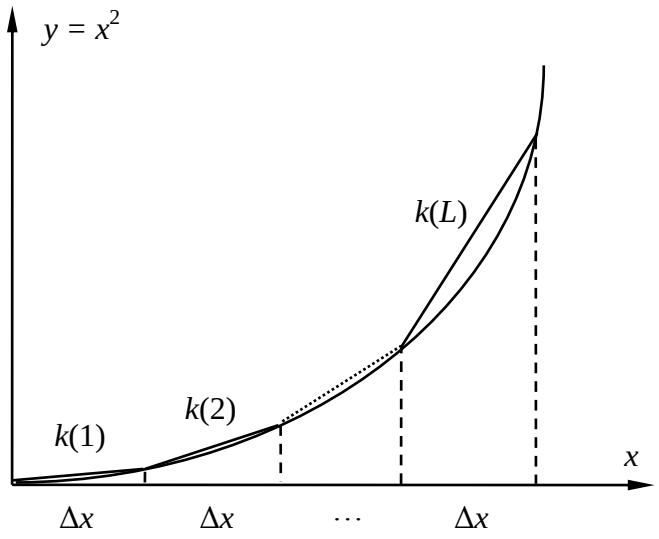

Fig. 3.4. Piecewise linearization for $y = ax^2$, $x \geq 0$

Based on (3.16) and (3.17), the following formulation is developed to linearize (3.15),

$$P_k = P_k^+ - P_k^- \tag{3.18}$$

$$\sum_{l=1}^{L} \Delta P_k(l) = P_k^+ + P_k^- \tag{3.19}$$

$$0 \leq \Delta P_k(l) \leq P_k^{\max} / L \tag{3.20}$$

$$PL_k = \left(g_k / b_k^2\right) \sum_{l=1}^{L} k(l) \Delta P_k(l) \tag{3.21}$$

$$k(l) = (2l-1)\, P_k^{\max} / L \tag{3.22}$$

$$P_k^+, P_k^- \geq 0\,,\ l = 1, 2, ..., L.$$

In (3.18) and (3.19), two non-negative slack variables P_k^+ and P_k^- are used to represent the active power P_k flows in the line. The upper and lower bounds for each interval $\Delta P_k(l)$ are defined in (3.20). The losses in the line are approximated by (3.21) and the slope of each linear block is given by (3.22). In most cases, the above piecewise linear loss model gives the correct line losses, however, when certain conditions are met, this model may

fail to converge to the correct solution and result in a "fictitious loss" that will not be observed in the real system [45]-[46]. To address this problem, a loss model with binary variables is presented in Chapter 5, in which the fictitious loss is eliminated.

3.4 The MILP-Based TEP Model

Based on the DC model, this section presents a MILP-based multi-stage TEP model that considers network losses and the $N-1$ criterion. The formulation of this TEP model is deterministic and the planners are assumed to have perfect information about the existing network as well as the parameters of the potential lines.

3.4.1 Linearized Operating Cost

The generator operating cost is usually assumed to be a linear function with respect to its active power output for simplicity purposes. However, a more realistic representation for the generator total energy cost should be a quadratic function with the following form,

$$CG_{gt} = a_g PG_{gt}^2 + b_g PG_{gt} + c_g . \tag{3.23}$$

Similar to the loss model presented in Section 3.3, the quadratic cost function (3.23) is also piecewise linearized using a series of linear blocks as shown in Fig. 3.4. The mathematical formulation of the piecewise linear cost model is shown as follows,

$$PG_{gt} = \sum_{l=1}^{L} \Delta PG_{gt}(l) \tag{3.24}$$

$$0 \le \Delta PG_{gt}(l) \le PG_g^{\max} / L \tag{3.25}$$

$$CG_{gt} = \sum_{l=1}^{L} k(l)\Delta PG_{gt}(l) + c_0 \tag{3.26}$$

$$k(l) = (2l-1)c_2 \left(PG_g^{\max} / L \right) + c_1 . \tag{3.27}$$

In (3.24), the generator output is modeled as the summation of a series of small intervals. The upper and lower bounds for each interval are defined in (3.25). The quadratic cost function is approximated by (3.26) and the slope of each linear block is calculated by (3.27). As shown in Fig. 3.5, the above piecewise linearized cost model is a better representation of the generator total operating cost as compared to a linear cost curve.

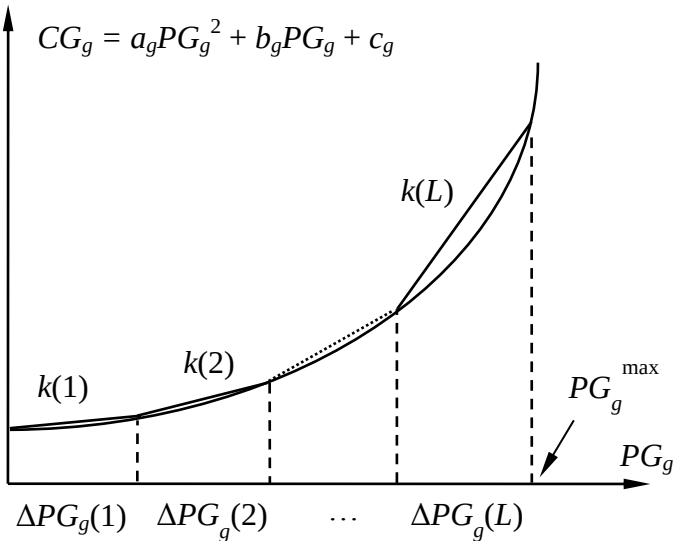

Fig. 3.5. Piecewise linearized generator total energy cost

3.4.2 Modeling the N – 1 Criterion

The $N - 1$ criterion states that the transmission network should be robust enough to handle the loss of any single element in the system. For the DC power flow model, this simply implies that no thermal limit violation and no load curtailment occurs with the outage of a single branch ($L - 1$) or a generator ($G - 1$).

Similar to the approach proposed in [13] two contingency scanning matrices **L** and **G** are introduced to model the $L - 1$ and $G - 1$ contingency respectively. Assume a power system that has *nl* lines and *ng* generators, the structure of the contingency scanning matrices are shown below,

$$\mathbf{L} = \left[\begin{array}{c|ccc} 1 & 0 & & 1 \\ \vdots & & \ddots & \\ 1 & 1 & & 0 \end{array}\right]_{nl\times(nl+1)} \qquad \mathbf{G} = \begin{bmatrix} 0 & & 1 \\ & \ddots & \\ 1 & & 0 \end{bmatrix}_{ng\times ng} \tag{3.28}$$

In (3.26), **L** is an *nl* by *nl* + 1 binary matrix and **G** is an *ng* by *ng* binary matrix. A '0' in the matrices means the status of the corresponding element is *outaged*, while a '1' means the status is *normal*. The first column of **L** has all ones, which represents the base case with all lines in service. In the matrices, each column is called a *state*, which represents the different operating modes. Generally, for a system with *nl* lines and *ng* generators, the total number of states for a complete $L - 1$ and $G - 1$ contingency scanning is $nl + ng + 1$.

A power system subjected to a $G - 1$ contingency usually requires generation re-dispatch. However, in real power systems, only certain generators can be re-dispatched. These generators usually have a higher ramp rate and serve non-base load. On the contrary, the base load generators, though cheaper in energy cost, usually have a low ramp rate. These base load generators are good resources to provide long-term system reserve, but are usually excluded as candidates for real time re-dispatch.

The total number of states for a complete $N - 1$ analysis is $nl + ng + 1$. However, for large power system planning studies, a complete $N - 1$ analysis is usually too expensive due to the computational burden. In real systems, only a few critical contingencies could cause serious overload issues, in this case, if the algorithm still goes through all the $nl + ng + 1$ states, the efficiency of the algorithm will be severely affected. In order to reduce the computational burden, the critical contingencies should be pre-screened and the total number of states should be set equal to the number of the critical contingencies plus one rather than $nl + ng + 1$. This function can be implemented by

adding a binary index in the input data indicating whether a line or a generator is a valid $N-1$ contingency. Before solving the TEP model, the program should count the number of contingencies and then form the scanning matrices accordingly.

3.4.3 The TEP Formulation

From an economic perspective, operating cost can play a substantial role in the total cost, therefore, considering only the investment cost may not accurately reflect the true cost of a TEP project. Furthermore, transmission planning will enhance the competitiveness of the power market when more players can participate. These market players, many of them are profit driven, consider the operating costs of their generation units as a major issue. As a result, it is important to coordinate the investment cost and the operating cost when formulating the objective function. Theoretically, the objective of a TEP problem is to maximize the social welfare, but in reality, the social welfare can be difficult to measure. Assuming a perfect inelastic demand curve, an equivalent objective to maximizing the social welfare is to minimize the sum of the investment cost and the operating cost [47]. The objective function jointly minimizes the total investment cost and the operating cost discounted to the present value,

$$\min\ C=\sum_{t=1}^{T_{pl}}\sum_{k\in\Omega_k}\frac{c_k\left(z_{kt}-z_{kt-1}\right)}{\left(1+d\right)^{t-1}}+\sum_{t=1}^{T_{op}}\sum_{g\in\Omega_g}\frac{8760CG_{gt}}{10^6\left(1+d\right)^{t-1}} \tag{3.29}$$

where the first and second terms represent the total investment cost and the total generator operating cost respectively. In the investment cost, $c_k(z_{kt}-z_{kt\text{-}1})$ guarantees that the cost of building a line c_k is not double counted. The value of the decision variable z_{k0} is set to be zero. Notice that the cost of losses is implicitly modeled in (3.29). This is because that the total power generated in the system is equal to the total loads plus the

losses, thus, the cost of losses is implicitly modeled in the generator operating cost. However, the proposed objective function does not necessarily minimize the losses. If one intends to minimize the losses, then the expression for losses should be the only term contained in the objective function. It could be argued that it is always good to have minimal losses, and they tend to penalize the term related to the losses by a large number to get a solution with fewer losses. Without entering into the discussion as to how to choose the penalty factor properly, this author believes that the investment cost and the operating cost should be treated in a nondiscriminatory manner. Since both costs are discounted to the present value, biasing one may identify a different TEP solution that reduces the overall economic value of the TEP project.

The complete constraints set of the proposed TEP formulation is as follows,

$$\sum_{k\in\Omega_k^i} P_{kct} + \sum_{g\in\Omega_g^i} PG_{gct} - \sum_{k\in\Omega_k^i} PL_{kt} = \sum_{d\in\Omega_d^i} PD_d \quad \forall i \in \Omega_b \tag{3.30}$$

$$-\left(1-x_{kt}\right)\cdot M_k \le \left(P_{kct} + b_k\theta_{kct}\right) \le \left(1-x_{kt}\right)\cdot M_k \quad \forall k \in \Omega_k \tag{3.31}$$

$$x_{kt}P_k^{\min} \le P_{kct} + PL_{kct} \le x_{kt}P_k^{\max} \quad \forall k \in \Omega_k \tag{3.32}$$

$$0 \le PG_{gct} \le PG_g^{\max}G(g,c) \quad \forall g \in \Omega_g \tag{3.33}$$

$$P_{kct} = P_{kct}^{+} - P_{kct}^{-} \quad \forall k \in \Omega_k \tag{3.34}$$

$$\sum_{l=1}^{L} \Delta P_{kct}(l) = P_{kct}^{+} + P_{kct}^{-} \quad \forall k \in \Omega_k,\ l = 1,\ 2,...,L \tag{3.35}$$

$$0 \le \Delta P_{kct}(l) \le x_{kt}\left(P_k^{\max}/L\right) \quad \forall k \in \Omega_k,\ l = 1,\ 2,...,L \tag{3.36}$$

$$P_{kct}^{loss} = \left(G_k/B_k^2\right)\sum_{l=1}^{L} k(l)\Delta P_{kct}(l) \quad \forall k \in \Omega_k,\ l = 1,\ 2,...,L \tag{3.37}$$

$$k(l) = (2l-1)\,P_k^{\max}/L \quad \forall k \in \Omega_k,\ l = 1,\ 2,...,L \tag{3.38}$$

$$PG_{gt} = \sum_{l=1}^{L} \Delta PG_{gt}(l) \quad \forall g \in \Omega_g,\ l = 1,\ 2, ..., L \tag{3.39}$$

$$0 \le \Delta PG_{gt}(l) \le PG_g^{\max} / L \quad \forall g \in \Omega_g,\ l = 1,\ 2, ..., L \tag{3.40}$$

$$CG_{gt} = \sum_{l=1}^{L} k_g(l) \Delta PG_{gt}(l) + c_0 \quad \forall g \in \Omega_g,\ l = 1,\ 2, ..., L \tag{3.41}$$

$$k_g(l) = (2l-1)c_2 \left(PG_g^{\max} / L \right) + c_1 \quad \forall g \in \Omega_g,\ l = 1,\ 2, ..., L \tag{3.42}$$

$$z_{kt} - z_{kt-1} \ge 0 \quad t = 2, 3, ...T \tag{3.43}$$

$$x_{kt} = \begin{cases} L(k,c) & \text{for existing lines} \\ z_{kt} L(k,c) & \text{for perspective lines} \end{cases}.$$

In this formulation, (3.30) is the nodal balance equation which guarantees the power balance at every bus. In (3.31) and (3.32), a disjunctive factor M_k is used to eliminate the nonlinearities that would otherwise appear. Constraint (3.31) indicates the following: if x_{kt} is 1, *i.e.* the line exists or the line is selected, then the DC power flow equation is enforced; otherwise, if x_{kt} is 0, *i.e.* the line is outaged or the line is not selected, then the disjunctive factor M_k ensures that the constraint is not binding. The disjunctive factor M_k should be sufficiently large, but a too large M_k will often cause numerical difficulties. The minimum sufficient value of M_k can be calculated using the approach in [48]. Similar logic also applies to (3.32): if the x_{kt} is 1. Then the power flow is limited by the rating of that line; otherwise, the power flow is forced to be 0. In (3.33), the power generated from a certain generator is limited in its capacity range if the generator is in service, and is zero if the generator is outaged. Constraints (3.34)-(3.42) represent the linearized loss model and generator cost model. Notice that in the objective function, only the base case operating cost is modeled. Operating under contingencies is not considered as a normal

operating mode, the operating cost for operating under contingencies is not included in the objective function. Constraints (3.43) ensures that once a line is built in one period, it will not be taken off in the next period.

3.5 Case Studies

In this section, the proposed TEP model is applied to two test systems. First, the performance of the proposed loss modeling approach is tested and analyzed on the IEEE 24-bus system [5]. A two-stage TEP is then performed on the IEEE 118-bus system [50]. All models are programmed in AMPL [51]. The solvers used are Gurobi [52]. The computer used for simulations has an Intel E8500 CPU with 3.2 GB of RAM.

3.5.1 The IEEE 24-bus System

The IEEE 24-bus system used in this case has 35 existing branches, 32 generators connected at 10 buses, and 21 loads. The total load is 2850 MW. All the system parameters including the line investment cost data can be found in [5]. The lower bounds of all the generators are set to zeros. The total operating horizon is twenty years.

First, the TEP solution obtained from the lossy DC model and the lossless DC model are compared for the cases that consider and do not consider $N - 1$ criterion, respectively. For every existing corridor, one more line can be added. Since there are 35 existing branches and no parallel branches, the number of binary decision variables is 35. A complete $N - 1$ analysis is performed for all lines (35 existing lines and 35 potential lines) and generators. The number of the piecewise linear sections for loss modeling and generator cost modeling are set to be 5 and 20 respectively. The comparison results are shown in Table 3.3. Define the term *cost turnover* as,

$$Cost\ turnover = \left| \frac{C_{loss}^{inv} - C_{lossless}^{inv}}{C_{loss}^{opr} - C_{lossess}^{opr}} \right| \tag{3.44}$$

where the numerator and the denominator represent the difference of investment cost and the operating cost between the lossy and the lossless DC models respectively. For any year beyond *cost turnover*, the expansion plan obtained from the lossy DC model will give a lower total cost as compared to the lossless DC model.

Table 3.3. TEP results comparison for the IEEE 24-bus system

Corridor	Not considering $N-1$		Considering $N-1$	
	Lossy	Lossless	Lossy	Lossless
3 – 9		No line needed		1
3 – 24			1	
7 – 8			1	
14 – 16			1	
15 – 21	1		1	
15 – 24			1	
16 – 17			1	1
17 – 18				1
20 – 23			1	
No. of lines needed	1	0	7	3
CPU time (s)	0.16	0.06	74.19	8.59
Investment cost (M$)	24.8	0	168.4	80.6
Losses (MW)	51.70	0	52.98	0
Annual operating cost (M$)	506.72	508.97	503.20	507.46
Cost turnover	11.0 years		20.6 years	

As observed from the above table, the lossy DC model results in completely different network expansion schemes as compared to the lossless DC model. For the case that considers the $N-1$ criterion, more lines are required to be built, this is because modeling network losses tend to shift the cost from operation to line investment, and thus influence the optimal transmission plan. The lossless DC model usually requires building fewer lines initially and gives a lower estimate of the planning cost, but in the long run,

the transmission expansion plan given by the lossless DC model will cost more because of the presence of losses in the real system. The annual operating cost in the Table is obtained from the ACOPF result with the corresponding expanded network. As observed from the table, the annual operating cost of the expanded network obtained from the lossy DC model is lower than the one obtained from the lossless model for both cases. For the IEEE 24-bus system studied in this section, the cost turnovers are 20.6 years and 11 years depending on whether the $N-1$ criterion is considered.

3.5.2 The IEEE 118-bus System

In this case study, a multi-stage planning study is performed on the modified IEEE 118-bus system. The system has 186 existing branches, 54 generators, and 91 loads. The line ratings have been reduced to create line congestion in the initial network. In this case study, seventeen lines have been selected as the candidate lines. The complete candidate line set is listed in Table 3.4.

Table 3.4. Candidate lines for the IEEE 118-bus system

Number	Corridor	Cost (M$)	Rating (MW)
1	3 – 5	8.73	120
2	8 – 5	8.17	200
3	8 – 9	16.43	200
4	30 – 17	21.22	200
5	8 – 30	8.67	120
6	26 – 30	11.22	200
7	55 – 56	14.66	120
8	38 – 65	13.74	200
9	77 – 78	8.97	120
10	83 – 85	10.65	120
11	85 – 86	22.77	200
12	65 – 68	18.41	200
13	38 – 37	19.24	200
14	103 – 110	15.7	120
15	110 – 112	18.71	120
16	17 – 113	17.54	120
17	12 – 117	3.18	120

The following simulations show the results for a two-stage security-constrained planning study on the IEEE 118-bus system. The time span of this planning problem is ten years. The planned lines are to be built at the beginning of Year 1 and Year 6 respectively. In total, 8 additional lines are required in this ten-year planning horizon, and no more than 5 lines should be built in the first stage due to a budget constraint. Starting from Year 1, the objective is to minimize the total cost of investment and operation in this ten-year horizon. The estimated load growth is 20% in five years, which means at the beginning of the sixth year, the total load is 20% higher than the initial load. Furthermore, the load is assumed to increase in proportion to each load bus. A complete $N-1$ analysis except for the single outlet transformer (line 9 – 10, 71 – 73, 86 – 87, 110 – 111 and 68 – 116) is performed for each stage. The optimal network expansion scheme and the total estimated cost obtained by the model is shown in Table 3.5.

Table 3.5. TEP results for the IEEE 118-bus system

Lines to build	Year 1	5 – 8, 8 – 9, 12 – 117, 26 – 30, 85 – 86
	Year 6	3 – 5, 8 – 30, 77 – 78
Total cost (M$)	4383.09	
Computing time (min)	68.5	

As observed from Table 3.5, four new lines are needed for this two-stage security-constrained planning problem, and all of them need to be built in Year 1 for economic purposes. During the ten-tear planning horizon, the total investment and the operating cost are about 4.38 billion dollars. The computation time is about 68.5 minutes. Notice that the result obtained above only gives a high-level picture of how the system can be designed reliably and economically for the long run based on the best estimate at the present. The line flow and the generator dispatch obtained in the planning studies,

however, may not be economical for real time operation due to unforeseen load levels and many uncertainty factors that cannot be forecast.

For the expanded system, a lower and flatter LMP profile is usually expected, and this is observed for most cases. However, notice that the objective of power system planning is not to minimize the LMP. Therefore, the planned system does not necessarily lower the LMP at every bus. The LMP profile of the initial network without additional lines, the expanded network at the end of Year 1, and the final expanded network at the end of Year 6 are plotted in Fig. 3.6. One can observe that the LMP profile for the expanded system at the end of Year 1 is much flatter than the initial network, because with the new lines added, the congestions that were originally present in the system are relieved. Due to the significant load growth at the end of Year 6, the ACOPF fails to converge for the initial network without any transmission lines additions, while for the expanded system, a higher LMP profile is observed.

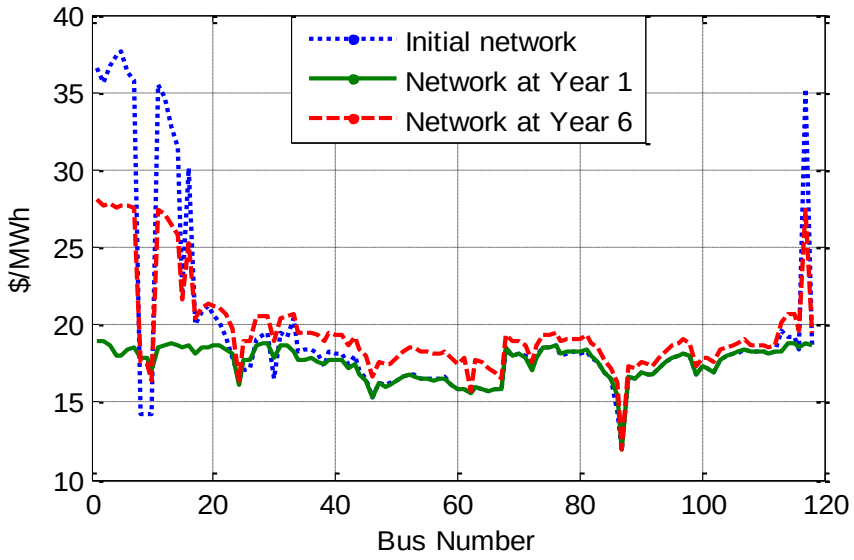

Fig. 3.6. Comparison of the LMPs at each bus

3.6 Summary

A MILP-based multi-stage TEP model is proposed in this chapter. In order to obtain an accurate TEP model, a piecewise linearization approach is developed to model the network losses as well as the quadratic generator cost. The $N-1$ criterion is modeled using two contingency scanning binary matrices. The first case study shows that the modeling of network losses can significantly influence the network expansion plan. The *cost turnover* index shows that the TEP model using the lossy DC model will eventually provide savings in the total cost. The multi-stage planning studies on the IEEE 118-bus system demonstrate that the proposed TEP model has the potential to be applied to large power system planning problems.

Chapter 4

TRANSMISION EXPANSION PLANNING USING THE AC MODEL

4.1 Chapter Overview

The AC modeling of the TEP problem is rarely seen in the literature. This is because the formulation of TEP problems using the AC model is generally a MINLP problem, which is extremely difficult to solve. A few solvers such as Knitro, Bonmin, Couenne and Baron are capable of solving MINLP problems and can obtain a reasonably good solution in an acceptable time. Among these solvers, Couenne and BARON are designed for solving both convex and non-convex MINLP problems. Knitro and Bonmin are designed for solving only convex MINLP problems exactly, while for non-convex MINLP problems, heuristic solutions will be given [53]-[55].

Solving MINLP problems directly is not the only choice. In fact, when the original problem is impossible or too expensive to solve, relaxation should be considered. By eliminating integer variables, the MINLP problems can be relaxed to an NLP problem, which usually has a potential for an easier solution. This chapter explores the possibility of applying AC-based models to the TEP problems. The AC-based TEP models and their possible relaxations are proposed and discussed in detail.

The rest of the chapter is organized as follows: Section 4.2 presents two MINLP-based TEP models. The relaxations of the models are investigated in Section 4.3. Simulation results are provided in Section 4.4 to compare the performance of the proposed TEP models. Finally, concluding remarks are drawn in Section 4.5.

4.2 MINLP-Based ACTEP Models

In this section, two MINLP-based TEP models are presented. The two models are denoted as *MIP*1 and *MIP*2 and the mathematical formulations are shown as follows,

*MIP*1:

$$\min \sum_{k\in\Omega_k} c_k z_k + \sum_{g\in\Omega_g} \left(c_2 PG_g^2 + c_1 PG_g + c_0\right) \tag{4.1}$$

$$\sum_{g\in i} PG_g - \sum_{d\in i} PD_d + \sum_{k\in i} P_k = 0$$

$$\sum_{g\in i} QG_g - \sum_{d\in i} QD_d + \sum_{k\in i} Q_k = 0$$

$$PG_g^{\min} \le PG_g \le PG_g^{\max}$$

$$QG_g^{\min} \le QG_g \le QG_g^{\max}$$

$$V_i^{\min} \le V_i \le V_i^{\max}$$

$$-\theta_k^{\max} \le \theta_k \le \theta_k^{\max}$$

$$0 \le P_k^2 + Q_k^2 \le \left(S_k^{\max}\right)^2$$

where the active and reactive line flows are given by,

$$P_k = z_k\left[V_i^2\left(g_k + g_{k0}\right) - V_i V_j\left(g_k \cos\theta_k + b_k \sin\theta_k\right)\right] \tag{4.2}$$

$$Q_k = z_k\left[-V_i^2\left(b_k + b_{k0}\right) + V_i V_j\left(b_k \cos\theta_k - g_k \sin\theta_k\right)\right]. \tag{4.3}$$

In the *MIP*1 model, the objective function (4.1) jointly minimizes the investment cost and the operating cost. The line flows are modeled as the products of binary variables z_k and the AC power flow equations as shown in (4.2) and (4.3). For existing lines, z_k is fixed to 1, while for perspective lines, z_k is a binary variable and can be chosen

freely as 0 or 1. It can be observed from (4.2) and (4.3) that if a line is not selected, then the power flow on that line is forced to be zero. Disjunctive programming methods can be applied to replace the equality constraints (4.2) and (4.3) and gives the following *MIP*2 model,

*MIP*2:

$$\min \sum_{k\in\Omega_k} c_k z_k + \sum_{g\in\Omega_g} \left(c_2 PG_g^2 + c_1 PG_g + c_0\right)$$

$$\sum_{g\in i} PG_g - \sum_{d\in i} PD_d + \sum_{k\in i} P_k = 0$$

$$\sum_{g\in i} QG_g - \sum_{d\in i} QD_d + \sum_{k\in i} Q_k = 0$$

$$PG_g^{\min} \le PG_g \le PG_g^{\max}$$

$$QG_g^{\min} \le QG_g \le QG_g^{\max}$$

$$V_i^{\min} \le V_i \le V_i^{\max}$$

$$-\theta_k^{\max} \le \theta_k \le \theta_k^{\max}$$

$$0 \le P_k^2 + Q_k^2 \le z_k \left(S_k^{\max}\right)^2 \tag{4.4}$$

where the active and reactive line flows are given by,

$$P_k - V_i^2\left(g_k + g_{k0}\right) + V_i V_j \left(g_k \cos\theta_{ij} + b_k \sin\theta_{ij}\right) \le (1-z_k) M_k \tag{4.5}$$

$$P_k - V_i^2\left(g_k + g_{k0}\right) + V_i V_j \left(g_k \cos\theta_{ij} + b_k \sin\theta_{ij}\right) \ge (z_k - 1) M_k \tag{4.6}$$

$$Q_k + V_i^2\left(b_k + b_{k0}\right) - V_i V_j \left(b_k \cos\theta_{ij} - g_k \sin\theta_{ij}\right) \le (1-z_k) M_k \tag{4.7}$$

$$Q_k + V_i^2\left(b_k + b_{k0}\right) - V_i V_j \left(b_k \cos\theta_{ij} - g_k \sin\theta_{ij}\right) \ge (z_k - 1) M_k . \tag{4.8}$$

Compared to the *MIP*1 model, the above *MIP*2 model splits the two power flow equations into four inequality constraints as shown in (4.5) – (4.8). Constraints (4.5) and (4.6) indicate that if a line is selected, which means that z_k equals to 1, then the two constraints act as akin to (4.2) and force the active power flow equation to hold; otherwise, the disjunctive factor M_k guarantees that the two constraints are not binding. Similar logic applies to (4.7) and (4.8) for reactive power flow on the line. Notice that the two TEP models presented in this section are straightforward, but they are both MINLP-based models and are extremely difficult to solve (refer to simulation results in Section 4.4). In order to obtain an efficient ACTEP model, relaxations of the above models are needed. Possible relaxations of the MINLP-based ACTEP models are investigated in the next section.

4.3 Relaxations of the MINLP-Based ACTEP Model

Mathematically, the relaxation refers to a modeling strategy that approximates the original problem. The relaxed problem typically creates a superset of the feasible region of the original problem so that solving the relaxed problem usually requires less effort than solving the original problem. The solution of the relaxed problem may not necessarily be the exact solution of the original problem but should be reasonably close and provides key information about the original problem. For ACTEP models, the main purpose of the relaxation is to eliminate the integer variables to reduce the complexity of the original problem. This section proposes three possible relaxations of the MINLP-based ACTEP models. The first two models are based on the NLP relaxations, and the third model is based on the RLT relaxation where all the constraints are linearized.

4.3.1 The NLP Relaxations

The two NLP relaxations are developed based on the *MIP*2 model presented in Section 4.2. By slightly changing the formulation, the integer constraints in *MIP*2 can be eliminated and NLP-based TEP model is formulated as follows,

*NLP*1:

$$\min \sum_{k\in\Omega_k} c_k z_k + \sum_{g\in\Omega_g} \left(c_2 PG_g^2 + c_1 PG_g + c_0\right)$$

$$\sum_{g\in i} PG_g - \sum_{d\in i} PD_d + \sum_{k\in i} P_k = 0$$

$$\sum_{g\in i} QG_g - \sum_{d\in i} QD_d + \sum_{k\in i} Q_k = 0$$

$$PG_g^{\min} \le PG_g \le PG_g^{\max}$$

$$QG_g^{\min} \le QG_g \le QG_g^{\max}$$

$$V_i^{\min} \le V_i \le V_i^{\max}$$

$$-\theta_k^{\max} \le \theta_k \le \theta_k^{\max}$$

$$0 \le P_k^2 + Q_k^2 \le z_k \left(S_k^{\max}\right)^2$$

$$z_k \left(1 - z_k\right) \le \varepsilon \tag{4.9}$$

$$0 \le z_k \le 1. \tag{4.10}$$

By adding (4.9) and (4.10) in the *NLP*1 model, z_k is relaxed as a continuous variable ranging from 0 to 1. The TEP formulation is therefore reduced to an NLP model. Notice that ideally, (4.9) should be written as $z_k(1 - z_k) = 0$. To satisfy this equation, z_k must equal either 0 or 1. In practice, the inequality form as shown in (4.9) is usually used with the right hand side equal to a small positive number ε instead of zero to prevent he

presence of numerical difficulties. Instead of using the *zero product* constraint as in (4.9), the same goal can be achieved by penalizing the objective function as shown in the following *NLP*2 model,

NLP2:

$$\min \sum_{k\in\Omega_k} c_k\left[A\sin\left(\pi z_k\right)+1\right]+\sum_{g\in\Omega_g}\left(c_2 PG_g^2+c_1 PG_g+c_0\right) \tag{4.11}$$

$$\sum_{g\in i} PG_g-\sum_{d\in i} PD_d+\sum_{k\in i} P_k=0$$

$$\sum_{g\in i} QG_g-\sum_{d\in i} QD_d+\sum_{k\in i} Q_k=0$$

$$PG_g^{\min}\le PG_g\le PG_g^{\max}$$

$$QG_g^{\min}\le QG_g\le QG_g^{\max}$$

$$V_i^{\min}\le V_i\le V_i^{\max}$$

$$-\theta_k^{\max}\le\theta_k\le\theta_k^{\max}$$

$$0\le P_k^2+Q_k^2\le z_k\left(S_k^{\max}\right)^2$$

$$0\le z_k\le 1.$$

As observed from the above *NLP*2 model, a penalty term [Asin(πz_k) + 1] is imposed on the objective function (4.11). When z_k is equal to either 1 or 0, the value of Asin(πz_k) is always zero and the resultant objective function is the same as (4.1). Otherwise, the large positive coefficient A of the sine function will impose a penalty on the objective function and make it impossible to be the optimal solution. In other words, the optimal solution can only be obtained when z_k is equal to 0 or 1. The sketch of the penalty function is shown in Fig. 4.1.

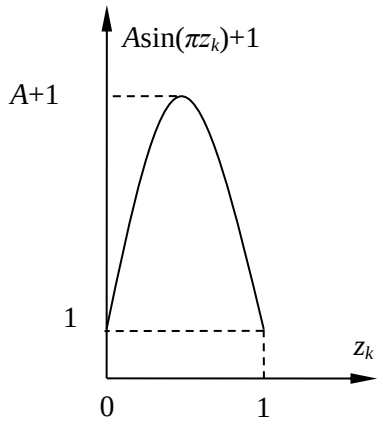

Fig. 4.1. Sketch of the penalty function in the *NLP*2 model

The NLP-based TEP model relaxes the binary decision variables by introducing a nonlinear constraint (4.9) or penalty term in the objective function (4.11). Compared with the original MINLP problem, the relaxed NLP problem is usually easier to solve. However, this relaxation also creates many local optimum. Since the NLP problem is solved using KKT condition, the solve may not "see" other solutions (could be better) once it reaches one of the local optimum. Therefore, Starting with different combination of starting point is important to obtain a solution with high quality.

4.3.2 The RLT-based Relaxation

The following example shows the basic concept of the RLT [56]. Considering the following minimization problem,

$$\min \; x + y \tag{4.12}$$

subject to,

$$x - y + xy = 1 \tag{4.13}$$

$$(x_L, y_L) \le (x, y) \le (x_U, y_U), x, y \in \mathbf{R}^+.$$

Since there is a bilinear term xy in (4.13), the model (4.12) is non-convex. In order to convexify the model, a new variable w is introduced to replace the binary term so that the (4.13) can be rewritten as,

$$x - y + w = 1. \tag{4.14}$$

In the above model, the upper bound and lower bound of the existing variables x and y are given respectively as (x_U, y_U) and (x_L, y_L), and there is no additional constraint on w, then a tight bound on w, which is also known as the McCormick convex relaxation [56] can be calculated by solving the following inequalities:

$$\begin{aligned} w &\geq x_L y + y_L x - x_L y_L \\ w &\geq x_U y + y_U x - x_U y_U \\ w &\leq x_U y + y_L x - x_U y_L \\ w &\leq x_L y + y_U x - x_L y_U \end{aligned} \tag{4.15}$$

By using the above RLT-based relaxation, the original bilinear problem can be relaxed to a linear programming problem, which is convex and much easier to solve. However, the main drawback of the RLT-based relaxation is the excessive size of the resulting LP relaxation. In addition, by using the RLT-based relaxation, it is difficult to control the degree of the relaxation. This means that the problem may easily become too relaxed and therefore lose some of the key information that should be maintained. In order to apply RLT to the TEP formulation, the rectangular form of the power flow equations as shown in Section 2.3.1 is used. By sequentially inserting the dummy variables, all the bilinear terms can eventually be rewritten as a linear expression. The RLT-based TEP model is shown as follows,

RLT:

$$\min \sum_{k\in\Omega_k} c_k z_k + \sum_{g\in\Omega_g} \left(c_2 PG_g^2 + c_1 PG_g + c_0\right)$$

$$\sum_{g\in i} PG_g - \sum_{d\in i} PD_d + \sum_{k\in i} P_k = 0$$

$$\sum_{g\in i} QG_g - \sum_{d\in i} QD_d + \sum_{k\in i} Q_k = 0$$

$$PG_g^{\min} \le PG_g \le PG_g^{\max}$$

$$QG_g^{\min} \le QG_g \le QG_g^{\max}$$

$$V_i^{\min} \le V_i \le V_i^{\max}$$

$$-\theta_k^{\max} \le \theta_k \le \theta_k^{\max}$$

$$0 \le P_k \le S_k^{\max} \tag{4.16}$$

$$P_k - g_{sh}\left(X1_k + X2_k\right) + g_k\left(X3_k + X4_k\right) + b_k\left(X5_k - X6_k\right) \le (1-z_k)M_k \tag{4.17}$$

$$P_k - g_{sh}\left(X1_k + X2_k\right) + g_k\left(X3_k + X4_k\right) + b_k\left(X5_k - X6_k\right) \ge (z_k - 1)M_k \tag{4.18}$$

$$Q_k + b_{sh}\left(X1_k + X2_k\right) - b_k\left(X3_k + X4_k\right) + g_k\left(X5_k - X6_k\right) \le (1-z_k)M_k \tag{4.19}$$

$$Q_k + b_{sh}\left(X1_k + X2_k\right) - b_k\left(X3_k + X4_k\right) + g_k\left(X5_k - X6_k\right) \ge (z_k - 1)M_k \tag{4.20}$$

where $g_{sh} = g_k + g_{k0}$, $b_{sh} = b_k + b_{k0}$, $X1 = e_i^2$, $X2 = e_j^2$, $X3 = e_i e_j$, $X4 = f_i f_j$, $X5 = e_j f_i$ and $X6 = e_i f_j$. For power systems in the steady state, it is usually assumed that $0.95 \le V_i \le 1.05$ and $-\pi/6 \le \theta_k \le \pi/6$. Recall that $e_i = V_i\cos\theta_i$ and $f_i = V_i\sin\theta_i$, the bounds on e_i, e_j, f_i and f_j can be therefore obtained as $0.8227 \le (e_i, e_j) \le 1.05$ and $-0.525 \le (f_i, f_j) \le 0.525$. Thus, (4.15) can be used for deriving the bounds on $X1$ to $X6$. Notice that in order to obtain a fully linearized model, reactive power term is neglected in (4.16).

4.4 Case Studies

In this section, the proposed TEP models are applies to two test systems and simulation results are demonstrated. First, the proposed MINLP-based ACTEP models and their relaxations are tested on Garver's 6-bus system. The performance of each model is compared and analyzed. Then, the *NLP*2 model is applied to solve the TEP problem of the IEEE 24-bus system. All the models are programmed in AMPL. The computing platform used to perform all the simulations is a Linux workstation that has an Intel *i*7 2600 4-core CPU at 3.40 GHz and with 16 GB of RAM.

4.4.1 Garver's 6-bus System

The Garver's system used in this section is the same as the one used in Section 3.2. The additional system data are provided in [14]. It is assumed in this section that the maximum number of lines allowable in a transmission corridor is 2. Since there are 6 existing lines, the maximum number of lines that can be built are 24. In order to compare with the TEP results in the literature, the objective is only to minimize the investment cost. First, three MINLP solvers: Couenne 0.4.0 [53], Bonmin 1.5.1 [54] and Knitro 8.0.0 [55] are used to solve the two MINLP-based TEP models presented in Section 4.2. The results are listed in Table 4.1.

Table 4.1. TEP results for the MINLP-based TEP models

Model		KNITRO	BONMIN	COUENNE
*MIP*1	Objective	1056	1056	Time limit reached
	TEP result	Build all lines	Build all lines	
*MIP*2	Objective	Iteration limit reached	677	Time limit reached
	TEP result		Build 17 lines	

As observed from Table 4.1, for the *MIP*1 model, the heuristic solutions given by Knitro and Bonmin are simply to build all the lines. This is rather a trivial feasible solution because the solvers are not really *selecting* a specific choice. For the *MIP*2 model, Knitro gives a solution of 130 M$, while Bonmin gives 667 M$. Notice that although Couenne claims that it can solve general MINLP problems exactly, the solution time could be extremely long. For both MINLP-based models, Couenne fails to return a solution within the 24-hour time limit. The capability of the solvers for handling MINLP-based TEP models is still quite limited.

The NLP models and the RLT model are solved only by Knitro and Bonmin. Although the first two models are reduced to NLP problems, they are still non-convex problems. However, the quality of the solution can be significantly affected by the starting points. As a heuristic approach, the *multi-start* option in Knitro and Bonmin is used. For both NLP models, the number of multi-starts is set to 2000. The optimality tolerance and the feasibility tolerance of the solvers are set to 10^{-9}, respectively. The TEP results of the relaxed models are presented in Table 4.2.

Table 4.2. TEP results for the relaxed ACTEP models

Model	Solver	KNITRO	BONMIN
*NLP*1	Objective (M$)	406	473
	Lines	Build 11 lines	Build 12 lines
*NLP*2	Objective (M$)	180	804
	Lines	(1-5), (2-3), (2-6)×2, (3-5), (4-6)×2	Build 21 lines
RLT	Objective (M$)	110	110
	Lines	(2-6), (3-5), (4-6)×2	(2-6), (3-5), (4-6)×2

As observed from Table 4.2, for *NLP*1 model, Knitro gives a lower objective value (406 M$) and fewer lines to build as compared to the results gives by Bonmin after 2000 restarts. For the *NLP*2 model, Knitro again gives a much lower objective value (180 M$) as compared to the results gives by Bonmin. It should be pointed out that the selection of the penalty factor *A* can significantly influence the results. A penalty factor that is not sufficiently large may cause the decision variables z_k fail to converge closely enough to 0 or 1, but a too large penalty factor could also make the problem difficult to converge. Based on the simulation experience, the value of coefficient *A* used for Knitro that gives the best solution is 10^9, while for Bonmin is 10^3. For the *RLT* model, both the solvers identify the same objective value and the same set of lines to be built. Among all the results in the table, the *RLT* model gives the lowest objective value.

During the process of the relaxations, it is likely that some key information of the original model is not strictly maintained in the relaxed models. Therefore, the "optimal" plan obtained by the TEP model may be infeasible in the AC power flow studies. As a result, a validation process is necessary to ensure that the TEP plans are AC feasible. In this section, the four TEP plans with the lowest objective functions are validated by running an ACOPF study and the results are shown in Table 4.3.

Table 4.3. Validation of the TEP results of Garver's system

Model	Solver	Objective (M$)	ACOPF Results
RLT	KNITRO / BONMIN	110	No convergence
***NLP*2**	**KNITRO**	**180**	**Converged**
*NLP*1	KNITRO	406	Converged
*NLP*1	BONMIN	473	Converged

As observed from Table 4.3, despite the *RLT* model giving the lowest objective value, the TEP result is, however, infeasible in the ACOPF. The TEP results given by the three NLP models are all feasible in the ACOPF, and the one given by the *NLP*2 model (marked in **bold**) has the lowest objective value. Therefore, one can conclude that among all the solutions in Table 4.3, the one given by the *NLP*2 model is the best expansion plan for Garver's test system. The expanded network is shown in Fig. 4.2. The dashed lines are new transmission lines to be added.

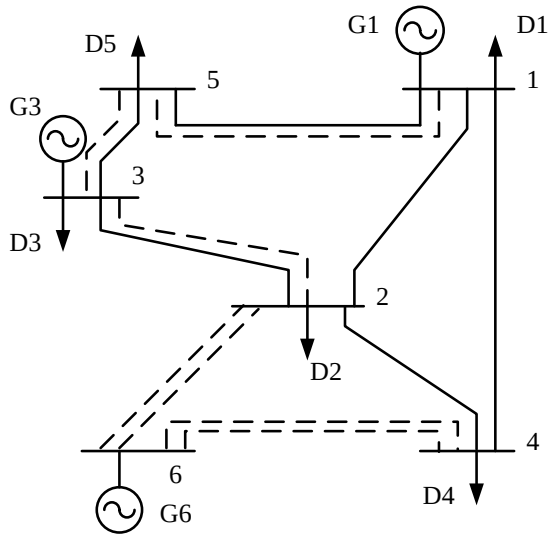

Fig. 4.2. The expanded Garver's 6-bus system

As a global optimization problem, different starting points should be tried to improve quality of the solution. Fig. 4.3 shows the effect of multi-starts on the ACTEP solutions using the *NLP*2 model. It can be observed that the quality of the solution is significantly improved with the increased number of multi-starts. However, one should be aware that this is at a cost of additional computing time.

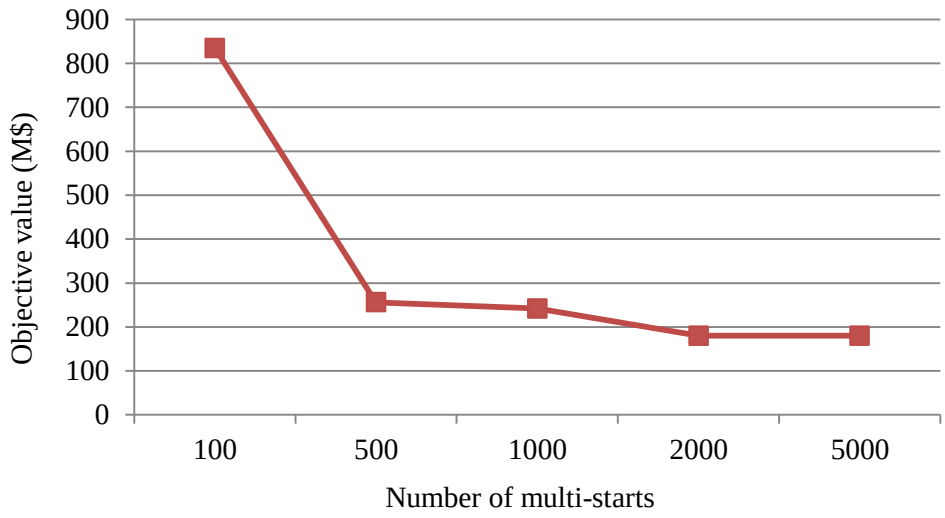

Fig. 4.3. Effect of multi-starts on the TEP solution

The results presented in Table 4.4 compare the TEP solutions of Garver's 6-bus system obtained from different models. One can observe that the AC model gives a higher objective value and requires building more lines. Notice that since the TEP models based on the lossless DC model and the lossy DC model are MILP models, the global optimality of the solution is guaranteed. However, TEP model based on the AC model is a non-convex NLP model and there is no guarantee to obtain a global optimal solution in polynomial time. The only conclusion that can be drawn is that this solution is the best possible TEP solution after 2000 multi-starts.

Table 4.4. Comparison of the TEP results

Model	DC Lossless [5]	DC Lossy [15]	AC
Objective (M$)	110	140	180
Lines to be added	(3-5), (4-6)×3	(2-6)×2, (3-5), (4-6)×2	(1-5), (2-3), (2-6)×2, (3-5), (4-6)×2
AC Feasible?	No	No	Yes

4.4.2 The IEEE 24-bus System

The IEEE 24-bus system used in this paper has 33 generators connected at 10 buses, and 21 loads [57]. The line investment cost data and the system parameters are provided in Appendix A, respectively. The total load is 2850 MW. The objective function in this case is to minimize the sum of line investment cost and the operating cost for 20 years. The AC model and solver used in this study are *NLP*2 and Knitro, respectively. Similar to the previous case, the penalty factor used in this case is 10^9, the number of multi-starts is set to 2000, and the optimality tolerance and the feasibility tolerance of the solvers are set to 10^{-9}. In order to perform the ACTEP studies, five lines that are related to bus 1, bus 2 and bus 7 are removed (1 – 2, 1 – 4, 1 – 5, 2 – 4 and 7 – 8), which means bus 1, bus 2 and bus 7 are isolated from the rest of the system. Instead, a new candidate line set is listed in Table 4.5.

Table 4.5. Candidate line parameters for IEEE 24-bus system

Number	Corridor	Cost (M$)	Rating (MW)
1	1 – 2	7.04	175
2	1 – 4	106.92	175
3	1 – 5	42.78	175
4	2 – 4	64.14	175
5	2 – 6	97.2	175
6	7 – 2	7.04	175
7	7 – 4	106.92	175
8	7 – 5	64.14	175
9	7 – 8	31.08	175

Two cases are studied for the IEEE 24-bus system. In Case 1, the TEP model is run without any additional constraints. In Case 2, an additional security constraint is added to make sure that the number of lines connected to a bus should be greater or equal to 2. The TEP results are shown in Table 4.6.

Table 4.6. Comparison of TEP results for the IEEE 24-bus system

Corridor	DC lossless model [5]	DC lossy model [11]	AC model (*NLP*2)	
			Case 1	Case 2
1 – 2	1	1		1
1 – 5			1	1
2 – 4				1
7 – 2	1	1	1	1
7 – 8	1	1	1	1
Investment cost (M$)	45.16	45.16	87.94	152.08
Losses[1] (MW)	58.77	58.77	55.72	54.06
Annual operating cost (M$)	560.3	560.3	558.7	558.0
CPU time	0.08 s	0.16 s	2.3 h (2000 restarts)	2.5 h (2000 restarts)

[1]The losses and the annual operating cost are obtained from ACOPF

As observed from Table 4.6, for Case 1, the AC model requires building 3 lines, thus bus 1, bus 2, bus 4, bus 5 and bus 7 in the system will be radially connected, while in Case 2 where the security requirement is added, two more lines 2 – 4 and 1 – 2 are required, and therefore eliminates the radial line. Both the lossless DC model and the lossy DC model give the same result of building 3 lines when security requirement is not considered. It should be pointed out that if considering the security constraints, then the DC-based models give the same results as Case 2 of the AC model.

4.5 Summary

Starting with two MINLP models, this chapter explores the possibility of applying the AC model to solve TEP problems. Two NLP-based TEP models are proposed by relaxing the binary variables in the model. A RLT-based model in which all the constraints are linearized is also studied. Based on the simulation results, the following general conclusions can be made:

- The AC model can be applied to model TEP problems, but solving the MINLP-based ACTEP models is still challenging.
- By relaxing the binary variables, it is possible to solve the NLP-based ACTEP problem and obtain a local solution. In order to obtain a high quality solution, it is necessary to use of the multi-start option. However, despite the observation that the multi-start option can improve the quality of the TEP solution, it is still difficult to judge the global optimality of the solution due to the non-convex nature of the problem.
- The potential of using the MINLP/NLP models for solving large-scale TEP problems requires more research.

Chapter 5

A RELAXED ACOPF MODEL BASED ON A TAYLOR SERIES

5.1 Chapter Overview

Due to the approximations made, the accuracy of the DC model may be poor in some cases [58]. Endeavors have been made recently to search for better approximations to the AC model. The core concepts of the work being done are convexification and relaxation. The purpose of formulating a convex model is to obtain the global optimal solution. During the convexification process, if certain conditions do not hold, then relaxations may be needed. A linear programming approximation to the AC power flow equations was presented in [59], where the cosine term in the power flow equations was piecewise linearized and other nonlinear terms are approximated by the Taylor series. In [60], the ACOPF problem was reformulated using a semi-definite programming (SDP) model and solved by the interior point method. A zero-duality SDP model based on the Lagrange dual of the ACOPF problem was proposed in [61]. For the zero-duality to hold, small modifications to the original systems may be needed. Studies including branch flow model [62] and branch-and-bound algorithms [63] have been conducted recently to further explore the zero-duality feature. Compared to the DC model, the models presented in the above work provide better approximations to the ACOPF model. However, these models are still incomplete and require further investigations. For example, the zero-duality may not hold when certain constraints, such as line flow or lower bounds on reactive power generation, are enforced [64]-[65]. In addition, these models are complicated and may not be easily extended to other applications such as transmission expansion planning. This chapter develops a relaxed OPF model based on a

Taylor series. The proposed model provides a better approximation to the AC network by retaining reactive power, off-nominal bus voltage magnitudes as well as network losses.

The rest of this chapter is organized as follows: Section 5.2 presents the relaxed ACOPF model. Section 5.3 investigates the loss model and its relaxations. Simulation results are presented in Section 5.4. Conclusions are drawn in Section 5.5.

5.2 The Relaxed ACOPF Model

The proposed relaxed ACOPF model is derived in this section. The model is based on the following assumptions:

- All bus voltage magnitudes are close to 1.0 p.u.
- The angle difference across a branch is small so that $\sin(\theta_k) \approx \theta_k$ and $\cos(\theta_k) \approx 1$ can be applied.

Similar to the standard ACOPF model, the proposed relaxed ACOPF model takes the following form:

$$\min \ f(\mathbf{x}) \tag{5.1}$$

subject to

$$\mathbf{h}(\mathbf{x}) = \mathbf{c} \tag{5.2}$$

$$\mathbf{g}(\mathbf{x}) \le \mathbf{b} \tag{5.3}$$

$$x^{\min} \le x \le x^{\max} \tag{5.4}$$

$$\mathbf{x} = \left(PG_g, QG_g, V_i, \theta_i \right)^T .$$

In the above model, bold-faced variables refer to vectors. The objective function (5.1) is the summation of the quadratic cost functions of each generator and has the following form:

$$C_g\left(PG_g\right) = a_g PG_g^2 + b_g PG_g + c_g\,. \tag{5.5}$$

The equality constraints (5.2), which are further elaborated in (5.6) and (5.7), represent the active and reactive power balance equations at every bus. The variables after the colon represent the associated dual variables. The terms corresponding to network losses PL_k and QL_k are explicitly added to the nodal balance equations. Define bus i and bus j to be the "from" bus and the "to" bus of branch k. The losses on the branch are split in half and attached to the two terminal buses as shown in Fig. 5.1. The expressions of PL_k and QL_k will be elaborated further in Section 5.3,

$$\sum_{g\in i} PG_g + \sum_{k\in i} P_k - \sum_{k\in i}\left(0.5PL_k\right) = \sum_{d\in i} PD_d \quad :\lambda_i \tag{5.6}$$

$$\sum_{g\in i} QG_g + \sum_{k\in i} Q_k - \sum_{k\in i}\left(0.5QL_k\right) = \sum_{d\in i} QD_d \quad :\eta_i \tag{5.7}$$

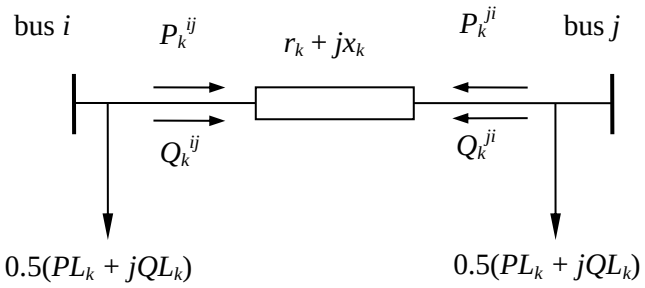

Fig. 5.1. Modeling of network losses as bus fictitious demands

Inequality constraints (5.3) represent the power flow limit on each branch:

$$P_k^2 + Q_k^2 \le (S_k^{\max})^2\,. \tag{5.8}$$

Notice that (5.8) is a set of second order cone constraints. This type of constraint is still convex and can be handled by linear solvers such as Gurobi. Neglecting the effects of off-nominal transformer turns ratios and phase shifters yield the full AC power flow through branch k as follows,

$$P_k = V_i^2 g_k - V_i V_j \left(g_k \cos\theta_k + b_k \sin\theta_k \right) \tag{5.9}$$

$$Q_k = -V_i^2 \left(b_k + b_{k0} \right) + V_i V_j \left(b_k \cos\theta_k - g_k \sin\theta_k \right). \tag{5.10}$$

Rewriting the bus voltage magnitude as,

$$V_i = 1 + \Delta V_i . \tag{5.11}$$

Based on the assumptions, ΔV_i is expected to be small. Substituting (5.11) into (5.9) and (5.10) and neglecting higher order terms,

$$P_k \approx \left(1 + 2\Delta V_i\right) g_k - \left(1 + \Delta V_i + \Delta V_j\right)\left(g_k + b_k \theta_k \right) \tag{5.12}$$

$$Q_k \approx -\left(1 + 2\Delta V_i\right)\left(b_k + b_{k0} \right) + \left(1 + \Delta V_i + \Delta V_j\right)\left(b_k - g_k \theta_k \right). \tag{5.13}$$

Notice that (5.12) and (5.13) still contain nonlinearities. However, since ΔV_i, ΔV_j and θ_k are expected to be small, the products $\Delta V_i \theta_k$ and $\Delta V_j \theta_k$ can be treated as second order terms and hence negligible. Therefore, the linearized power flow through branch *k* metered at bus *i* are obtained as follows,

$$P_k = \left(\Delta V_i - \Delta V_j \right) g_k - b_k \theta_k \tag{5.14}$$

$$Q_k = -\left(1 + 2\Delta V_i\right) b_{k0} - \left(\Delta V_i - \Delta V_j \right) b_k - g_k \theta_k . \tag{5.15}$$

The bounds on variables (5.4) include upper and lower limits on bus voltage magnitudes and angles as well as the generator active and reactive outputs,

$$\Delta V_i^{\min} \le \Delta V_i \le \Delta V_i^{\max} \tag{5.16}$$

$$-\theta^{\max} \le \theta_k \le \theta^{\max} \tag{5.17}$$

$$PG_g^{\min} \le PG_g \le PG_g^{\max} \tag{5.18}$$

$$QG_g^{\min} \le QG_g \le QG_g^{\max} . \tag{5.19}$$

The complete relaxed ACOPF model is described by (5.5)-(5.8) and (5.14)-(5.19).

5.3 Network Losses Modeling

As shown in (5.6) and (5.7), the network losses can be included in the proposed model. This section derives the network losses PL_k and QL_k and investigates the possible relaxations. Applying the second order approximation of $\cos\theta_k$ and neglecting high order terms, the active and reactive network losses can be approximated as,

$$PL_k \approx g_k \theta_k^2 \tag{5.20}$$

$$QL_k \approx -b_k \theta_k^2 . \tag{5.21}$$

Notice that (5.20) and (5.21) are still nonconvex. The following two approaches are developed to render them convex.

5.3.1 Piecewise Linearized Relaxation

The piecewise linearized model is to approximate θ_k^2 by a series of linear blocks. Since (5.20) and (5.21) are nonconvex, certain line losses in the resultant linear model may fail to converge to the correct value and cause the "fictitious loss" problem as pointed out in [45] and [46]. The following MILP model introduces a series of binary variables to prevent the presence of the fictitious losses:

$$PL_k \approx g_k \sum_{l=1}^{L} k(l)\Delta\theta_k(l) \qquad :\gamma_k \tag{5.22}$$

$$QL_k \approx -b_k \sum_{l=1}^{L} k(l)\Delta\theta_k(l) \qquad :\omega_k \tag{5.23}$$

$$\theta_k = \theta_k^+ - \theta_k^- \qquad :\alpha_k \tag{5.24}$$

$$\sum_{l=1}^{L} \Delta\theta_k(l) = \theta_k^+ + \theta_k^- \qquad :\beta_k \tag{5.25}$$

$$-\Delta\theta_k(l) \le 0, \quad l = 1,...,L \qquad :\underline{\rho}_k^l \tag{5.26}$$

$$\Delta\theta_k(l) \le \theta^{\max}/L, \quad l = 1,...,L \qquad :\bar{\rho}_k^l \tag{5.27}$$

$$-\theta_k^+ \le 0 \qquad :\underline{\upsilon}_k \tag{5.28}$$

$$\theta_k^+ \le \delta_k \theta_k^{\max} \qquad :\bar{\upsilon}_k \tag{5.29}$$

$$-\theta_k^- \le 0 \qquad :\underline{\sigma}_k \tag{5.30}$$

$$\theta_k^- \le (1-\delta_k)\theta_k^{\max} \qquad :\bar{\sigma}_k \tag{5.31}$$

$$\Delta\theta_k(l) \le \Delta\theta_k(l-1), \quad l = 2,...,L \tag{5.32}$$

$$\theta^{\max}/L - \Delta\theta_k(l-1) \le u_k(l-1)\theta^{\max}/L, \quad l = 2,...,L \tag{5.33}$$

$$\Delta\theta_k(l) \le \left[1-u_k(l-1)\right]\theta^{\max}/L \quad l = 2,...,L \tag{5.34}$$

$$k(l) = (2l-1)\,\theta^{\max}/L\,.$$

In (5.24), θ_k is replaced by slack variables θ_k^+ and θ_k^-. Binary variable δ_i together with (5.28) to (5.31) ensures the right-hand side of (5.25) equals the absolute value of θ_k, *i.e.*, at most one of θ_k^+ and θ_k^- can be nonzero. Constraints (5.32)-(5.34) guarantee that the linear block on the left will always be filled up first to eliminate fictitious losses. The piecewise linearization is illustrated in Fig. 5.2.

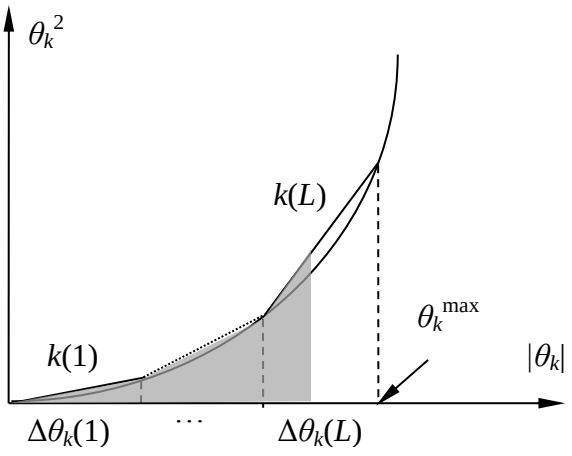

Fig. 5.2. Piecewise linearization of θ_k^2

The above MILP model eliminates the fictitious losses by adding the binary variables. These binary variables, however, could prevent the resultant model from being solved efficiently. In fact, the MILP model can be relaxed to the linear programming (LP) model that was presented in Section 3.3 by discarding the binary variables δ_k from (5.29) and (5.31) and retaining only (5.22)-(5.31). When certain conditions are met, this relaxation is exact. The conditions are investigated in the following. First, let $\mathcal{L}(\mathbf{x})$ be the Lagrangian function.

$$\mathcal{L}(\mathbf{x}) = f(\mathbf{x}) + \boldsymbol{\varphi}^T \left[\mathbf{c} - \mathbf{h}(\mathbf{x})\right] + \boldsymbol{\mu}^T \left[\mathbf{b} - \mathbf{g}(\mathbf{x})\right] \tag{5.35}$$

where, $\boldsymbol{\varphi}$ and $\boldsymbol{\mu}$ represent the Lagrange multipliers associated with the equality and inequality constraints respectively. Bounds on variables are converted to inequality constraints and included in $\mathbf{g}(\mathbf{x})$. The dual variables needed are given in (5.22) to (5.31). According to Lagrangian duality theory, the dual variables are non-positive for "$\leq$" constraints, and are free of sign restriction for equality constraints. All terms are moved to the right-hand side of the constraints. The optimality condition requires the following constraints hold simultaneously,

$$\partial\mathcal{L}/\partial PL_k = 0.5(\lambda_i + \lambda_j) - \gamma_k = 0 \tag{5.36}$$

$$\partial\mathcal{L}/\partial QL_k = 0.5(\eta_i + \eta_j) - \omega_k = 0 \tag{5.37}$$

$$\partial\mathcal{L}/\partial\Delta\theta_k(l) = (g_k\gamma_k - b_k\omega_k)k(l) - \beta_k + \underline{\rho}_k^l - \bar{\rho}_k^l = 0 \tag{5.38}$$

$$\partial\mathcal{L}/\partial\theta_k^+ = \alpha_k + \beta_k + \underline{\upsilon}_k - \bar{\upsilon}_k = 0 \tag{5.39}$$

$$\partial\mathcal{L}/\partial\theta_k^- = -\alpha_k + \beta_k + \underline{\sigma}_k - \bar{\sigma}_k = 0 \tag{5.40}$$

Theorem 1: If $(g_k\gamma_k - b_k\omega_k) > 0$, then the MILP model and the LP model are equivalent.

Proof: Without loss of generality, consider $\Delta\theta_k(l)$ to be the l^{th} linear block for θ_k where $1 < l < L$. If $0 < \Delta\theta_k(l) < \theta^{\max}/L$, then by complementary slackness (CS), (5.38) becomes:

$$(g_k\gamma_k - b_k\omega_k)k(l) = \beta_k . \tag{5.41}$$

Let $\Delta\theta_k(l - m)$ and $\Delta\theta_k(l + n)$ be any linear block before and after $\Delta\theta_k(l)$ respectively, where $1 \le m < l$ and $1 \le n \le (L - l)$, then for these two linear blocks, (5.38) gives:

$$(g_k\gamma_k - b_k\omega_k)k(l-m) = \beta_k - \underline{\rho}_k^{l-m} + \overline{\rho}_k^{l-m} \tag{5.42}$$

$$(g_k\gamma_k - b_k\omega_k)k(l+n) = \beta_k - \underline{\rho}_k^{l+n} + \overline{\rho}_k^{l+n} . \tag{5.43}$$

Provided the OPF model is feasible, (5.41)-(5.43) must have a solution. Since $(g_k\gamma_k - b_k\omega_k) > 0$ and $k(L) > k(l) > 0$, by CS, $\underline{\rho}_k^{l-m} = \overline{\rho}_k^{l+n} = 0$. This indicates that any linear block before $\Delta\theta_k(l)$ must be at its upper bound, *i.e.*, $\Delta\theta_k(l - m) = \theta^{\max}/L$ and any linear block after $\Delta\theta_k(l)$ must be at its lower bound, *i.e.*, $\Delta\theta_k(l + n) = 0$. Referring to Fig. 5.2, the linear blocks will be filled continuously starting with the leftmost one.

Equation (5.41) shows that $\beta_k > 0$. By CS, it can be observed from (5.39) and (5.40) that if either θ_k^+ or θ_k^- is nonzero, then the other must be at its lower bound, *i.e.*, zero. This indicates that θ_k is either equal to θ_k^+ or $-\theta_k^-$ depending on the sign of θ_k. Hence, *Theorem 1* is proved. ■

For the piecewise linearized model, *Theorem 1* provides an approach to identify the branches where the fictitious losses may be created. Binary variables are needed only for these branches instead of all the branches in the system. Additionally, if the model only considers active power constraints, the following corollary can be derived:

Corollary 1: For an OPF model that only considers active power constraints, if the sum of the locational marginal price (LMP) at two terminal buses of a branch is positive, then the LP relaxation is exact.

Proof: LMPs are the dual variables associated with the active power nodal balance constraints, *i.e.*, λ_i. If reactive power is neglected, then the term $-b_k\omega_k$ will drop out from (5.38). From (5.36), it is clear that γ_k is positive. If $g_k > 0$, then $g_k\gamma_k > 0$ and according to *Theorem 1*, the LP relaxation is exact. If $g_k = 0$, then the active power loss for that branch is always zero. Hence, *Corollary 1* is proved. ■

5.3.2 Quadratic Inequality Relaxation

If reactive power losses are neglected, *i.e.*, (5.21) is removed, then (5.20) can be relaxed using the following inequality constraint,

$$PL_k \geq g_k\theta_k^2 \qquad :\gamma_k . \tag{5.44}$$

This inequality relaxation is exact when (5.44) is binding. The following condition needs to be satisfied.

Theorem 2: If the sum of the LMPs at the two terminal buses of a branch is positive, then (5.44) is binding.

Proof: Let $\mathcal{L}$ be the Lagrangian function and consider (5.44), then (5.36) can be rewritten as:

$$\partial\mathcal{L}/\partial PL_k = 0.5(\lambda_i + \lambda_j) - \gamma_k = 0 \tag{5.45}$$

In (5.45), it is easy to show that if $(\lambda_i + \lambda_j)$ is greater than zero, then γ_k must be great than zero as well. By CS, (5.44) must be binding. ■

5.4 Case Studies

The proposed model and its relaxations are evaluated in this section. All models are programmed in AMPL. The solvers used are Gurobi. The computer used for simulation has an Intel E8500 CPU with 3.2 GB of RAM.

First, a case is presented to illustrate *Theorem 1*. The test system is constructed based on the IEEE 24-bus RTS system [57] with modified generator cost data to create fictitious losses. The OPF is solved using the relaxed LP loss model presented in Section 5.3. The LMP is positive at every bus. The $(g_k\gamma_k - b_k\omega_k)$ value of each branch is plotted in Fig. 5.3. As one can observe from the figure, $(g_k\gamma_k - b_k\omega_k)$ values of all the branches are positive except for branch 16, which is zero. According to *Theorem 1*, the LP relaxation should be exact and no fictitious losses should be created except for branch 16. The active power loss for each branch is plotted in Fig. 5.4 using (5.20) and (5.22) respectively. In the figure, fictitious losses are observed at branch 16. This is because with $(g_{16}\gamma_{16} - b_{16}\omega_{16})$ equals to zero, the piecewise linear model fails to select the correct linear blocks for branch 16 and causes excessive losses which will not be observed in reality. For other branches, since $(g_k\gamma_k - b_k\omega_k) > 0$, the LP relaxation is exact and therefore no fictitious loss is created.

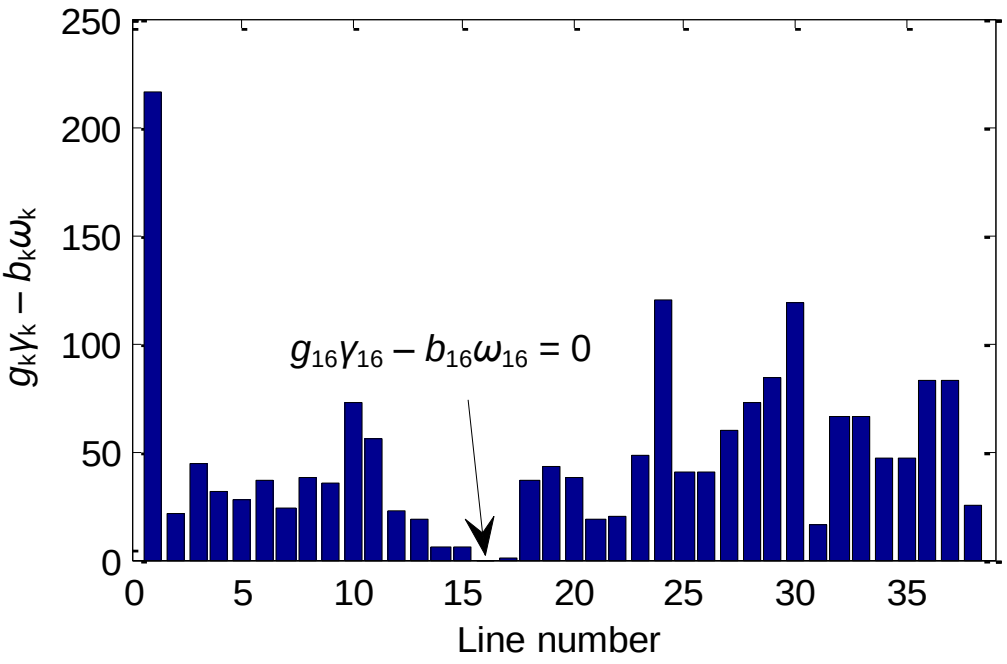

Fig. 5.3. $(g_k\gamma_k - b_k\omega_k)$ value of each branch

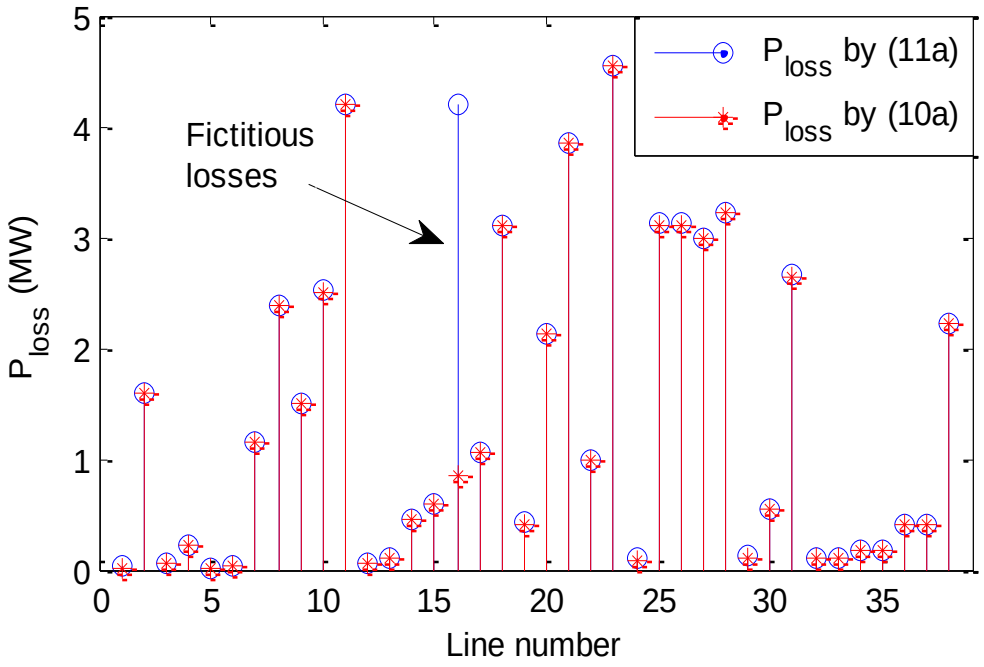

Fig. 5.4. Active power loss of each branch

As shown in the Table 5.1, the LP model creates 8.9 MW fictitious losses at branch 16, whereas the full MILP model and the reduced MILP model are free of fictitious losses. In terms of simulation time, the LP model is the fastest among the three models, which is solved in less than 0.1 s. The full MILP model is solved in 2.3 s and this time is reduced by 35% if the reduced MILP model is used.

Table 5.1. Comparison of different loss models

Loss model[1]	Problem Type[2]	Fictitious losses (MW)	Simulation time (s)
Full MILP	MISOCP	0	2.3
Reduced MILP	MISOCP	0	1.5
LP	SOCP	8.9 (at branch 16)	< 0.1

1. Full MILP model: binary variables are added for every branch.
   Reduced MILP model: binary variables are only added to branches with $(g_k\gamma_k - b_k\omega_k) = 0$
2. MISOCP: Mixed-integer second order cone programming.
   SCOP: Second order cone programming

The proposed model and its relaxations are also applied to multiple test cases [66] and the results are reported in Table 5.2. The number of linear blocks used is 40. It can be observed that for all test cases, the optimal solutions obtained from the proposed model provide good approximations to the full ACOPF solutions. The proposed model is also computationally efficient compared to solving the full ACOPF model.

Table 5.2. Performance comparison of the proposed models

Test cases	Piecewise linearized loss model			Quadratic inequality loss model		
	Objective	*Gap*†(%)	*Time* (s)	*Objective*	*Gap*†(%)	*Time* (s)
IEEE 14	8067	0.2	0.06	8094	0.3	0.06
IEEE 24	63397	0.07	0.11	63352	$< 10^{-6}$	0.09
IEEE 39	41876	0.03	0.17	41861	< 0.01	0.16
IEEE 57	41497	0.6	0.27	41448	0.7	0.22
IEEE 118	129612	0.04	0.55	129471	0.1	0.52
IEEE 300	718549	0.2	1.74/2.8 (AC)	718227	0.3	2.37
3120SP	1646320	0.2	70.2/154 (AC)	/	/	/

† *Gap* is the percentage mismatch between the objective values given by the proposed models and the full ACOPFs solution using MATPOWER [66].

5.5 Summary

This chapter develops a relaxed OPF model based on a Taylor series. The proposed model retains the reactive power, off-nominal bus voltage magnitudes as well as network losses. A MILP-based loss model is developed to eliminate the fictitious losses. Relaxations of the MILP model are investigated. It is proved that the relaxations are exact if the system meets certain specified conditions. Based on the results in this paper, the following conclusions are drawn:

- In the piecewise linear model, the branches that may create fictitious losses can be identified. Binary variables are only needed for these branches instead of all the branches in the system.
- In the piecewise linearization model, even if the all the LMPs are positive, the fictitious losses may still be present if the reactive power losses are considered.
- If reactive power losses are neglected, then the quadratic inequality relaxation is exact for active power losses.
- Inclusion of reactive power and the off-nominal bus voltage magnitudes improves the model accuracy. The proposed model is computationally efficient and provides a better approximation to the full ACOPF model.

Chapter 6

TRANSMISSION EXPANSION PLANNING USING THE RELAXED AC MODEL

6.1 Chapter Overview

It has been widely acknowledged that there is a "gap" between the solutions obtained from the DC model and the AC model [58]. In some cases, the gap could be large enough to result in a TEP solution that is problematic in the AC network. On the other hand, it is still extremely challenging to solve a TEP problem using the AC model. This chapter extends the relaxed ACOPF model developed in Chapter 5 to TEP studies and proposes a novel TEP model (LACTEP) that includes a linear representation of reactive power, off-nominal bus voltage magnitudes and network losses. An iterative approach for considering the $N-1$ criterion during the planning process is also developed and demonstrated on the test system.

The remainder of this chapter is organized as follows: Section 6.2 presents the mathematical formulation of the LACTEP model. The modeling of $N-1$ criterion is investigated in Section 6.3. In Section 6.4, the proposed LACTEP model is validated and compared with other existing models. Concluding remarks are given in Section 6.5.

6.2 Mathematical Formulation of the LACTEP Model

Based on the linearized network model presented in Chapter 5, the mathematical formulation of the LACTEP model is presented in this section. It is assumed that the planners have perfect information about the existing network as well as the parameters of the potential lines. The planning work is carried out at the peak loading hour for a single future scenario. In real world applications, however, multiple scenarios can be developed

to account for uncertainties and a two-stage stochastic programming planning model can be readily formulated using the LACTEP model proposed in this paper.

6.2.1 Objective Function

The objective function used in this paper jointly minimizes the investment cost and the total operating cost,

$$\min\ C = \sum_{k\in\Omega_k^+} \frac{c_k z_k}{(1+d)^{TP-1}} + \sum_{t=TP}^{TP+TO} \sum_{g\in\Omega_g} \frac{8760 CF_{gt} CG_{gt}}{10^6 (1+d)^{t-1}}. \tag{6.1}$$

In (6.1), the first term represents the line investment cost and the second term corresponds to the total operating cost over a time horizon scaled by the generator capacity factor, both in M$ and are discounted to the present value. Notice that the scaled operating cost provides only an estimate of the true operating cost, and can be replaced by a more accurate production cost model if the yearly load profile is available. As implied by the planning timeline in Fig. 6.1, all the selected lines are committed in the targeted planning year, and the operating costs are evaluated over multiple years thereafter. In reality, it is difficult to control the choice of the line to be built in a particular year over the planning horizon. Issues such as project review process, construction and the load forecast accuracy could bring too many uncertainties and make the dynamic planning process intractable. This TEP model presented in this chapter is based on a static planning framework and focuses only on the large economic impact of the TEP project. Thus, the incremental economic benefit is lumped into the single targeted planning year.

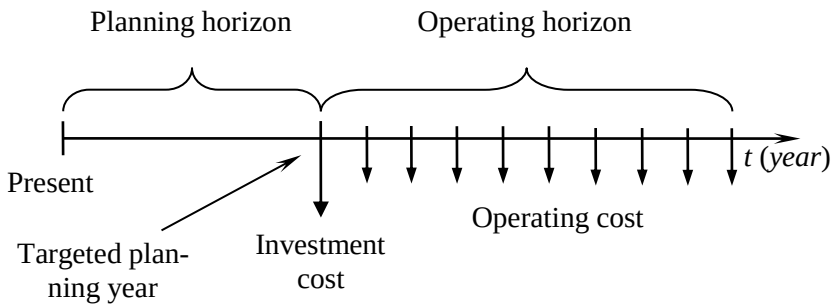

Fig. 6.1. Typical transmission planning timeline

6.2.2 Power Flow Constraints

In order to build the TEP model, the linearized power flow equations derived in Chapter 5 need to be reformulated. The constraints set related to the power flow equations in the LACTEP model are shown as follows,

$$P_k = \left(\Delta V_i - \Delta V_j\right) g_k - b_k \theta_k \quad \forall k \in \Omega_k \tag{6.2}$$

$$Q_k = -\left(1 + 2\Delta V_i\right) b_{k0} - \left(\Delta V_i - \Delta V_j\right) b_k - g_k \theta_k \quad \forall k \in \Omega_k \tag{6.3}$$

$$\left(z_k - 1\right) M \le P_k - \left(\Delta V_i - \Delta V_j\right) g_k + b_k \theta_k \le \left(1 - z_k\right) M \quad \forall k \in \Omega_k^+ \tag{6.4}$$

$$\left(z_k - 1\right) M \le Q_k + \left(1 + 2\Delta V_i\right) b_{k0} + \left(\Delta V_i - \Delta V_j\right) b_k + g_k \theta_k \le \left(1 - z_k\right) M \quad \forall k \in \Omega_k^+ \tag{6.5}$$

$$-z_k S_k \le P_k \le z_k S_k \quad \forall k \in \Omega_k^+ \tag{6.6}$$

$$-z_k S_k \le Q_k \le z_k S_k \quad \forall k \in \Omega_k^+ \tag{6.7}$$

$$P_k^2 + Q_k^2 \le (S_k^{\max})^2 \quad \forall k \in \Omega_k \cup \Omega_k^+ \tag{6.8}$$

$$-\theta^{\max} \le \theta_k \le \theta^{\max} \quad \forall k \in \Omega_k \tag{6.9}$$

$$\left(z_k - 1\right) \pi - \theta^{\max} \le \theta_k \le \left(1 - z_k\right) \pi + \theta^{\max} \quad \forall k \in \Omega_k^+ . \tag{6.10}$$

Constraints (6.2)-(6.5) represent the linearized power flow equations for existing lines and prospective lines. For existing lines, the power flow equations are given by

(6.2) and (6.3). For prospective lines, the disjunctive constraints (6.4)-(6.5) are used to avoid the nonlinearity that would otherwise appear. The power flow on the potential lines is forced to be zero by (6.6) and (6.7) if the line is not selected. The line MVA flow is limited by (6.8). Constraints (6.9) and (6.10) put a limit on the phase angle difference across existing lines and prospective lines respectively. If the two buses are directly connected, then θ_k is limited by $\theta^{\max}$ and $-\theta^{\max}$; otherwise, (6.10) is not binding.

6.2.3 Network Losses

The following constraint set extends the concept of linearized loss modeling to the proposed TEP model,

$$\theta_k = \theta_k^+ - \theta_k^- \quad \forall k \in \Omega_k \cup \Omega_k^+ \tag{6.11}$$

$$\sum_{l=1}^{L} \Delta\theta_k(l) = \theta_k^+ + \theta_k^- \quad \forall k \in \Omega_k \cup \Omega_k^+ \tag{6.12}$$

$$0 \le \theta_k^+ \le \delta_k \theta^{\max} \quad \forall k \in \Omega_k \tag{6.13}$$

$$0 \le \theta_k^- \le (1-\delta_k)\theta^{\max} \quad \forall k \in \Omega_k \tag{6.14}$$

$$0 \le \theta_k^+ \le \delta_k \theta^{\max} + (1-z_k)\pi \quad \forall k \in \Omega_k^+ \tag{6.15}$$

$$0 \le \theta_k^- \le (1-\delta_k)\theta^{\max} + (1-z_k)\pi \quad \forall k \in \Omega_k^+ \tag{6.16}$$

$$0 \le \Delta\theta_k(l) \le \theta^{\max}/L \quad \forall k \in \Omega_k \tag{6.17}$$

$$0 \le \Delta\theta_k(l) \le \theta^{\max}/L + (1-z_k)\pi/L \quad \forall k \in \Omega_k^+ \tag{6.18}$$

$$PL_k = g_k \sum_{l=1}^{L} k(l)\Delta\theta_k(l) \quad \forall k \in \Omega_k \tag{6.19}$$

$$QL_k = -b_k \sum_{l=1}^{L} k(l)\Delta\theta_k(l) \quad \forall k \in \Omega_k \tag{6.20}$$

$$0 \le PL_k \le z_k g_k (\theta^{\max})^2 \quad \forall k \in \Omega_k^+ \tag{6.21}$$

$$0 \le -PL_k + g_k \sum_{l=1}^{L} k(l)\Delta\theta_k(l) \le (1 - z_k) M \quad \forall k \in \Omega_k^+ \tag{6.22}$$

$$0 \le QL_k \le -z_k b_k (\theta^{\max})^2 \quad \forall k \in \Omega_k^+ \tag{6.23}$$

$$0 \le -QL_k - b_k \sum_{l=1}^{L} k(l)\Delta\theta_k(l) \le (1 - z_k) M \quad \forall k \in \Omega_k^+ \tag{6.24}$$

$$\Delta\theta_k(l) \le \Delta\theta_k(l-1) \quad \forall k \in \Omega_k \cup \Omega_k^+ \tag{6.25}$$

$$\theta^{\max}/L - \Delta\theta_k(l-1) \le u_k(l-1)\theta^{\max}/L \quad \forall k \in \Omega_k \tag{6.26}$$

$$z_k\theta^{\max}/L - \Delta\theta_k(l-1) \le u_k(l-1)\theta^{\max}/L \quad \forall k \in \Omega_k^+ \tag{6.27}$$

$$\Delta\theta_k(l) \le [1 - u_k(l-1)]\theta^{\max}/L \quad \forall k \in \Omega_k \cup \Omega_k^+ \tag{6.28}$$

$$k(l) = (2l-1)\,\theta^{\max}/L \quad \forall k \in \Omega_k \cup \Omega_k^+ .$$

Constraints (6.13)-(6.16) ensure that the right hand side of (6.12) equals $|\theta_k|$ for existing lines and the selected prospective lines respectively. Constraints (6.17) and (6.18) determine the upper and lower bound of a linear block $\Delta\theta_k(l)$ for existing lines and prospective lines respectively. For existing lines and the selected prospective lines, $\Delta\theta_k(l)$ is bounded by zero and $\theta^{\max}/L$, otherwise, (6.18) is not binding. The active and reactive power losses for existing lines are given by (6.19) and (6.20) respectively. For prospective lines, the active and reactive power losses are determined by (6.21)-(6.22) and (6.23)-(6.24) respectively. Constraints (6.25)-(6.28) guarantee that the linear blocks on the left will be filled up first. Constraints (6.12)-(6.28) present a full MILP formulation that linearizes the network losses rigorously without generating fictitious losses. Relaxed models can be formed by removing (6.25)-(6.28) or even (6.13)-(6.16).

The linearized line losses are then split in half and attached to the two terminal buses as "virtual demands". The terms corresponding to the network losses are added to the nodal balance equations as follows,

$$\sum_{g\in i} PG_g + \sum_{k\in i} P_k - \sum_{k\in i} \left(0.5PL_k\right) = \sum_{d\in i} PD_d \tag{6.29}$$

$$\sum_{g\in i} QG_g + \sum_{k\in i} Q_k - \sum_{k\in i} \left(0.5QL_k\right) = \sum_{d\in i} QD_d \ . \tag{6.30}$$

6.2.4 Generator Capacity Limits

In the planning study, all the generators in the system are assumed to be on-line. The generator outputs are limited by their minimum and maximum generating capacities as shown in (6.31) and (6.32). Unit commitment is regarded as an operational problem and is therefore not considered in this model. The generator limits are,

$$PG_g^{\min} \le PG_g \le PG_g^{\max} \quad \forall g \in \Omega_g \tag{6.31}$$

$$QG_g^{\min} \le QG_g \le QG_g^{\max} \quad \forall g \in \Omega_g \ . \tag{6.32}$$

The complete LACTEP model is described by (6.1)-(6.32).

6.3 The N – 1 Modeling

The computational burden is a major concern in MIP problems. Typically, increasing the number of binary variables could potentially slow the solution process. Therefore, the candidate line set should be carefully selected and only the applicable transmission corridors should be included. With a large-scale MIP problem, the solver may have trouble finding an initial feasible solution. In this case, providing a feasible starting point will help reduce the overall simulation time.

The $N-1$ contingency modeling is another major source of the computational burden. In fact, a complete $N-1$ analysis in the TEP model for a well-designed power system is generally unnecessary because the number of contingencies that will cause serious overloads is generally limited. The $N-1$ modeling approach used in [11] was to explicitly invoke the set of network constraints for all possible operating conditions and satisfy all the constraints when solving the optimization problem. However, the model presented in this paper is more complicated. If the approach in [11] were used, the size of the problem could easily become too large to be solvable. Moreover, the TEP problem uses only a relaxed network model, which means that the solution that satisfies the $N-1$ criterion in the TEP model may not represent the actual case in the AC network. In order to make the planned system comply with the $N-1$ criterion without imposing too much computational burden, an iterative approach is proposed in Fig. 6.2.

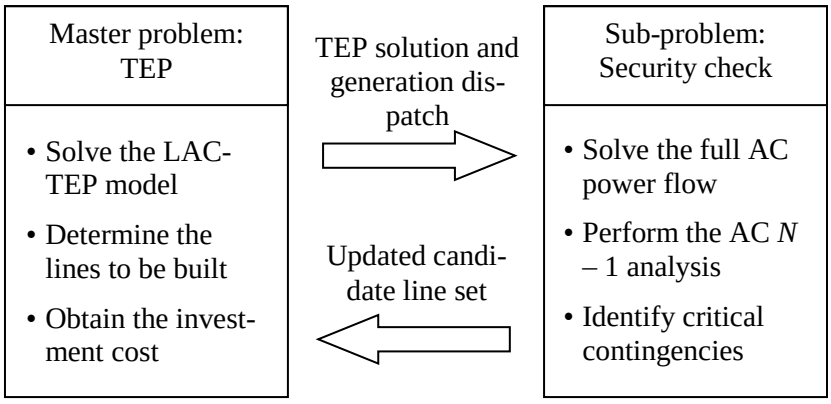

Fig. 6.2. The iterative approach for the $N-1$ contingency modeling

Using the approach in Fig. 6.2, the original problem is decomposed into a *master problem*, which solves the optimization model and a *sub-problem*, which verifies the network security. The master problem passes the TEP solution and the generator dispatch to the sub-problem, while the sub-problem passes the network violations back to the

master problem. The approach solves the two problems iteratively until there is no violation or all the violations identified in the sub-problem are within preset limits.

6.4 Case Studies

In this section, Garver's 6-bus system and the IEEE 118-bus system are studied and the simulation results are demonstrated. The work presented in this dissertation is programmed using AMPL. The DC lossless, DC lossy and the LACTEP models are solved by Gurobi. The ACTEP models are solved by Knitro. PowerWorld [66] is used for AC power flow and the $N-1$ contingency analysis. All simulations are done on a Linux workstation with an Intel *i*7-2600, 4-core CPU @ 3.40 GHz with 16 GB of RAM.

6.4.1 Garver's 6-bus System

Garver's 6-bus system has 6 existing lines, 5 loads and 3 generators Initially, the generator connected at bus 6 is isolated from the main system. The system parameters are listed in Tables 6.1 and 6.2. It is assumed that at most 3 lines are allowed in each transmission corridor. The total number of candidate lines is 39. The objective function is to minimize the line investment cost **only**. The bus voltage magnitude range is 1 – 1.05 p.u. The following two cases are analyzed:

- **Case 1:** Compare the TEP solutions given by the LACTEP model and other existing models.
- **Case 2:** Network losses sensitivity analysis.

Table 6.1. Candidate line data for Garver's 6-bus system

Corridor	r_k (p.u.)	x_k (p.u.)*	Capacity (MW)	Cost (M$)
1 – 2	0.04	0.4	100	40
1 – 3	0.038	0.38	100	38
1 – 4	0.06	0.6	80	60
1 – 5	0.02	0.2	100	20
1 – 6	0.068	0.68	70	68
2 – 3	0.02	0.2	100	20
2 – 4	0.04	0.4	100	40
2 – 5	0.031	0.31	100	31
2 – 6	0.03	0.3	100	30
3 – 4	0.059	0.59	82	59
3 – 5	0.02	0.2	100	20
3 – 6	0.048	0.48	100	48
4 – 5	0.063	0.63	75	63
4 – 6	0.03	0.3	100	30
5 – 6	0.061	0.61	78	61

*100 MVA base

Table 6.2. Generator and load data for Garver's 6-bus system

Bus No.	Load parameters		Generator parameters			
	PD (MW)	*QD* (MVAr)	PG^{min} (MW)	PG^{max} (MW)	QG^{min} (MVAr)	QG^{max} (MVAr)
1	80	16	0	160	-10	65
2	240	48				
3	40	8	0	360	-10	150
4	160	32				
5	240	48				
6			0	610	-10	200

Case 1: In this case, the TEP solution obtained from the LACTEP model is compared with the solutions obtained from other available TEP models. The full MILP approach is used for modeling the network losses. The number of linear blocks is 7. The comparison results are shown in Table 6.3.

Table 6.3. TEP results comparison of Garver's system

TEP model	Expansion plan	Investment cost (M$)	Comments
DC lossless	(3-5), (4-6)×3	110	Need additional reactive power to make the AC power flow converge. Overloads and undervoltage issues are detected.
DC lossy	(2-6)×3, (3-5)×2	130	
LACTEP	(2-3), (2-6)×2, (3-5)×2, (4-6)×3	210	No additional reactive power needed. All indices are within limits.
ACTEP	(2-6)×3, (2-3), (3-5)×2, (4-6)×3, (2-5)×2	302[1]	

[1]The ACTEP is a non-convex global optimization problem. The result shown in the table is the best solution after five thousand restarts.

The two DC-based TEP models in Table 6.3 seem to be superior in the sense that the investment costs are less. However, the reactive power needed for these two models in the AC network actually exceeds the amount that the three generators can supply. In order to make the AC power flow converge, an additional 189 MVAr and 129 MVAr are needed for the lossless and the lossy DC model respectively. Meanwhile, overloads and under voltage issues are observed in the system, which require additional investment for network reinforcement. The solution obtained from the LACTEP model requires building more lines than the DC-based models do, but needs no additional reactive power and there are no overloads and undervoltage problems in the AC power flow. The expanded Garver's system with all indices within the preset limits is plotted in Fig. 6.3.

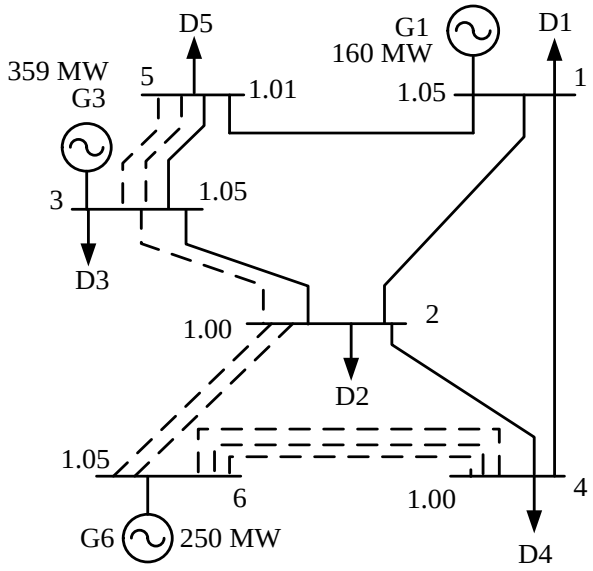

Fig. 6.3. The TEP results of Garver's 6-bus system

As a non-convex global optimization problem, multiple starting points are tried to obtain a good solution for the ACTEP model. As shown in Table 6.3, the best objective value for the ACTEP model after five thousand restarts is still much higher than the objective function given by the LACTEP model. It will also be computationally too expensive to apply the ACTEP model to larger power system planning problems. This comparison reveals that the solutions given by the DC-based TEP models may not represent the actual case in the AC network and additional network reinforcement is likely to be needed. The LACTEP model better approximates the AC network and therefore provides a more realistic TEP solution.

For small systems such as the 6-bus example, reactive power can be a critical issue to make the AC power flow converge. As indicated by Table 6.3, the LACTEP model chooses to build more lines to provide reactive power support. In reality, increasing generator reactive power capacity and installing VAr support devices can certainly be considered as alternative solutions if a DC-based TEP solution is adopted,

but one should be aware that it may not be easy to increase reactive power capacity of existing generators, and can be costly to install VAr support devices at high voltage buses. For real world applications, different solution options can be compared to find the most cost effective TEP plan. For larger systems with more meshed topology, the value of the LACTEP model is that it dispatches the generators more accurately, gives a better estimation of the line flows, and provides a realistic TEP solution which the DC-based models usually fail to do.

Case 2: As discussed in Section 6.2, the linearized network losses can be rigorously modeled using the MILP formulation. However, addition of the binary variables also increases the complexity of the TEP model. The number of linear blocks can significantly affect the solution time as well as the model accuracy. Table 6.4 shows how the number of linear blocks changes the size of the problem and the TEP solution. The full MILP formulation is used for the results shown in Table 6.4.

Table 6.4. The effects of number of linear blocks

Linear blocks	Variable types		Objective (M$)	Total *P* losses (MW)	Time (s)
	Continuous	Binary			
1	281	84	Infeasible	/	/
2	323	126	378	16.3	> 413
3	407	171	259	11.8	69
4	449	213	230	8.8	97
5	489	253	230	8.7	33
6	579	298	230	8.2	89
7	**621**	**340**	**210**	**8.2**	**34**
8	666	385	210	8.2	43
9	708	427	210	8.2	116
10	748	467	210	8.2	97

The variable types in Table 6.4 show that the size of the problem increases as the number of linear blocks increases. This behavior coincides with the intuition that more variables are needed to model the additional linear blocks. It should be noted that the linearization intrinsically overestimates the losses in the system. If too few linear blocks are used, e.g., 1, then the overestimation can be significant and the problem will be infeasible with the given set of candidate line set. This is reflected from both the trends of losses and the objective values listed in Table 6.4. It is worth noticing that due to the mixed-integer nature of the problem, the change in solution time does not follow a linear pattern. When too few linear blocks are used, the TEP results may contain unnecessary lines due to the significant overestimation of the network losses. It may also take a long time to branch out an initial feasible solution. On the other hand, too many linear blocks will impose unnecessary computational burden and slow the solution time. The key idea of the study is to find the number of linear blocks that gives the best balance between the model accuracy and the solution time. In this case, 7 is an appropriate number.

The results contained in Table 6.5 compare the accuracy of the relaxed losses models and the solution time. The number of linear blocks used for this study is 7. Among all the loss modeling approaches listed in Table 6.5, the full MILP formulation is the most accurate and serves as a basis of the study. The *R*1 approach relaxes the constraints for prioritizing the lower linear blocks. This approach reduces the solution time by approximately 41%, but the drawback is that it creates 2.4 MW fictitious active power losses. The *R*2 approach relaxes the constraints for modeling the absolute value. It reduces the solution time by approximately 35%, and creates only 0.2 MW fictitious losses. The *R*3 approach relaxes both the constraints that were relaxed in *R*1 and *R*2. It

reduces the solution time by approximately 38%, but creates 2.5 MW fictitious losses. Additionally, if losses are ignored, the solution time will be significantly reduced by 91%, but the TEP solution no longer satisfies preset the voltage requirement. Except for the no loss case, the TEP solutions remain the same for all other loss modeling approaches. One explanation is that the impact of fictitious losses is not significant enough to change the TEP results in this case. The study results show that the *R*2 approach is considered as the best trade-off between model accuracy and solution time.

Table 6.5. Comparison of different network losses models

Losses modeling approach[1]	Total *P* losses (MW)	Objective (M$)	Time (s)/Δ (%)
Full MILP	8.2	210	34/(0%)
Relaxation 1 (*R*1)	10.6	210	20/(-41%)
Relaxation 2 (*R*2)	8.4	210	22/(-35%)
Relaxation 3 (*R*3)	10.7	210	21/(-38%)
Do not model losses[2]	0	150	3/(-91%)

[1]Full MILP: Use (6.1)-(6.32) to model the linearized network losses
Relaxation 1: Remove (6.25)-(6.28)
Relaxation 2: Remove (6.13)-(6.16)
Relaxation 3: Remove (6.13)-(6.16) and (6.25)-(6.28)
[2]Losses are not modeled, but r_k, Q and V are retained

6.4.2 The IEEE 118-bus System

The IEEE 118-bus system [50] is used to demonstrate the potential of applying the proposed LACTEP model to large power systems. The system has 186 existing branches, 54 generators and 91 loads. The line ratings are reduced to create congestions. The system is divided into three zones with the zonal data listed in Table 6.6. The load assumed is the peak loading level. The discount rate is assumed to be 10%, and the number of linear blocks used for loss modeling is 10. The planning horizon is ten years.

The objective function used in this case jointly minimizes the line investment cost and the scaled ten-year total operating cost. The average capacity factors published in [67] are used in this paper. The capital costs of transmission lines are assumed proportional to the length of the lines. Due to the absence of real data, all prospective lines are assumed to share the same corridor and have the same parameters as the existing lines. The planning criteria are given in Table 6.7. The detailed planning procedure is described in the following steps.

Table 6.6. Zonal data of the IEEE 118-bus system

	Bus	Branch	Generation (MW)	Load (MW)
Zone 1	42	62	2280	1865
Zone 2	48	81	4160	3125
Zone 3	28	43	2544	1271
Total	118	186	8884	6261

Table 6.7. TEP planning criterion for the IEEE 118-bus system

	Normal ($N-0$)	Contingency ($N-1$)
Voltage (p.u.)	$0.96 \leq V \leq 1.06$	$0.92 \leq V \leq 1.06$
Power flow	$P_k^2 + Q_k^2 \leq (S_k^{\max})^2$	$P_k^2 + Q_k^2 \leq (1.1S_k^{\max})^2$

- **Step 1:** Run a regular AC power flow on the system to be planned, and identify the lines that are overloaded or heavily loaded. These lines will form the initial candidate line set.
- **Step 2:** Use the candidate line set and run the LACTEP model. Obtain the TEP solution and update the system.
- **Step 3:** Rerun a regular AC power flow on the expanded system and identify any overloaded lines/transformers. Notice that it is still possible to observe

violations in this step because the network model used in the TEP problem is essentially a relaxation of the AC network model. If this happens, one should slightly reduce the line ratings used in the TEP problem and redo Step 2 to Step 3. If no violation is identified in this step, then proceed to Step 4.

- **Step 4:** Perform a complete $N-1$ analysis on the expanded system. Identify the worst contingency and take the line out of service. Form a new candidate line set and return to Step 2. Do this iteratively until all violations are within the preset threshold (as specified in Table 6.7). It is assumed that the generator dispatch do not change during this process.

The flowchart of the iterative approach is plotted in Fig. 6.4.

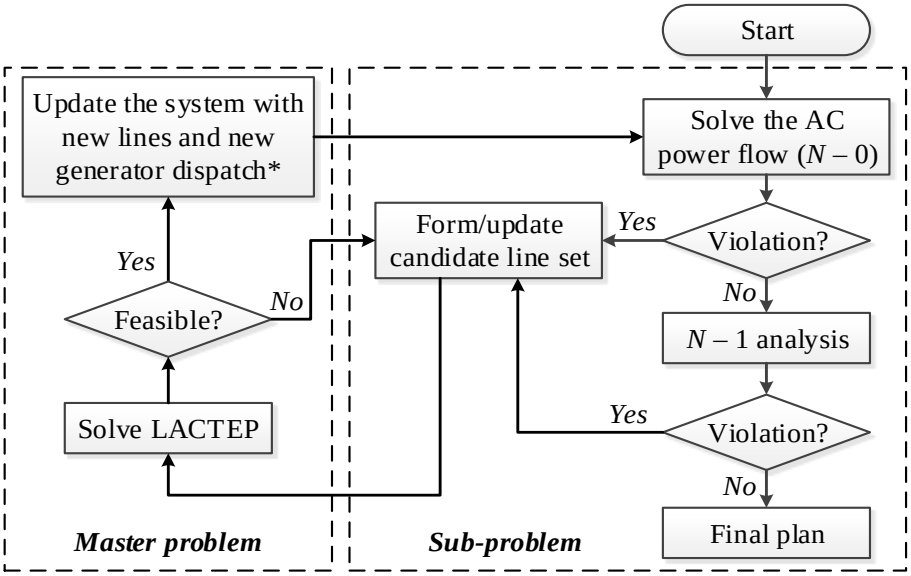

Fig. 6.4. Flowchart of the iterative approach for considering $N-1$ contingency

Table 6.8 shows the 15 initial candidate lines and their cost data. The candidate lines for the $N-1$ contingency analysis are not included in the table.

Table 6.8. Initial candidate lines for the IEEE 118-bus system

No.	Lines	Cost (M$)	No.	Lines	Cost (M$)
1	(3 – 5)	16.2	9	(38 – 37)	6.8
2	(5 – 6)	9.7	10	(69 – 67)	15.2
3	(8 – 9)	5.5	11	(77 – 78)	2.8
4	(8 – 5)	6.0	12	(80 – 99)	30.9
5	(9 – 10)	5.8	13	(82 – 83)	6.6
6	(17 – 113)	5.4	14	(94 – 100)	10.4
7	(23 – 32)	17.3	15	(99 – 100)	14.6
8	(26 – 30)	15.5			

The cost of building a transmission line can be roughly estimated by its length, cost per mile and the cost multipliers [68]. Assuming all lines are 230 kV double circuit lines, then the capital cost of a transmission line is calculated as,

$$C_{line} = 1.5\beta(Line\ length) \tag{6.33}$$

where 1.5 is the per mile cost multiplier in $/mile for 230 kV double circuit lines and β is the transmission length cost multiplier. For lines longer than 10 miles, 3 – 10 miles and shorter than 3 miles, the β values are 1.0, 1.2 and 1.5 respectively. Notice that (6.33) only gives a rough estimate of the line capital cost, more factors need be included in order to obtain a better estimate. The TEP results are demonstrated in Table 6.9 and 6.10 for $N-0$ and the $N-1$ contingency case respectively. The expanded system for $N-0$ condition is illustrated in Fig. 6.5.

Table 6.9. The TEP results for $N-0$

Lines to be built	(3 – 5), (8 – 9), (9 – 10), (26 – 30)
Investment cost (M$)	43
Total operating cost (M$)	1567.4 (10-year)
Solution time (s)	4

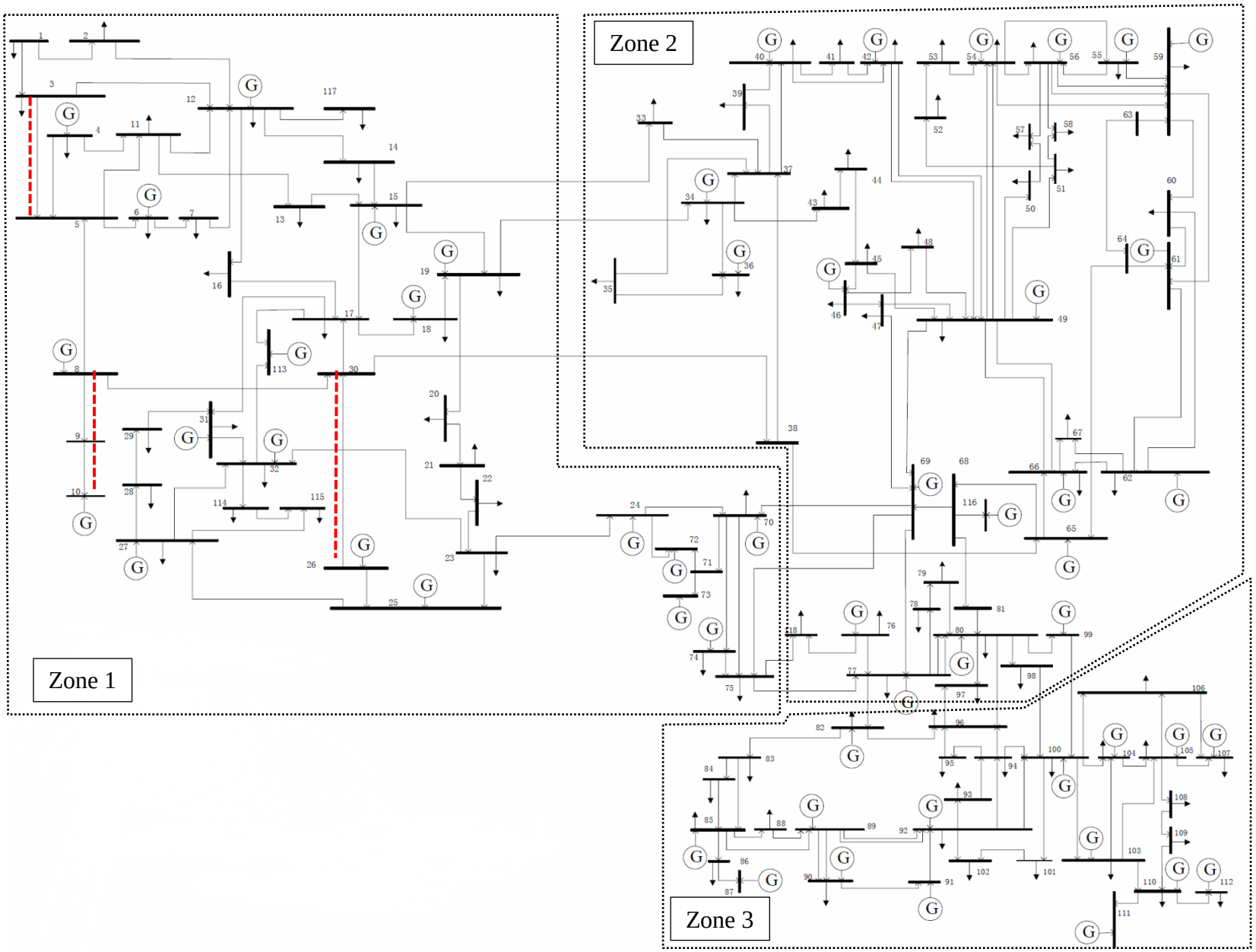

Fig. 6.5. Expanded IEEE 118-bus system under $N-0$

It is observed from Table 6.9 that four lines need to be added in order to relieve the overloads in the original system with all lines in service ($N - 0$). The investment cost is 43 M$, and the estimated 10-year total operating cost is 1567.4 M$, which is approximately 156.7 M$ per year. The original system is then expanded using the TEP solution in Table 6.9 and solved using the AC power flow with all indices within the limits. Therefore, with the four lines being added, the system is $N - 0$ secure. Meanwhile, it is worth mentioning that the TEP solution given by the DC lossless model requires building no line for this case. However, significant overloads and undervoltage issues are observed in the AC power flow. In order for the system to comply with the $N - 1$ criterion, the planning process needs to proceed to Step 4. In this case, only line (do not include transformers) contingencies are considered. During the contingency, the monitored violations monitored are overloads, loss of loads as well as undervoltages. The iterative planning process is elaborated in Table 6.10.

Table 6.10. The iterative planning process for $N - 1$

Iterations	Contingency line	Violation type	Lines added
1	(77 – 78)	Line overloading	(77 – 78) circuit 2
2	(80 – 99)		(80 – 99) circuit 2
3	(25 – 27)		(23 – 32)
4	(38 – 65)		(30 – 38)
5	(1 – 3)		(1 – 3) circuit 2
6	(86 – 87)		(86 – 87) circuit 2
7	(64 – 65)		(64 – 65) circuit 2
8	(60 – 61)		(60 – 61) circuit 2
9	(15 – 17)		(15 – 17) circuit 2
10	(12 – 117)	Loss of loads	(12 – 117) circuit 2
11	(110 – 117)		(110 – 117) circuit 2

In Table 6.10, the second column lists the lines that are manually outaged in each iteration. The contingencies in the table are ranked in the order of the severity of overload

caused in the system. The line that causes severe overloads and results in a large number of associated overloaded lines will be addressed first. The third column shows the type of the violations and the last column provides the solution to mitigate the potential overloads or loss of loads. After 11 iterations, all indices are within the limits set in Table 6.7 and the system complies with the $N-1$ contingency criterion. Mathematically, this iterative approach does not guarantee an optimal solution, but in terms of the computational burden, this approach attains the same goal more efficiently.

6.5 Summary

This chapter presents a new approach to linearize the full AC network model, based on which a TEP model is developed. The proposed LACTEP model retains a linear representation of reactive power, off-nominal bus voltage magnitudes and network losses. A MILP formulation for network losses modeling is developed to eliminate fictitious losses. An iterative approach is also presented to incorporate the $N-1$ contingency criterion in TEP problems. The simulation results of Garver's 6-bus system show that additional network reinforcements may be needed if a DC-based TEP model is adopted. The proposed LACTEP model, approximates the AC network more accurately, and therefore provides more realistic TEP solutions. The loss modeling sensitivity study shows that the *R*2 approach tends to give the best trade-off between accuracy and solution time. The fictitious losses are not significant enough to change the TEP results in the 6-bus example studied in this paper. However, this conclusion can be case dependent. The simulation results on the IEEE 118-bus system show that the proposed LACTEP model can be applied to solve large power system planning problems and the iterative approach is a computationally effective way to include the $N-1$ criterion in the TEP study.

Chapter 7

TRANSMISSION EXPANSION PLANNING UNDER UNCERTAINTIES

7.1 Chapter Overview

The planning horizon of a long term TEP study usually spans from ten to twenty years. Developing a practical system expansion plan for such a long time frame will inevitably involve extensive uncertainties including resources, budgets as well as policies. Modern TEP exercise focuses on improving the overall market efficiency and simultaneously enhancing the system reliability. In order for a practical transmission expansion plan to balance these two criteria, it is necessary to consider the uncertainties in the system and properly include them in the TEP model. The value of each transmission project must be evaluated accurately so that the correct set of lines can be chosen. This chapter addresses the important issue of modeling uncertainties in the TEP model. A two-stage stochastic TEP model is proposed and several decomposition methods are developed for solving the model.

The remainder of this chapter is organized as follows: Section 7.2 classifies the uncertainties in the system and highlights the necessity of the transition to a stochastic TEP model. A two-stage stochastic TEP model is presented in Section 7.3 and two decomposition-based solution algorithms are developed in Section 7.4. The concept of scenario generation and clustering are discussed in Section 7.5. Three cases studies are demonstrated in Section 7.6 and concluding remarks are given in Section 7.7.

7.2 TEP under Uncertainty

In power systems, load is the primary sources of uncertainties. From a long-term perspective, the annual load growth is dependent on some of the key variables such as

economics and fuel price that are inherently uncertain in the future. A promising economy will stimulate the customers' demands and will eventually lead to an increase in electricity consumption. While a bad economy, on the other hand, is likely to shrink the customers' demands and eventually reduce the electricity consumption. For short term, e.g., a daily basis, loads can be sensitive to factors such as weather and temperature that are uncertain by nature. Fig. 7.1 shows the WECC hourly forecasted loads for 2020. From the figure, one can observe that the load varies substantially during a year.

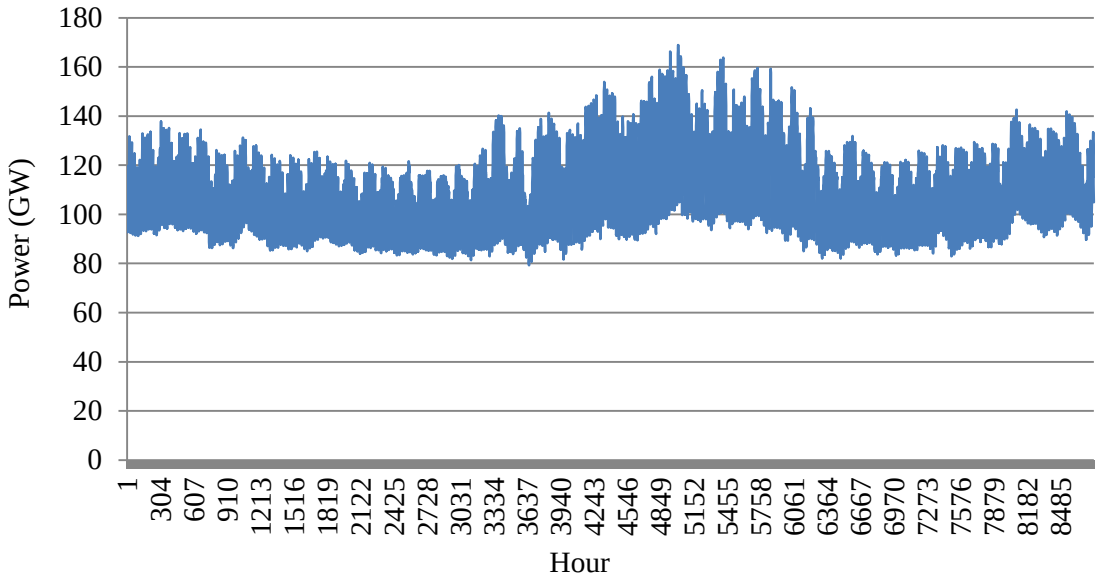

Fig. 7.1. Forecast hourly load for WECC for Year 2020 [69]

In recent years, with the increasing penetration of the renewable resources in the power system, the uncertainties at the generation side, especially the impact of uncertain renewable resources such as wind and solar on bulk power systems, should be appropriately addressed. From the planning perspective, it is important to select the mix of generators to satisfy the RPS requirement and at the same time, meet the future energy balance as well as the system reliability criteria.

The traditional TEP approach focused on protecting the system from the "worst case" scenario. In other words, the system expansions were largely determined by the most severe $N-1$ contingency at the peak load level. This approach was based on the assumption that if a system survives the worst case contingency, then it would be robust enough to survive any contingency. While this assumption could be valid in some cases, the worst case-based TEP approach is not suited for contemporary power systems. The reasons are twofold: First, most severe contingencies are very unlikely to occur, so that protecting against these contingencies through transmission expansion could be excessively expensive. In fact, special protection schemes (SPSs) are usually developed to mitigate the impact of the most critical contingencies. In addition, the deregulated market environment and high penetration of renewable resources could cause the generation pattern to vary significantly during different hours of a year, for which the real "worst case" is usually difficult to define / identify (may not be at peak load).

The proposed framework for the next generation TEP exercise is demonstrated in Fig. 7.2. The proposed TEP framework is classified into four stages with each stage as specified in the dotted box. In the first stage, in order to develop a planning base case, one can take the operational case of the current year, adjust the load level according to the forecast of the load growth, remove the generators to be retired and add the generators that are likely to be in service in the targeted planning year. Federal policy requirements, e.g., RPS, and stakeholders' inputs will also be addressed at this stage. The reference planning base case will be developed to represent the "standard" future. It should be noted that due to the potential load increase, it is normal to observe some overloads in this reference case. These overloads will serve as an incentive for the later transmission

expansions. The base case development is crucial in the TEP process because it serves as a basis for the entire planning framework. After the base case has been developed, different scenarios can be derived in stage two based on stakeholders' specific inquiries with the parameters in the base case adjusted to different levels. Typical alternative scenarios include a combination of variations in loads, energy costs, as well as the generation mixes. The candidate lines together with the scenarios are will serve as inputs to the next stage for network optimization.

The network optimization is the core of the entire TEP framework. Traditionally, due to the lack of efficient algorithms, this step was primarily done by using a trial and error approach, which is, the value of the expansion projects were evaluated by running multiple production cost analysis with different set of new lines inserted. However, this approach is by nature a heuristic and is only doable when the candidate line pool is small because as the number of candidate lines increases, the computational burden can easily become intractable. With the development of computing facilities and optimization solvers, the next generation TEP is expected to combine the production cost analysis together with the network expansion using a unified MIP formulation, which simultaneously optimizes the network expansions and generator dispatch. As for now, it is still computationally challenging to perform a study of this kind for a system with practical size. Various decomposition methods and heuristics are developed later in this chapter to tackle this problem. Alternatively, after an expansion plan is obtained for each scenario, lines or corridors that are selected in most scenarios can be viewed as the transmission projects with high value and therefore should be considered to build. Last, the resource adequacy and the system security, e.g., static and dynamic stability of the

expanded system should be evaluated in the final stage where possible sub-regional reinforcement projects are identified. The AC power flow model should be used to verify the transmission expansion plan obtained from the network optimization model, in which the DC model is usually used.

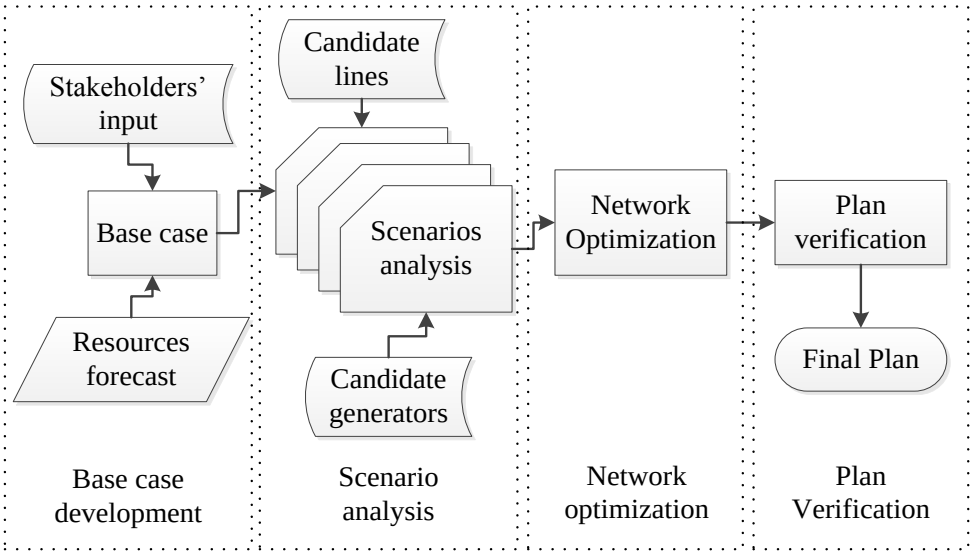

Fig. 7.2. Proposed next generation TEP framework

7.3 Stochastic Reformulation of the TEP Model

In this section, a two-stage stochastic TEP model that considers the load uncertainties is introduced. The decision variables in this stochastic model can be categorized into two sets. The decision that needs to be made immediately with limited information about future environments is called the first-stage decision (also known as the *here and now* decision), while given the first stage decisions made, the second stage decisions (also known as the *wait and see* decisions) can be made based on the realization of a series of random scenarios [69]. A general two-stage stochastic (mixed) linear programming problem with recourse can be formulated as follows,

$$\begin{aligned} &\min_{x} c^T x + E_s\left[Q(x,\tilde{s})\right] \\ &\text{s.t. } Ax = b \\ &\qquad x \geq 0 \end{aligned} \tag{7.1}$$

where

$$\begin{aligned} &Q(x,s) = \min_{y} \; q(s)^T y(s) \\ &\text{s.t. } T(s)x + W(s)y(s) = h(s) \\ &\qquad y \geq 0 \end{aligned} \tag{7.2}$$

In (7.1), x is the first-stage variables that need to be determined immediately. E_s represents the mathematical expectation of an uncertain set, and $\tilde{s}$ denotes as a set of random events. Among the set of second-stage random events, each given realization s is corresponding to a scenario *sub-problem* as defined in (7.2). For computational viability, the second-stage has a finite number of realizations with associated weight p^s. Combining the two stages together, the compressed *deterministic equivalent* (DE) form of the stochastic programming problem defined by (7.1) and (7.2) can be written as,

$$\begin{aligned} &\min_{x,y} c^T x + \sum_{s\in\Omega_s} p^s q^s y^s \\ &\text{s.t. } Ax = b \\ &\qquad T^s x + W^s y^s = h^s \qquad \forall s \in \Omega_s \\ &\qquad x,\; y^s \geq 0\;,\; \sum_{s\in\Omega_s} p^s = 1 \qquad \forall s \in \Omega_s \end{aligned} \tag{7.3}$$

In order to apply the above formulation to TEP problems, let the first-stage be the line investment decision problem and the second-stage be the operating sub-problems, the stochastic version of the TEP model (3.1)-(3.7) are formulated as follows,

$$\min_{x,y} c_k^T z_k + \sum_{s\in S} p^s \sum_{g\in\Omega_g} \left(c_g^s PG_g{}^s\right) \tag{7.4}$$

$$\sum_{k\in\Omega_k^i} P_k^s + \sum_{g\in\Omega_g^i} PG_g^s = \sum_{d\in\Omega_d^i} PD_s^s \quad \forall i \in \Omega_b \tag{7.5}$$

$$P_k^s = -b_k \theta_k^s \quad \forall k \in \Omega_k \tag{7.6}$$

$$-(1-z_k)\cdot M_k \le \left(P_k^s + b_k \theta_k^s\right) \le (1-z_k)\cdot M_k \quad \forall k \in \Omega_k^+ \tag{7.7}$$

$$-P_k^{\max} \le P_k^s \le P_k^{\max} \quad \forall k \in \Omega_k \tag{7.8}$$

$$-z_k P_k^{\max} \le P_k^s \le z_k P_k^{\max} \quad \forall k \in \Omega_k^+ \tag{7.9}$$

$$PG_g^{\min} \le PG_g^s \le PG_g^{\max} \quad \forall g \in \Omega_g \,. \tag{7.10}$$

Considering the complexity of the problem, the DC model is used in the above formulation and loads are considered as the only uncertain parameter in the model, which means the *T* and *W* matrices in (7.3) are fixed and not scenario dependent. The objective function (7.4) is to minimize the total investment cost and the expectation of a series of different operating scenarios with each weighted by a weight p^s. Compared with the deterministic TEP model in which the operating cost is calculated at a single load level, the stochastic version gives a more realistic estimate of the expected operating cost. The superscript *s* denotes variables and parameters that are scenario dependent. The network constraints for each scenario in the second-stage are in (7.5)-(7.10). As one can easily observe, the size of the above problem expands almost proportionally to the number of scenarios. If there are many scenarios in the second-stage, then solving a problem with this kind will be extremely difficult. However, by expanding the compact DE form in (7.3) and examining the *A* matrix of the constraints, it is not difficult to observe that the extensive form of the problem has a block angular structure as illustrated in Fig. 7.3. This special structure can be readily utilized by various decomposition algorithms such as the *L*-shaped method and progressive hedging (PH) method. The derivation of these algorithms will be presented in Section 7.4.

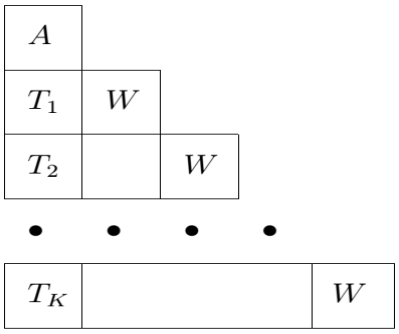

Fig. 7.3. Block structure of the two-stage stochastic formulation

7.4 Decomposition-based Solution Techniques

Considering the size and the number of scenarios a problem has, intensive computations are usually expected when solving stochastic programming problems. For decades, various decomposition methods have been developed for solving problem of this kind efficiently, among which, the *L*-shaped method [71] and progressive hedging (PH) [72] are the two approaches that have been widely adopted. This section briefly introduces these two approaches.

7.4.1 The L-Shaped Method

The *L*-shaped method is a *stage decomposition* method, which is in essence the application of Benders' decomposition (BD) in stochastic programming, designed to solve large-scale stochastic problems that cannot be solved directly using the DE form [71]. The classic *L*-shaped method requires second-stage variables to be continuous, while having no assumption on the first-stage variables. The stochastic TEP formulation developed in Section 7.3 contains purely binary variables in the first-stage (investment problem) and purely continuous variables in the second-stage (scenario-based operating problems). Therefore, the classic *L*-shaped method can be easily applied. Take problem (7.3) for example, the procedure of the single-cut *L*-shaped method is outlined as follows:

Step 0: Set $v = r = k = 0$, where v, r and k are number of iterations, feasibility sets and optimality sets respectively.

Step 1: Set $v = v + 1$. Solve the first-stage master problem:

$$\min_x c^T x + \eta \tag{7.11}$$

$$\text{s.t. } Ax = b \tag{7.12}$$

$$D_l x \geq d_l \qquad l = 1, ..., r \tag{7.13}$$

$$E_l x + \eta \geq e_l \qquad l = 1, ..., k \tag{7.14}$$

$$x \geq 0$$

where in (7.11), η can be viewed as an estimation (lower bound) of the second-stage objective. Constraint (7.12) represents those constraints that are only related to the first-stage variables, *i.e.*, line investment decision in the TEP problem. Constraints (7.13) and (7.14) are called the feasibility cut and the optimality cut respectively, and may not both appear in the first several iterations. In (7.11), η is initially set to $-\infty$ or whatever the practical lower bound is. Notice that η is included in (7.11) only if (7.14) is present. Let x^v and η^v be the optimal solution of (7.11) and then proceed to **Step 2**.

Step 2: For each sub-problem $s \in \Omega_s$, solve:

$$\begin{aligned} &\min_y \ q^s y^s \\ &\text{s.t. } W^s y^s = h^s - T^s x^v \\ &\quad y^s \geq 0 \end{aligned} \tag{7.15}$$

where x^v is the first-stage decision variable determined in **Step 1**. If for any s (7.15) is infeasible, then let σ_s be the dual extreme ray. Define

$$D_{r+1} = (\sigma^v)^T T^s \tag{7.16}$$

and

$$d_{r+1} = (\sigma^v)^T h^s \tag{7.17}$$

to generate a feasibility cut $D_{r+1}x \geq d_{r+1}$ and add it to (7.13). If (7.15) is feasible for all sub-problems, then let π_s^v be the dual multipliers of each sub-problem. Define

$$E_{k+1} = \sum_{s \in \Omega_s} p^s (\pi_s^v)^T T^s \tag{7.18}$$

and

$$e_{k+1} = \sum_{s \in \Omega_s} p^s (\pi_s^v)^T h^s . \tag{7.19}$$

Check if $\eta^v \geq e_{k+1} - E_{k+1}x^v$ holds. If yes, the algorithm stops and x^v is the optimal solution, otherwise, add the optimality cut $E_{k+1}x^v + \eta^v \geq e_{k+1}$ to (7.14), return to **Step 1** and resolve the restricted master problem. In every iteration, the distance between $(e_{k+1} - E_{k+1}x^v)$ and η^v is known as the *optimality gap*. In practice, instead of requiring $\eta^v \geq e_{k+1} - E_{k+1}x^v$ holds strictly, a tolerance can be set. Once the gap is within the tolerance, the algorithm can be terminated and the optimality can be declared.

The single-cut version *L*-shaped method as described above aggregates the dual multipliers of all sub-problems to generate a single optimality cut at a time. This may cause information loss and potentially results in a large number of iterations. A multi-cut version of the *L*-shaped method was proposed with an optimality cut is generated for each sub-problem if necessary. The multi-cut version utilizes all the information in the second-stage, which is therefore expected to generate cuts that are more effective. However, cases do exist in which the single-cut version outperforms the multi-cut version. In addition, the master problem could become huge in a few iterations since the multi-cut version adds a large number of cuts to it in an iteration. To improve the performance of the multi-cut version *L*-shaped method, methods have been developed by partially aggregating the dual multipliers in the second-stage. These extensions of the *L*-shaped

method are programmed in AMPL for solving the stochastic TEP model developed in this chapter. The detailed descriptions of these extensions are provided in [73]. It should be noted that if the scale of the stochastic programming problem is not large enough, then the *L*-shaped method may not be superior to solving the DE form of the problem directly in terms of execution time. The value of the *L*-shaped method, however, is that it breaks down a very large-scale (mixed-integer) stochastic programming problem that cannot be solved directly into many smaller problems. And then approaches the optimal solution in an iterative manner.

7.4.2 Progressive Hedging Algorithm

Progressive hedging (PH) is a heuristic algorithm that was originally proposed in [72] for solving uncertain problems in financial investment. PH has been widely used in solving stochastic programming problems and has served as an alternative for other Benders' decomposition-based methods such as the *L*-shaped method. Different from the *L*-shaped method that decomposed stages, the PH algorithm decomposes scenarios. Take the TEP problem for example, in each iteration, the *L*-shaped method solves the master problem using the same set of decision variables but different number of constraints. That is, the planning decisions in the first-stage are scenario independent (there is only one transmission plan). The PH algorithm, as illustrated in Fig. 7.4, temporarily relaxes the scenario independent constraint and develops a sub-plan for each scenario. During each iteration, penalties will be added to eliminate the dissimilarity among sub-plans until all sub-plans yield the same result. Compared to the *L*-shaped method in which the size of the master problem (MILP) keeps increasing while the size of the sub-problems (LPs) remain the same, one advantage of PH is that it evenly distributes the workloads to each

sub-problem (MILPs). This feature makes it not only easily parallelizable, but also computationally beneficial when each MILP problem is not too difficult to solve. The steps for applying the PH algorithm to TEP problems are derived followed by a heuristic strategy to accelerate the convergence of the algorithm in what follows.

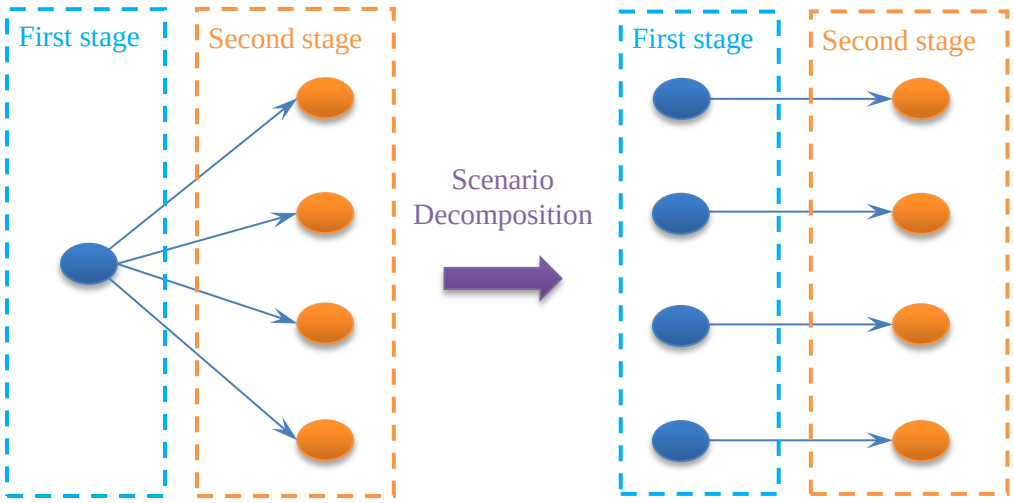

Fig. 7.4. Scenario decomposition in the PH algorithm

Applying scenario decomposition to (7.3) assuming the first-stage variables x are all binary, the decomposed DE form can be rewritten as follows,

$$\begin{aligned}
&\min_{x,y} \sum_{s\in\Omega_s} p^s \left(c^T x^s + q^s y^s\right) \\
&\text{s.t. } Ax^s = b \\
&\quad T^s x^s + W^s y^s = h^s \qquad \forall s \in \Omega_s \\
&\quad x^s = x^M \qquad\qquad (7.20) \\
&\quad x^s, x^M \in \{0,1\} \\
&\quad y^s \geq 0 \qquad \forall s \in \Omega_s
\end{aligned}$$

where (7.20) is known as the non-anticipative constraint and x^M denotes the master plan that all sub-plans should be equal to. By copying the decision variables x to each scenario, now the problem becomes completely scenario separable. To solve the problem,

(7.20) is first relaxed by the augmented Lagrangian formulation. The augmented objective function can be obtained as,

$$\min_{x,y} \sum_{s\in\Omega_s} p^s \left[c^T x^s + q^s y^s + \lambda^s \left(x^s - x^M \right) + 0.5\rho \left(x^s - x^M \right)^2 \right] \tag{7.21}$$

where λ^s is the Lagrangian multiplier of the relaxed constraint (7.20) and ρ is the penalty factor. Since x is binary, the quadratic term in (7.21) can be further simplified as:

$$0.5\rho \left(x^s - x^M \right)^2 = 0.5\rho \left(x^s - 2x^s x^M + x^M \right) \tag{7.22}$$

Substitute (7.22) into (7.21) and rearrange the order of the terms, the augmented objective function can be expressed as follows,

$$\min_{x,y} \sum_{s\in\Omega_s} p^s \left[\left(c^T + \lambda^s + 0.5\rho - \rho x^M \right) x^s + q^s y^s - \lambda^s \overline{x} + 0.5\rho x^M \right]. \tag{7.23}$$

For a given master plan $\overline{x}$, λ^s, p^s, and ρ are all fixed. Thus, the full scenario decomposable problem with the modified cost can be written as follows,

$$\begin{aligned} &\min_{x,y} \sum_{s\in\Omega_s} p^s \left[\left(c^T + \lambda^s + 0.5\rho - \rho x^M \right) x^s + q^s y^s - \lambda^s \overline{x} + 0.5\rho \overline{x} \right] \\ &\text{s.t. } Ax^s = b \\ &\quad T^s x^s + W^s y^s = h^s \qquad \forall s \in \Omega_s \\ &\quad x^s, \in \{0,1\} \\ &\quad y^s \geq 0 \qquad \forall s \in \Omega_s \end{aligned} \tag{7.24}$$

where in the objective function, the term ($\lambda^s + 0.5\rho - \rho x^M$) can be viewed as the penalty factor that adds to the original investment cost c at each iteration. The classic PH algorithm proceeds as follows,

Step 0: Initialization: Set $\lambda^s = \rho = k = 0$.

Step 1: $k = k + 1$. For each scenario s, solve (7.24) and obtain x^s. Calculate the master plan x^M and let $\lambda^s = \lambda^s + \rho(x - x^M)$.

Step 2: For each scenario s, solve (7.24) and obtain x0s. If $x_{k+1} = x_k$ and $\lambda^s = \lambda^s - 1$ then the algorithm stops and x is the optimal solution.

Table 7.1. Comparison of the *L*-shaped method and PH Algorithm

Method	Pros	Cons	Fix	Applications
L-shaped	Guarantees global optimum if convex	Master problem size keep increasing	Partial aggregation	Scenarios not too many
PH	Evenly distributes workload, parallelism	Very slow convergence, optimum not guaranteed	Heuristics	MILPs easy to solve

7.5 Scenario Generation and Clustering

As described in previous sections, the second-stage of the stochastic TEP problem needs the solution of a series of sub-problems. These sub-problems, differentiated by their load levels, represent different power system operating conditions over a time horizon. Typically, scenarios can be generated using two approaches. The first approach is through load forecast. Based on historical analysis and future load projection, forecast data can be obtained and used to generate weekly, daily and even hourly scenario set. The scenarios generated by this approach usually provide a reasonably good representation of the targeted planning year. However, for many test cases, usually a single load level is given and the forecast data are not available. If this is true, then a load growth rate can be assumed and a statistical distribution can be assigned to the load at every bus. A random sampling can then be performed to obtain the scenarios.

No matter which approach is taken, a large number of scenarios is usually expected. Before sending a problem with all these scenarios to the solver, one important step is scenario clustering, that is, to cluster similar scenarios into groups. The reasons why this step is important are twofold: First, even with the decomposition methods, the

two-stage stochastic TEP formulation is still computationally very intensive. A problem with too many scenarios usually takes too long a time to solve. This is unacceptable from the CPU time budget point of view. Second, with a large number of scenarios, only a limited number is unique in the sense that there are significant differences between each of them, the differences between the rest of the scenarios are insignificant and therefore can be views as redundant scenarios. Solving these redundant scenarios will not result in a new transmission expansion plan but will substantially slow down the execution time. Therefore, scenarios with high similarity need to be grouped and only the representative scenario should be retained in the final problem. To achieve this goal, the *K*-means clustering algorithm is used. The *K*-means algorithm is a model free method for data clustering by partitioning *n* sets of multivariate data observations into *k* clusters with their closest mean [74]. The basic idea of the *K*-means algorithm is illustrated in Fig. 7.5.

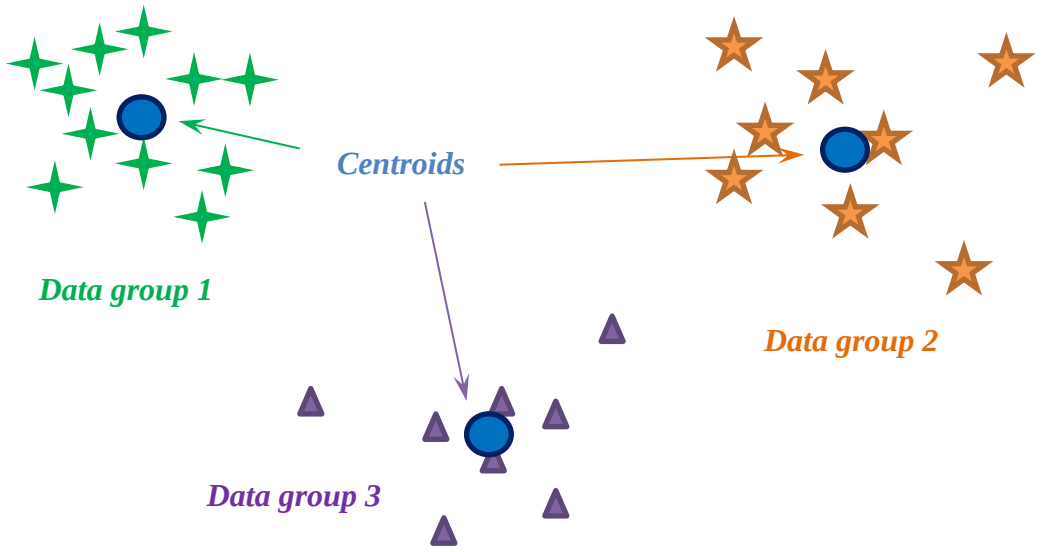

Fig. 7.5. Illustration of the *K*-means algorithm

The steps of the *K*-means algorithm are as follows,

Step 1: Determine *k* sets of initial centroids in the *n* sets of data point.

Step 2: Assign each of the *n* data points to its closest centroid.

Step 3: Recalculate the means of the clusters determined in **Step 2** as the new centroids. Repeat until the centroids do not move between two iterations.

The choice of initial centroids could greatly affect the performance of the *K*-means algorithm. An initialization strategy, known as the "*K*-means++ initializer", is proposed in [75]. Instead of selecting all initial centroids at once, this initialization strategy selects the initial centroids one at a time based on the "D^2-weighting" approach, where *D* is the shortest distance from a data point to the closest centroid that have been chosen. It has been proved that *K*-means++ generally gives better clustering results than the classic *K*-means method [75].

7.6 Case Studies

This section investigates the performance of the decomposition TEP algorithms developed in this chapter on the IEEE 24-bus RTS system and the IEEE 118-bus system. The TEP models and the decomposition algorithms are programmed using AMPL. In the following studies of this chapter, the relative optimality gap is set to be 10^{-5} (0.01%) if not otherwise specified. All simulations are done on a Linux workstation with an Intel *i*7-2600, 4-core CPU @ 3.40 GHz with 16 GB of RAM.

7.6.1 The IEEE 24-bus System

The 1996 IEEE 24-bus RTS system [57] has 39 existing lines, 17 loads and 33 generators. It is assumed that for each existing transmission corridor, a new line can be considered as a transmission line candidate. Therefore, the total number of candidate lines is 39. All the system parameters used in this study can be found in Appendix A.

First, the performance of the *L*-shaped method is evaluated by the following simulation. Based on the data in Appendix B, each daily peak load is selected and 365 scenarios are constructed for the second-stage operating problem. Multi-cut *L*-shaped method is used to solve this case. The TEP results are shown in Table 7.2.

Table 7.2. TEP results of IEEE 24-bus system with 365 scenarios

Problem size	Execution time (s)	Iterations	Investment cost (M$)	Annual operating cost (M$)	Selected lines
Rows: 184690 Columns: 48218 None zeros: 465010	308.6	24	40.1	355.55	14 – 16 16 – 17 17 – 18

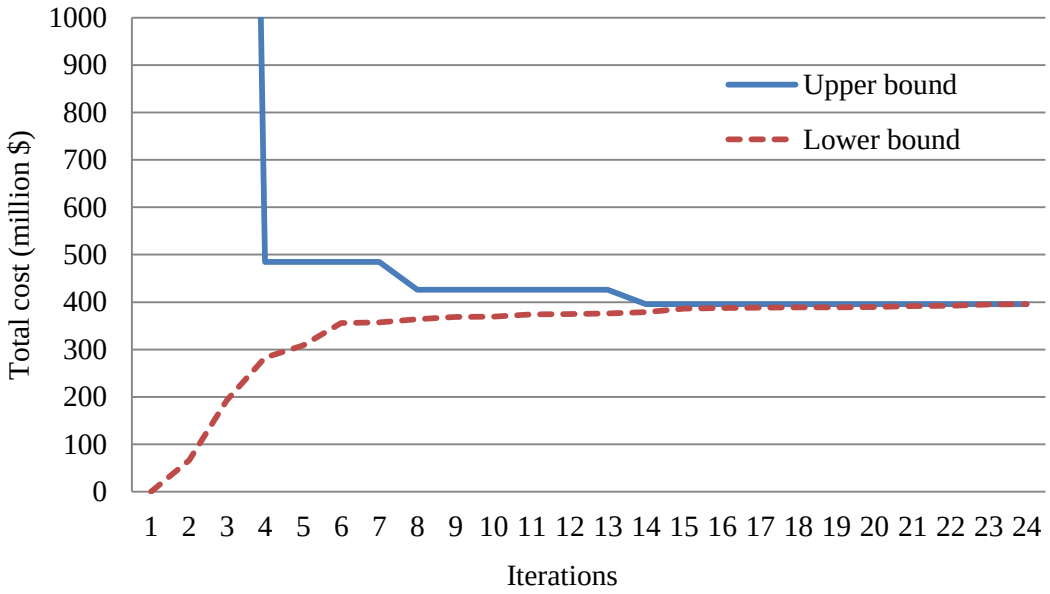

Fig. 7.6. Upper and lower bounds of the *L*-shaped method in each iteration

As one can observed from Table 7.2, the TEP problem with 365 scenarios is solved in approximately five minutes after 24 iterations using the multi-cut version *L*-shaped method. Three candidate lines are selected with an investment cost of 40.1 M$. The estimated annual operating cost is 355.55 M$. Fig. 7.6 shows the upper and lower

bounds of the *L*-shaped method at each iteration. The difference between the upper bound and the lower bound in the figure is known as the "optimality gap" or "gap" for short. It can be observed that the gap reduces very fast in the first a few iterations, and then converge slowly to the optimum. The reason is that in this case, the optimality cuts generated in the first a few iterations are effective cut planes that substantially reduce the feasible solution set and help the branch-and-bound search. As iterations proceed, the optimality cut generated may not be as effective in reducing the feasibility set, hence the convergence rate becomes slow. The expanded IEEE 24-bus system is shown in Fig. 7.7, where the dashed lines are the new lines to be added.

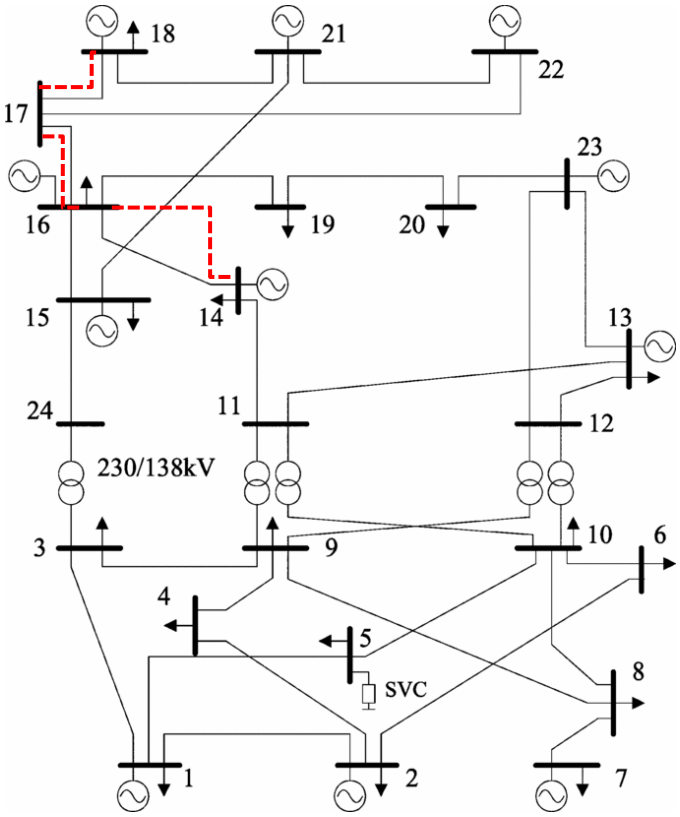

Fig. 7.7. One line diagram of the expanded IEEE 24-bus RTS system

In order to elaborate the value of the stochastic TEP model, the deterministic TEP model that considers only the annual peak load level is also studied and the results are provided in Table 7.3 for comparison.

Table 7.3. Deterministic TEP results of the IEEE 24-bus system

Problem size	Investment cost (M$)	Annual operating cost (M$)	Selected lines
Rows: 506 Columns: 170 None zeros: 1274	66.4	570.81	14 – 16 *15 – 24* 16 – 17 17 – 18

Comparing the results in Table 7.2 with 7.3, it is not difficult to observe that both the investment cost and the operating cost given by the deterministic TEP model are higher than those were obtained from the stochastic TEP model. The operating cost is higher in the deterministic TEP model because it assumes the peak load level for every single day of a year. This assumption in the real world, however, tends to be very conservative and may generate unrealistic results. In the deterministic TEP model, four lines are selected, which is one line more than the TEP result in Table 7.2. The additional line is *italicized* in Table 7.3. The reason why the investment cost for the deterministic TEP model is also higher is because that if it were to be calculated lower, e.g., the investment cost in Table 7.2, then the resultant operating cost in the deterministic TEP model would be even higher than 570.81 M$. The value of stochastic TEP model is that the annual operating cost can be more accurately estimated as compared to the deterministic model, which only focuses on the peak load level. The deterministic TEP

model tends to overestimate the annual operating cost and therefore potentially results in an uneconomical transmission expansion plan.

For the stochastic TEP model, the number of scenarios in the second-stage could affect the number of iterations and execution time significantly. In order to investigate this effect, three cases are created with 1 scenario (annual peak), 52 scenarios (weekly peak) and 365 scenarios (daily peak) in the second-stage operating problem, respectively. The relationship between iterations and execution time versus the number of scenarios are illustrated in Fig. 7.8.

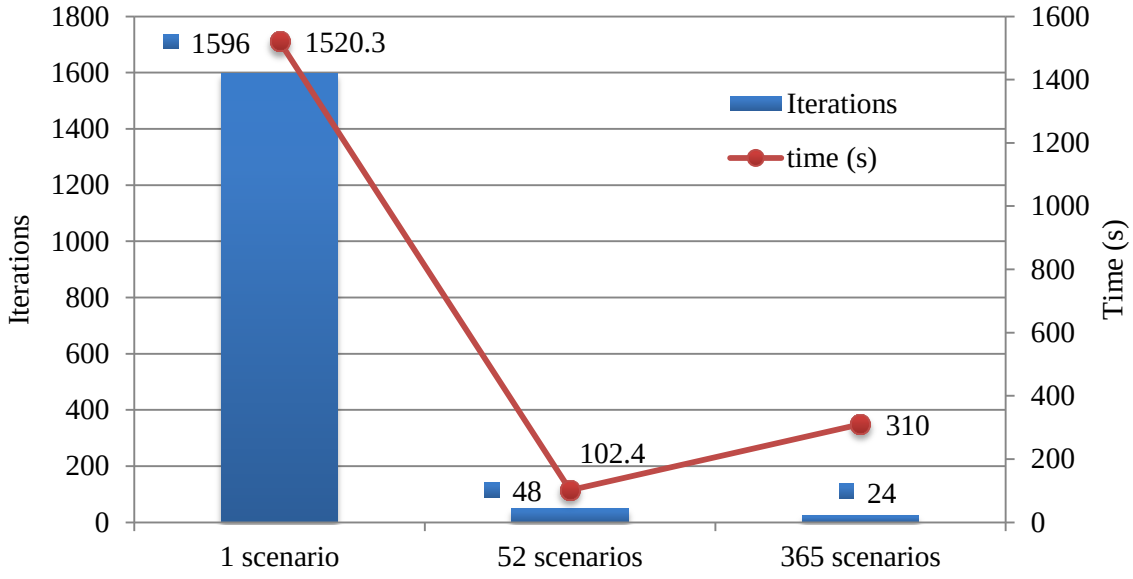

Fig. 7.8. Impacts of number of scenarios on the iterations and the execution time

From Fig. 7.8, one can observe that as the number of scenarios increases, the number of iterations for solving the problem drops drastically from 1596 to only 24. This is again because that with more scenarios in the second-stage, there will usually be a high possibility to generate efficient cut planes. In terms of execution time, it is interesting to notice that the execution time drops dramatically when the number of scenarios increases

from 1 to 52, while it increases marginally when the number of scenarios further increases from 52 to 365. To explain this, recall that the *L*-shaped method adds a number of optimality cuts (constraints) to the master problem in each iteration if the optimality has not been reached. For the multi-cut version, the number of constraints added to the master problem in each iteration can be as many as the number of scenarios in the second-stage. Hence, if the number of scenarios is large, then the size of the master problem will increase fast after each iteration. Since the master problem is a MILP problem, it could take a longer time to solve a large MILP master problem with fewer iterations as compared to a smaller MILP problem with slightly more iterations.

Similarly, the performance of the *L*-shaped method can be greatly affected by the number of clusters used in the algorithm. Taking the case with 365 scenarios for example, the 365 scenarios are aggregated into 1 cluster (single-cut), 5 clusters (73 scenarios per cluster), 73 clusters (5 scenarios per cluster) and 365 clusters (1 scenario per cluster, multi-cut), respectively. Fig 7.9 illustrates the relative gaps of these four clustering strategies in each iteration while Fig. 7.10 shows how the number of clusters influences the number of iterations and execution time. By observing the two figures, similar conclusions as for Fig. 7.8 can be drawn. The single-cut *L*-shaped method adds only one optimality cut into the master problem after each iteration, in this case, the size of the master problem increases slowly but the cutting planes generated in each iteration are inefficient in reducing the number of branching nodes needed to reach optimality. This explains why the single-cut version of the *L*-shaped method fails to yield a solution with 3600 seconds and still leave a gap of about 31%. On the other hand, in spite of the fact that the multi-cut version needs the least number of iterations to solve the problem, the

massive number of constraints that needs to be added to the master problem after each iteration slows down the overall computing performance. Among these four clustering strategies, the clustering strategy with 5 scenarios per cluster yields the most efficient solution.

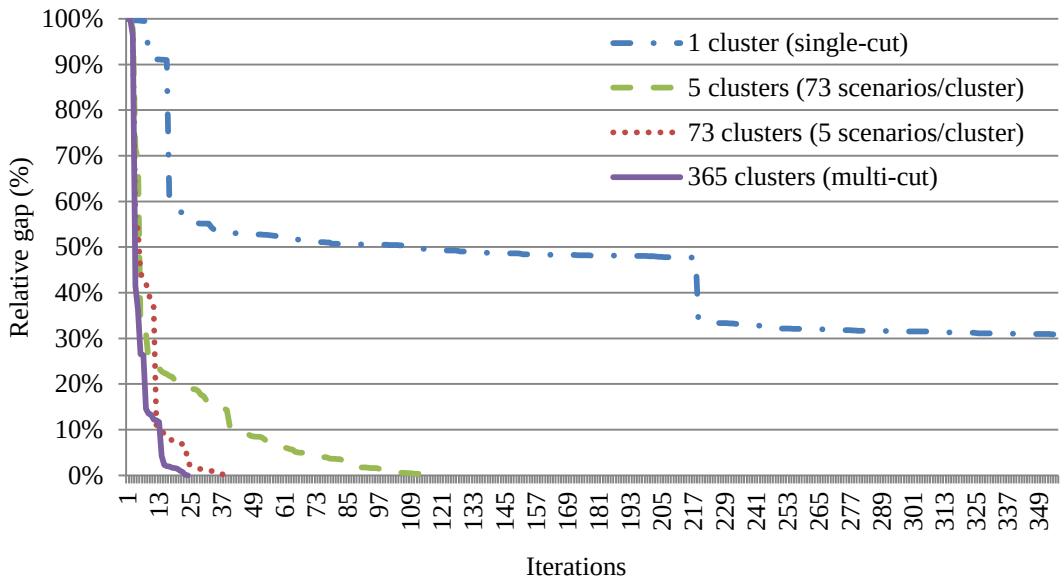

Fig. 7.9. Relative optimality gaps at every iteration

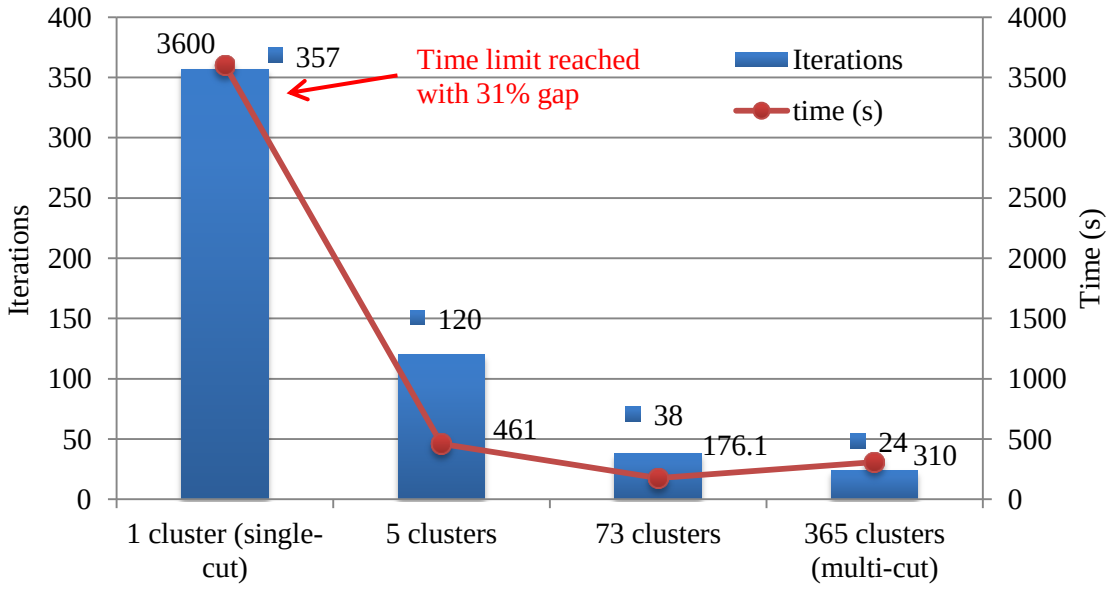

Fig. 7.10. Impacts of number of clusters on the iterations and the execution time

The performance of the *L*-shaped method algorithm is evaluated above. The following study compares the performance of the *L*-shaped method, PH and DE. Again, the same three cases with 1 scenario (annual peak), 52 scenarios (weekly peak) and 365 scenarios (daily peak) are used in this study, and there is an execution time limit of 3600 s. The TEP results from the three methods are summarized in Table 7.4.

Table 7.4. TEP results from the *L*-shaped method, DE and PH

Case	*L*-shaped	DE	PH
1 scenario	14 – 16 15 – 24 16 – 17 17 – 18	14 – 16 15 – 24 16 – 17 17 – 18	14 – 16 15 – 24 16 – 17 17 – 18
52 scenarios	14 – 16 16 – 17 17 – 18	14 – 16 16 – 17 17 – 18	Time limit reached
365 scenarios	14 – 16 16 – 17 17 – 18	14 – 16 16 – 17 17 – 18	

From Table 7.4, it can be observed that for all cases, the *L*-shaped method and DE always give the same TEP result. This verifies the accuracy of the *L*-shaped method based TEP algorithm. The PH gives the same TEP result for the 1 scenario case, but fails to generate a integer solution within the time limit for the other two cases. This indicates that PH tends to take a long time to converge, especially when the decision variables are integer. In order to accelerate the convergence rate of PH, some heuristic methods for lines selection need to be developed.

As mentioned in Section 7.4.1, the idea of the *L*-shaped method is to break down a big problem that cannot be solved directly into a master problem and many small sub-problems and then solve them iteratively. Due to this reason, even for a problem with

only a few scenarios, it could still take a long time for the *L*-shaped method to converge because the sub-problems do not "see" and "coordinate" with each other when they are being solved. DE, on the other hand, treats the problem as a whole and therefore can outperform the *L*-shaped method when the problem scale is not large. This fact is illustrated in Fig. 7.11, where the execution time of the *L*-shaped method and DE is compared for the three cases developed in Table 7.4.

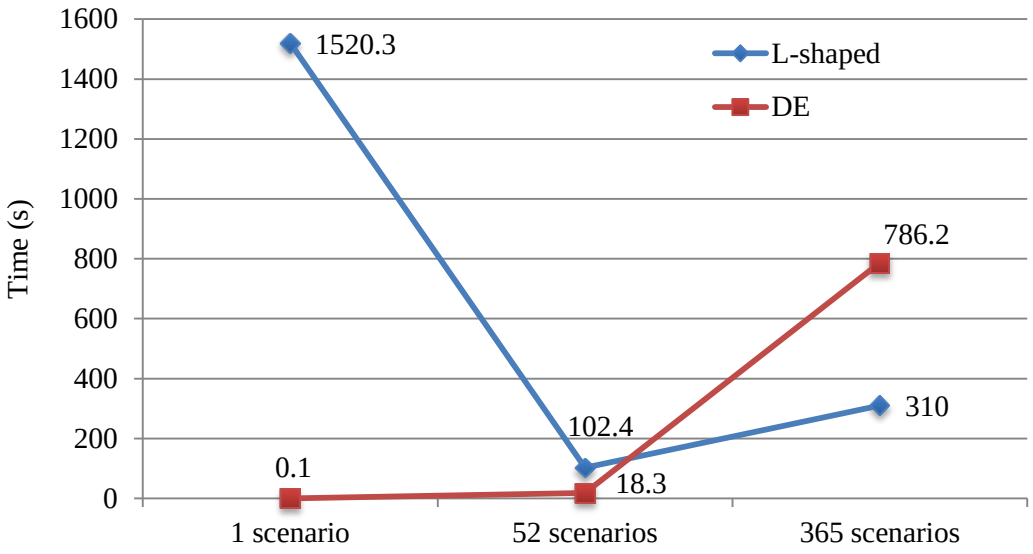

Fig. 7.11. Execution time vs. scenarios comparison of the *L*-shaped method and DE

From Fig. 7.11, it can be easily observed that when the problem scale is small, e.g., 1 scenario, the DE outperforms the *L*-shaped method dominantly. As the problem scale becomes larger, the difference between the *L*-shaped method and the DE becomes small, e.g., 52 scenarios. The computing advantage of the *L*-shaped method only shows up when the problem scale becomes really large, e.g., 365 scenarios. In this case, the execution time of DE increases substantially due to numerical difficulty, while the *L*-shaped method, because of its decomposition nature, becomes the efficient algorithm.

Various heuristics can be developed to accelerate the *L*-shaped method; one of them is to prescreen the candidate lines and reduce the solution set. The prescreening strategy should be carefully selected so that it should reduce the number of branching nodes effectively while leave the set where the optimal solution lies intact. A scenario decomposition based prescreening approach that enlightened by the PH algorithm is introduced in the following:

Step 1: For each scenario $s \in \Omega_s$, solve (7.24) and obtain the set of decision variable z^s for each scenario.

Step 2: Calculate the master plan $z^M = \sum_{s \in \Omega_s} \left(\rho^s z^s \right)$, where $\rho^S = 1/S$, S is the number of scenarios.

Step 3: Fix any element in z^M that is 0, remove them from the candidate line set and form the reduced candidate line set z^R.

Step 4: Proceed to solve the problem with the reduced candidate line set.

Notice that one assumption of this heuristic is that $z^* \subset z^M$ must hold, where z^* is the optimal solution. Otherwise, this prescreening process will result in only the sub-optimal solution being found or even make the problem infeasible. In this case, more candidate lines need to be included by unfixing some of the variables. Considering the problem with 365 scenarios, after running the prescreening algorithm, 24 out of the 39 decision variables are fixed to zero. Fig. 7.12 illustrates the change in the number of iterations with and without the prescreening. It can be observed that after the prescreening, the number of iterations reduces from 24 to 17. The number of iterations and the execution time with and without prescreening are compared in Fig. 7.13. Notice that the single-cut version without the prescreening fails to give a solution within the time

limit; therefore, it is not plotted out in the figure. It can be observed that with prescreening, both the number of scenarios and the execution time drop significantly, which proves the effectiveness of the heuristic prescreening approach.

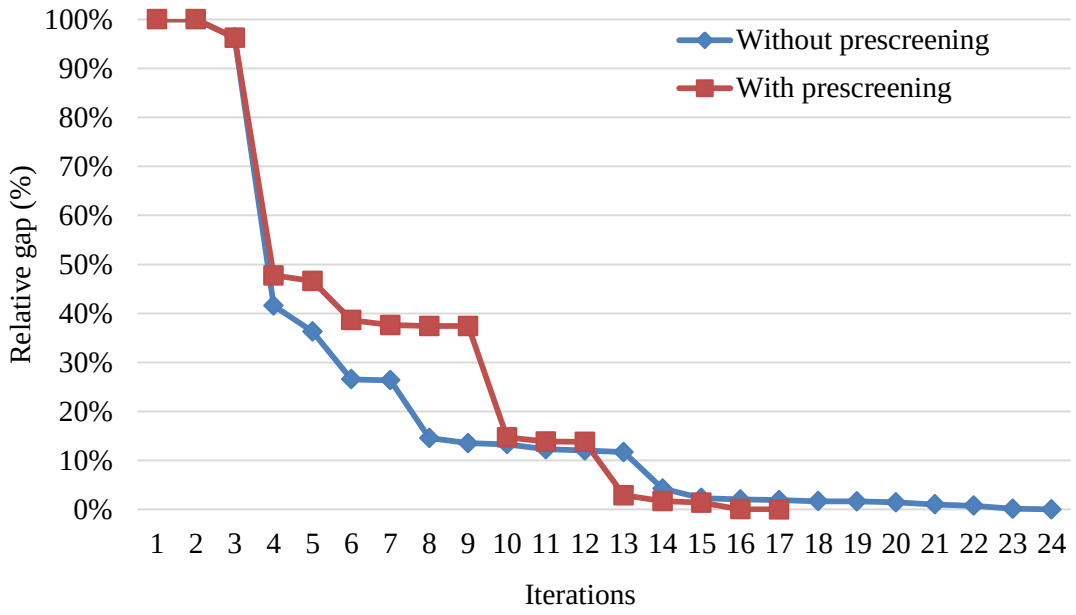

Fig. 7.12. Number of iteration w/ and w/o prescreening

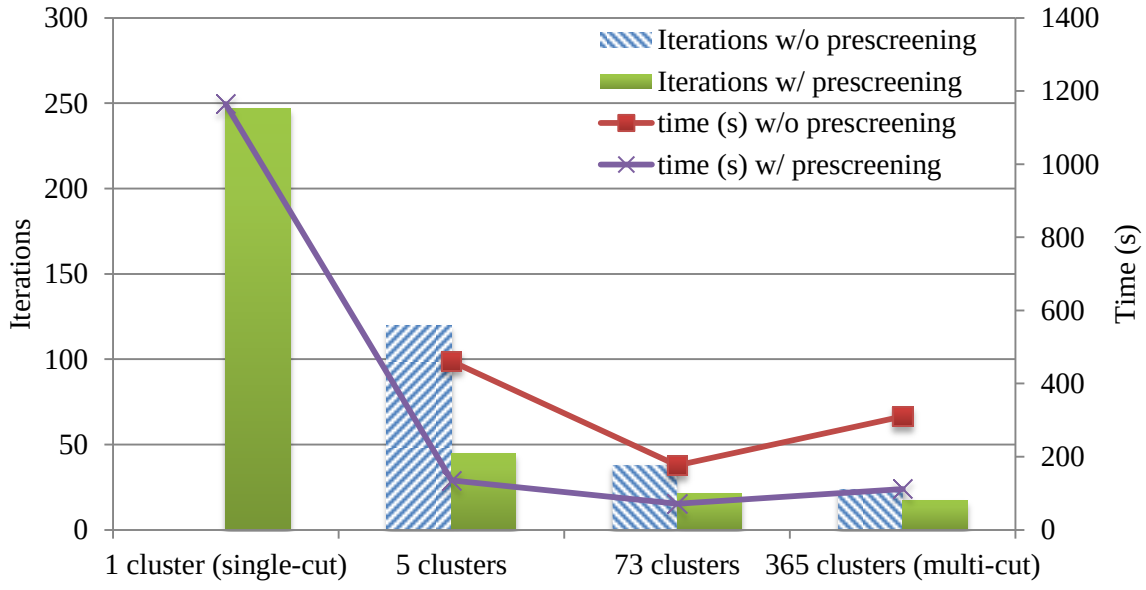

Fig. 7.13. Comparison of iterations and the execution time w/ and w/o prescreening

7.6.2 The IEEE 118-bus System

The IEEE 118-bus system [50] has 186 existing branches, 54 generators and 91 loads. The line ratings are reduced to create congestions. Detailed system parameters are provided in Appendix B. The system is divided into three zones as shown in Fig. 6.4 with the zonal data listed in Table 6.6. Unlike the 24-bus system, the IEEE 118-bus system does not have a load profile data for a year. Therefore, random loads are generated to construct different operating scenarios. The random loads are generated based on the assumptions that all the loads in the system independently follow the Gaussian distribution $N(\mu, 0.15\ \mu)$, where the given load level is used as the mean value μ. Based on the power flow result and the use the heuristics approach discussed previously, the following 20 lines selected as the candidate lines.

Table 7.5. Candidate lines parameters for IEEE 118-bus system

Number	From bus	To bus	Reactance (p.u.)	Rating (MW)	Cost (M$)
1	4	5	0.00798	400	1.8
2	5	6	0.054	120	9.7
3	30	17	0.0388	400	7
4	64	65	0.0302	400	5.4
5	94	95	0.0434	120	7.8
6	8	9	0.0305	400	5.5
7	8	5	0.0267	400	6
8	9	10	0.0322	400	5.8
9	23	32	0.1153	120	17.3
10	69	77	0.101	120	15.2
11	77	78	0.0124	120	2.8
12	99	100	0.0813	120	14.6
13	17	113	0.0301	120	5.4
14	3	5	0.108	120	16.2
15	5	6	0.054	120	9.7
16	82	83	0.03665	120	6.6
17	26	30	0.086	400	15.5
18	38	37	0.0375	400	6.8
19	80	99	0.206	120	30.9
20	94	100	0.058	120	10.4

First, 1000 random load scenarios are generated in the operating stage. The TEP problem is solved using the *L*-shaped method with 500 clusters (2 scenarios per cluster). The results are shown in Table 7.6, the relative gap in each iteration is shown in Fig. 7.14 and the expanded system one-line diagram is illustrated in Fig. 7.15.

Table 7.6. TEP results of IEEE 118-bus system with 1000 scenarios

Execution time (s)	Iterations	Investment cost (M$)	Expected annual operating cost (M$)	Selected lines
1336	25	80.4	807.85	3 – 5, 8 – 5, 8 – 9, 9 – 10, 64 – 65, 77 – 78, 80 – 99, 94 – 95

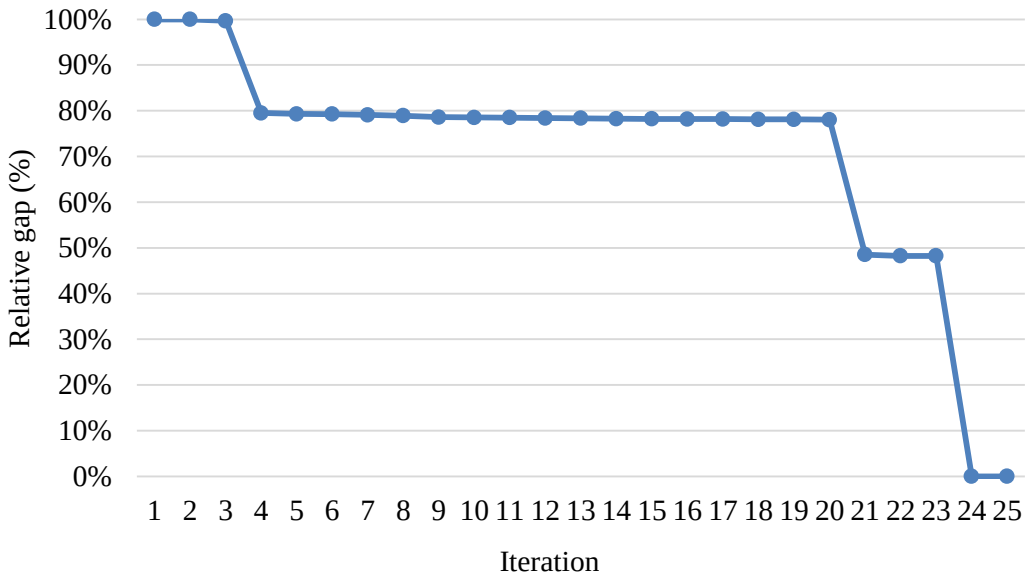

Fig. 7.14. Relative optimality gaps at every iteration (1000 scenarios)

In order to accelerate the computing speed while obtaining a solution with similar quality, the *K*-mean++ algorithm is used and the original 1000 scenarios are grouped into 500 and 100 clusters respectively. The weight of each cluster is proportional to the number of scenarios in the cluster, which can be calculated as follows,

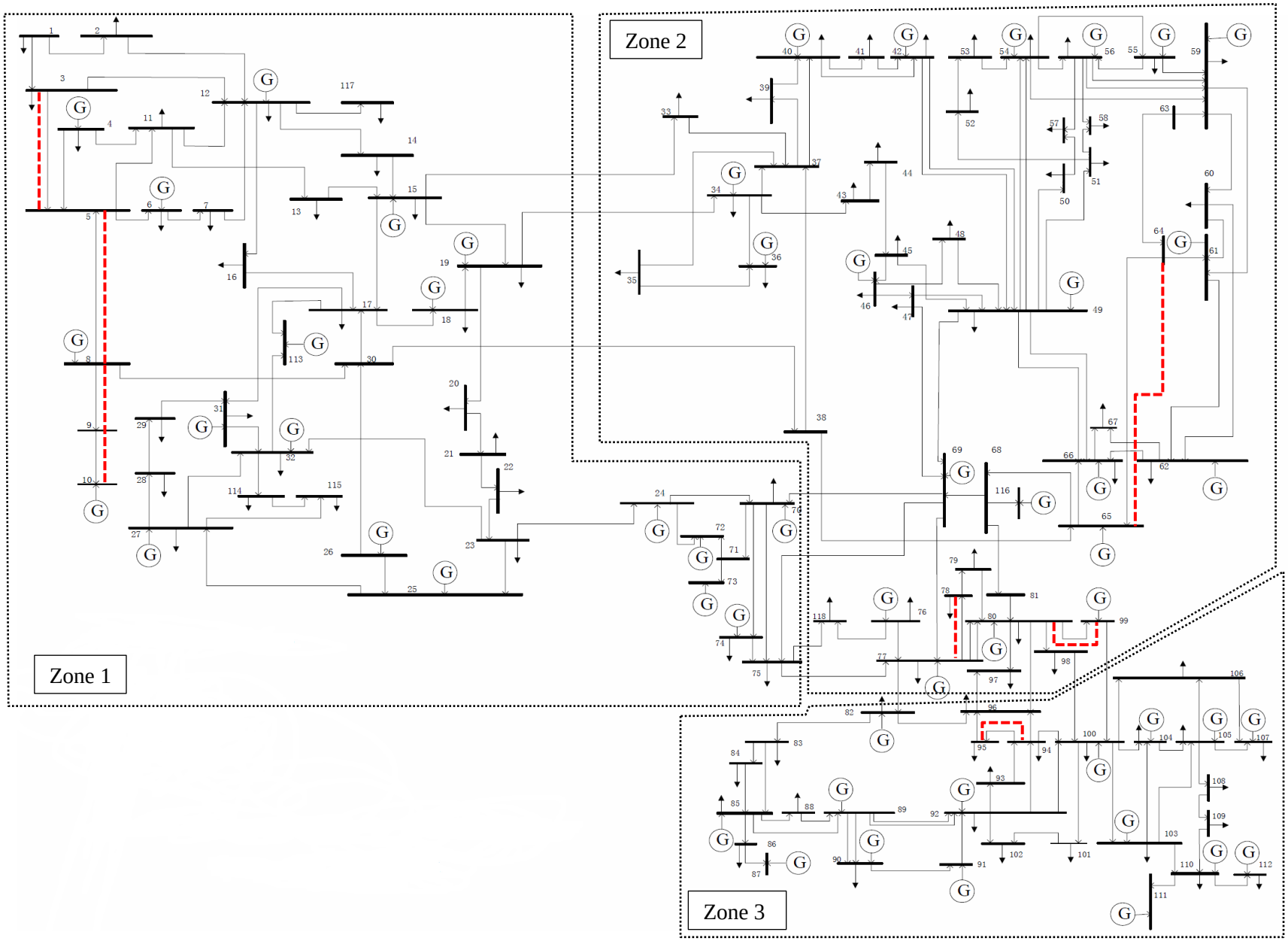

Fig. 7.15. One line diagram of expanded IEEE 118-bus system [50]

$$w^c = N^c \left(C/S \right) \tag{7.25}$$

where w^c is the weight of cluster c, S, C and N^c are number of total scenarios, number of total clusters, and number of scenarios falls in cluster c respectively. Taking the 500 clusters problem for example, if 10 out of the 1000 scenarios appear in the first cluster, then this cluster is assigned a weight of 5. The planning results are summarized in Table 7.7.

Table 7.7. TEP results of IEEE 118-bus system with scenarios grouping

Case	Investment cost (M$)	Annual operating cost (M$)	Selected lines	Execution time (s)
500 clusters	50	812.26	5 – 6, 8 – 5, 8 – 9, 9 – 10, 30 – 17, 64 – 65, 77 – 78, 94 – 95	466.3
100 clusters	52.9	816.17	8 – 5, 64 – 65, 77 – 78, 80 – 99, 94 – 95	38.1

The results shown in Table 7.7 indicate that the *K*-means clustering algorithm effectively reduces the number of scenarios and computing time; however, the quality of the solution after clustering needs to be closely examined. The essence of the *K*-mean based algorithms is to find the centroids that can best classify the original set of scenarios. The grouping process will modify the original problem by discarding some extreme cases. Therefore, the TEP result after the scenario grouping is expected to be different from what it would have been for the original problem. Clearly, this is observed from the results shown in Table 7.7. In fact, extreme cases can play an important role in the original problem solution. By discarding these extreme cases, the TEP result obtained from the clustered problem may cause an infeasible issue in the original problem. To rectify this problem, after solving the clustered problem, the original problem must also be solved with lines that are selected in the clustered problem fixed. Since the number of the

binary variables reduces, it is easier to solve the original problem with more scenarios and obtain at least a sub-optimal solution.

7.6.3 The 569-bus Reduced WECC System

The 569-bus reduced WECC system is created from the 2022 WECC full power flow case in .epc format. Since this is an interregional planning study for the entire WECC system, only the 500 kV and 230 kV backbone transmission lines in the full power flow case are retained in this reduced system. The reduced system has 805 existing transmission lines and an additional 689 candidate lines to be selected. There are a total number of 3751 generators. In order to study the impact of increase penetration of renewable resources on the entire WECC transmission system, potential renewable plants that are likely to be in service by 2022 are included in the reduced system. This planning study focus on the transmission paths among Balancing Authorities (BA), therefore, the system loads are aggregated to 39 load hubs, each corresponds to an individual BA in the Western Interconnection. There are 8 HVDC lines in the system, each is modeled as a power source or sink connected at an AC bus. The WECC 10-year and 20-year planning horizon are illustrated in Fig. 7.16.

Cycles:	Operational planning	Long term planning
Studies:	Scenario-based production cost analysis. Network is fixed	Scenario-based network expansion and generation resource planning
Time:	Year 2013 – Year 2022	Year 2023 – Year 2032

Fig. 7.16. WECC 10-year and 20-year planning horizon [1]

As indicated in Fig. 7.16, the planning framework that WECC is following can be divided into the operating planning cycle and the long term planning cycle with the em-

phasis on different time horizons. From present to 10-year ahead is known as the operating planning cycle. In this cycle, the transmission projects that were selected in the last long term planning cycle are included in the base case and the network topology is assumed fixed throughout this cycle. Scenario-base production cost analyses are performed in this cycle to evaluate the reliability of the system by monitoring the power flow on important transmission path. Sensitivity analyses are also performed to examine how certain parameters change, e.g., gas price, carbon price or renewable penetration, could affect the transmission utilizations as well as the cost of economic dispatch. Beyond the operating planning cycle, the following 10-years are known as the long term planning cycle. In this cycle, generation resources are planned based on the state RPS requirements to meet the forecasted load. All costs including generation and transmission expansions are financed in this cycle to obtain the present dollar value of the costs. Transmission corridors and candidate lines are selected to perform the network expansion studies. Similar sensitivity analyses are performed to examine how changes in gas price, carbon price or renewable penetration could affect the transmission expansion plans.

The 2032 reference case represents the "standard future". In order to study the seasonal impact, four scenarios are created for light spring (LSP), heavy summer (HS), light fall (LF) and heavy winter (HW) conditions, respectively. The generation dispatch is fixed for each season, which is calculated based on the state RPS goal and the annual capacity factor of each generator type. The objective function is to minimize the investment cost only. Fig. 7.17 to 7.20 visualizes the transmission expansion plan for each seasonal condition with the power flow direction marked by arrows. The visualizations are done using a Microsoft Excel tool originally developed by Mr. Ben Brownlee at WECC.

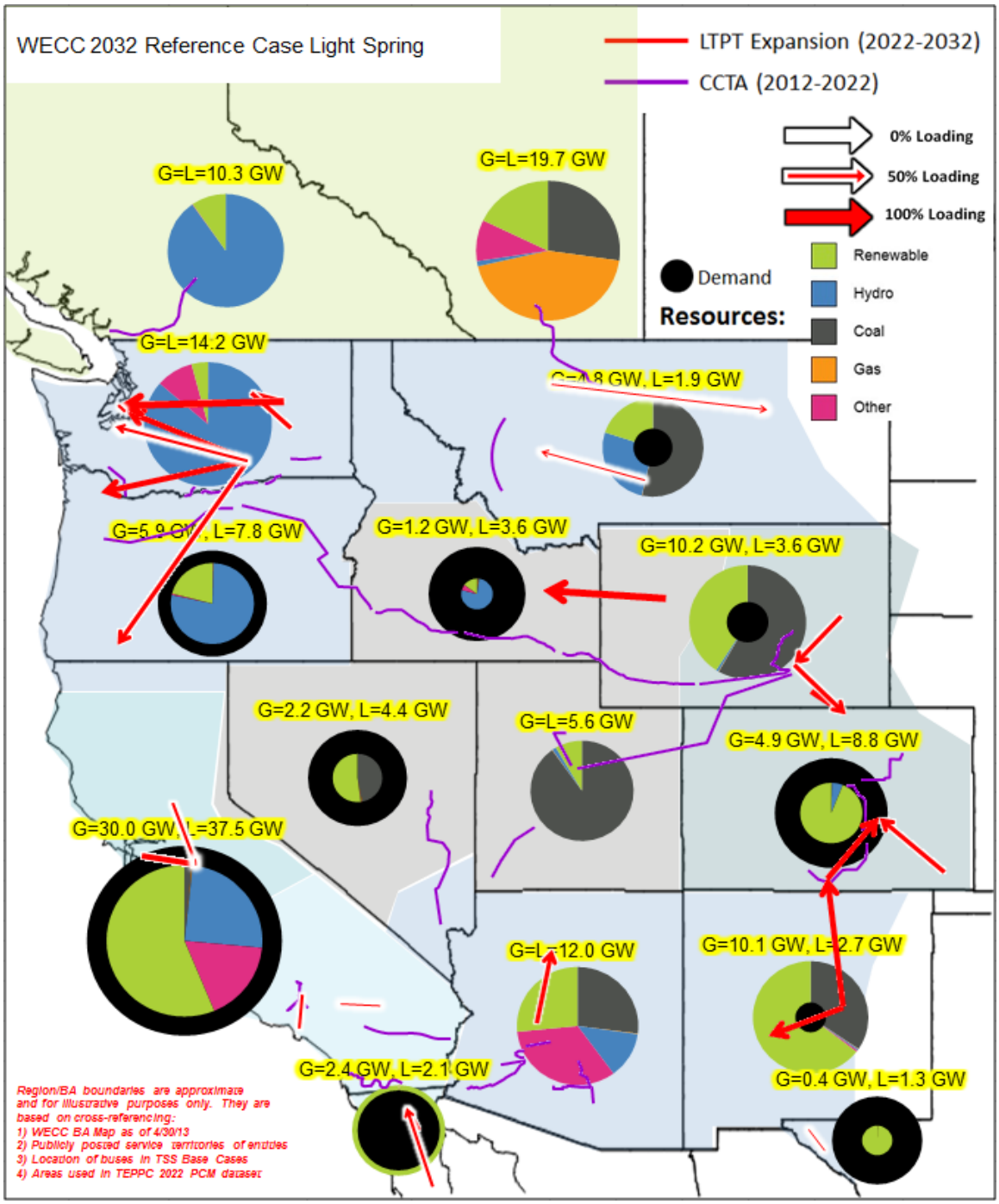

Fig. 7.17. Transmission expansion plan for WECC 2032 reference case – Light Spring

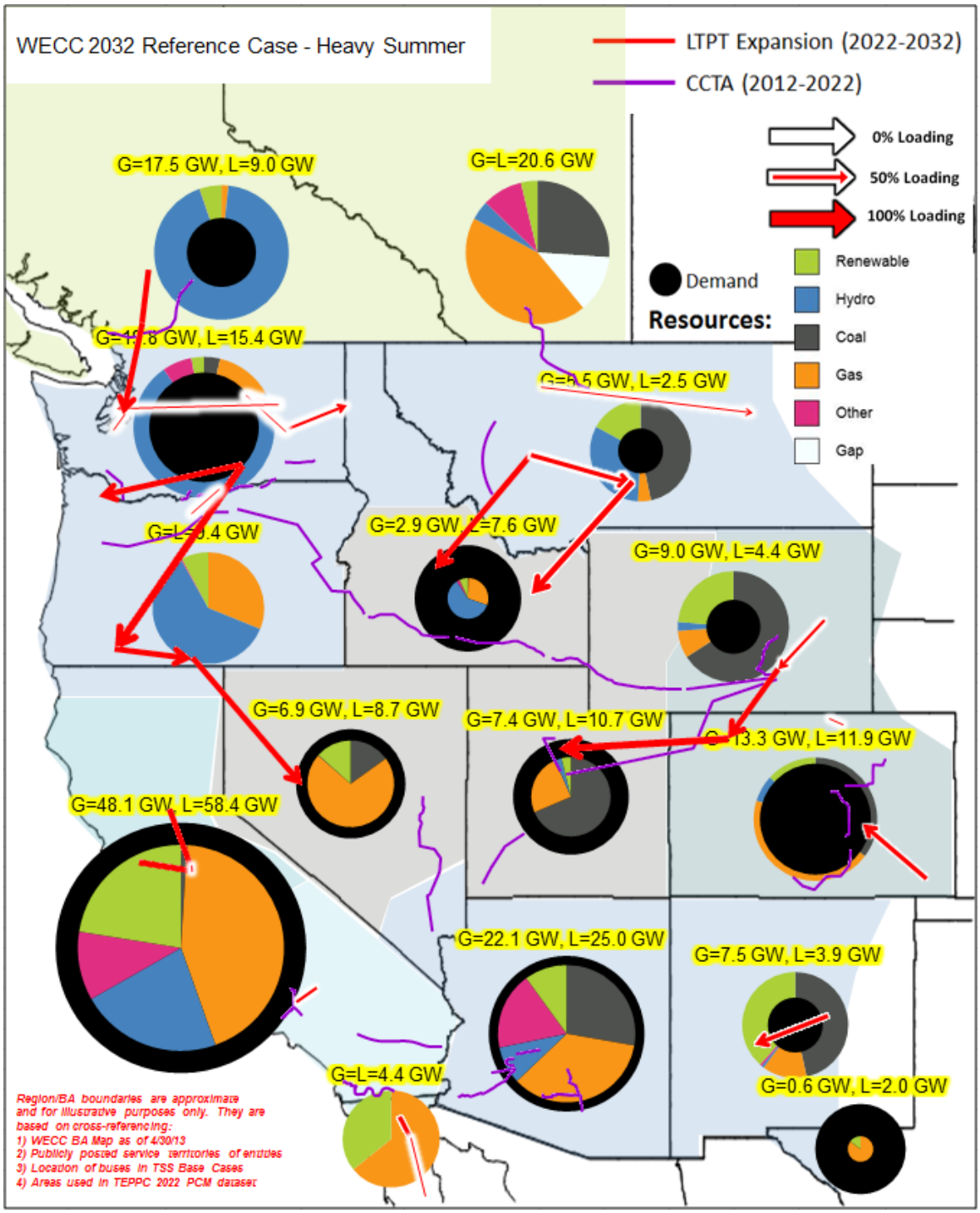

Fig. 7.18. Transmission expansion plan for WECC 2032 reference case – Heavy Summer

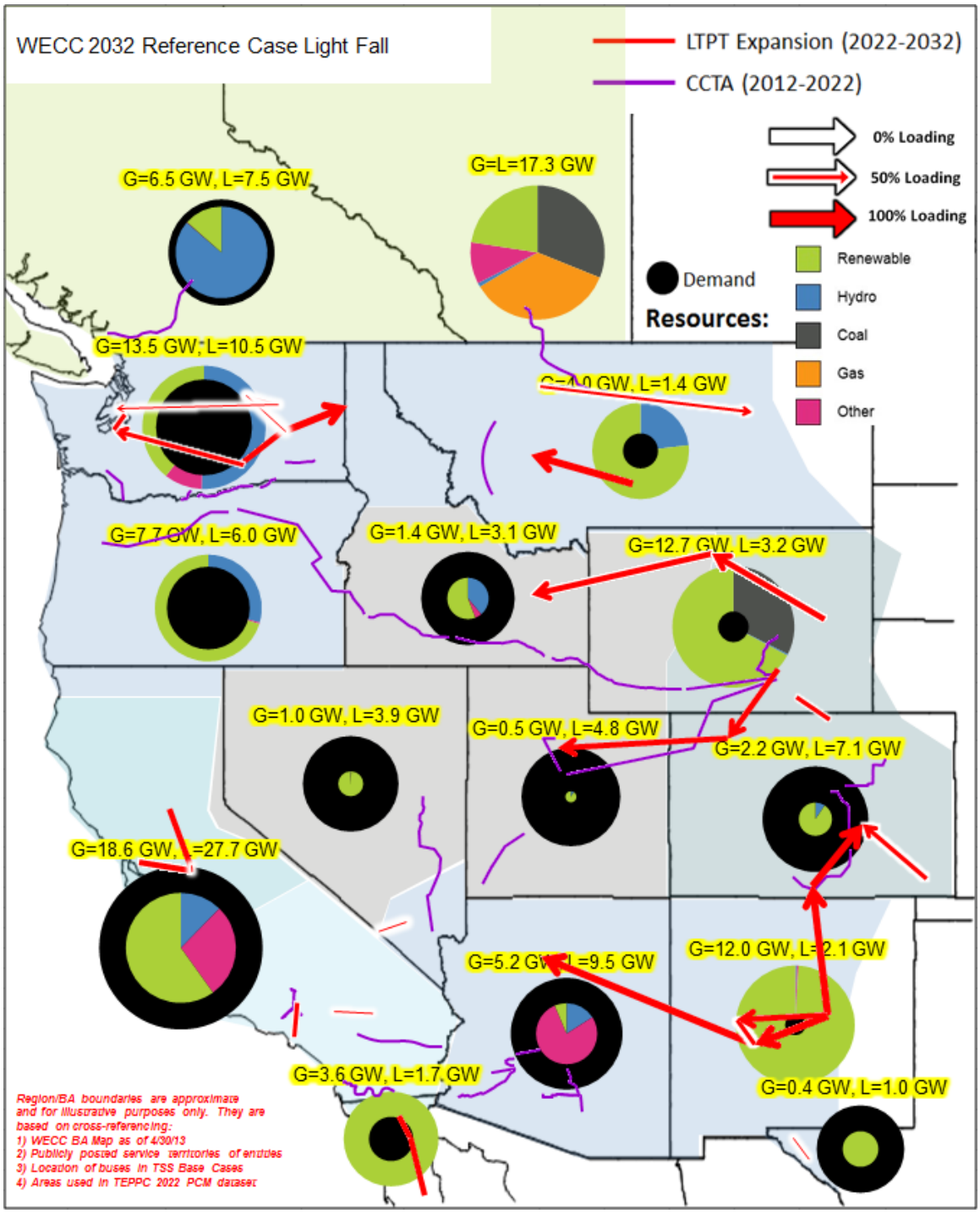

Fig. 7.19. Transmission expansion plan for WECC 2032 reference case – Light Fall

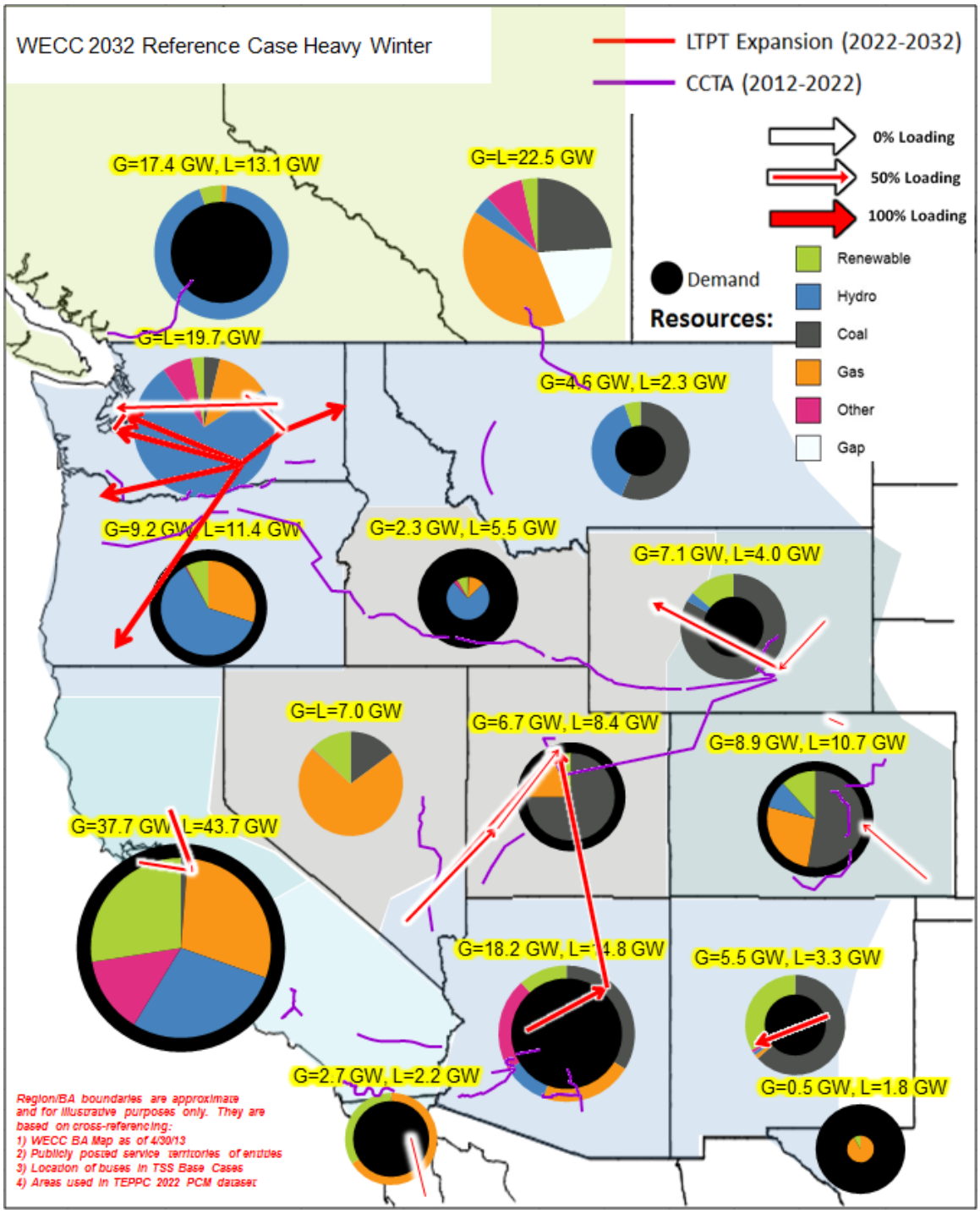

Fig. 7.20. Transmission expansion plan for WECC 2032 reference case – Heavy Winter

It is indicated from Fig. 7.17 to 7.20 that additional lines are usually selected to connect areas with generation surplus to areas have generation deficiency. It can be ob-

served that Wyoming and Montana, due to massive wind generation installation in the planning horizon, become power sources that serve other areas that do not have enough generations. Note that even though no new line is selected between some areas, it does not mean that there is no power transfer. Power can be transferred through the existing lines that are not plotted on the map or through the common case transmission assumptions (CCTA) lines that are built between 2013 and 2022. The summary of the planning result of these four seasons are provided in Table 7.8.

Table 7.8. Planning summary of the WECC 2032 reference case

Condition	Total load (MW)	Investment cost (M$)	Number of Selected lines
LSP	133969	9882.4	28
HS	194935	10333	30
LF	106658	12731.3	33
HW	170094	10719.4	24

There are only 5 lines that are in common within the above four expansion plans. This means that with different generation dispatches, the optimal network topologies could vary substantially. In order to find the overall optimal expansion plan, the original problem is reformulated as a stochastic programming problem with four operating conditions in the sub-problem. To solve the problem within an acceptable time, the number of candidate lines is reduced by starting fixing lines that are not selected by any of the four conditions to zero. With this heuristic, a good solution is obtained with 50 lines selected. The planning summary is shown in Table 7.9; the expansion plan and line utilizations for each condition are visualized in Fig. 7.21 – 7.24 respectively.

Table 7.9. Planning summary of the WECC 2032 reference case – all conditions

Condition	Total load (MW)	Investment cost (M$)	Number of Selected lines
All	605656	22461	50

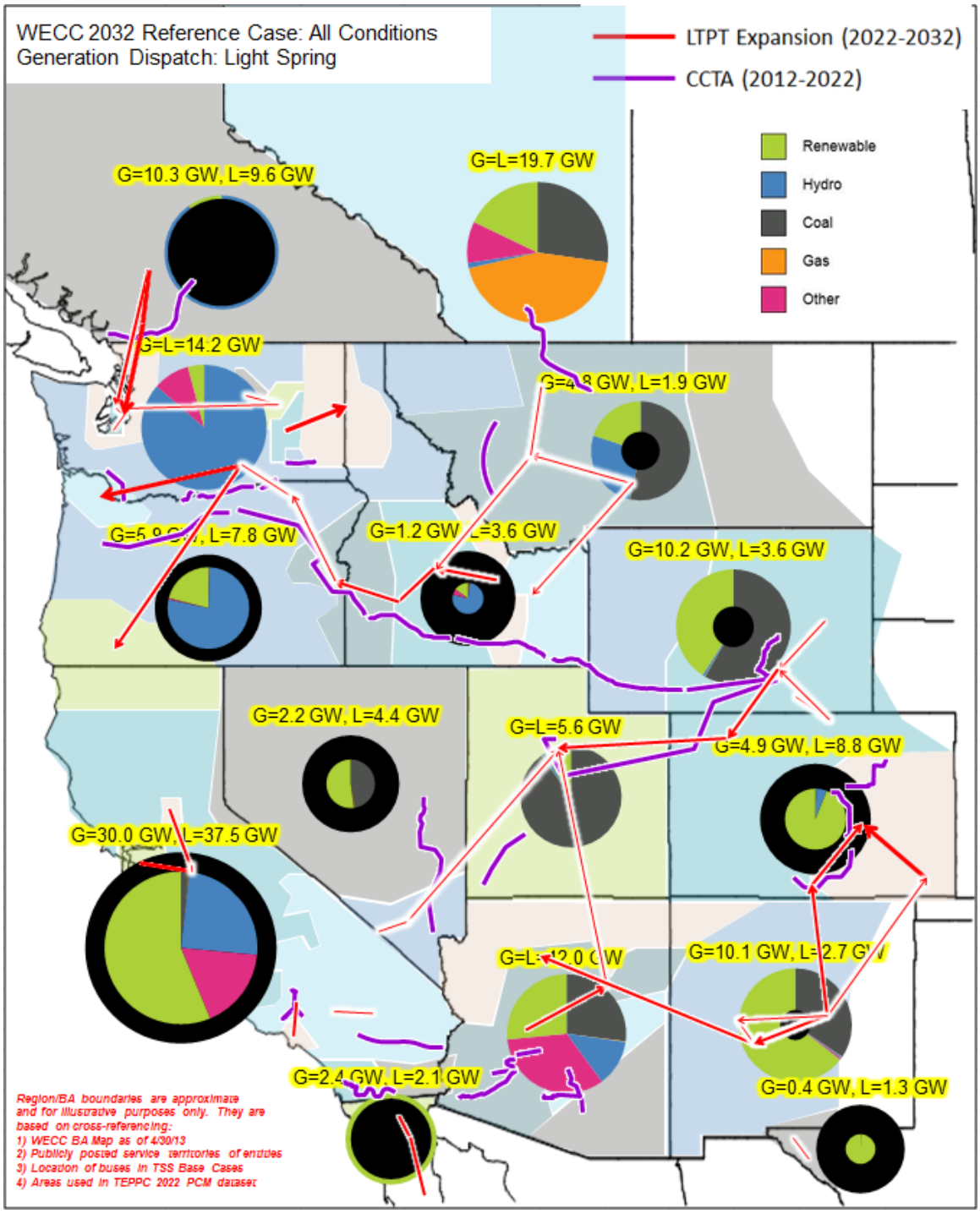

Fig. 7.21. WECC 2032 reference case line utilization – Light Spring

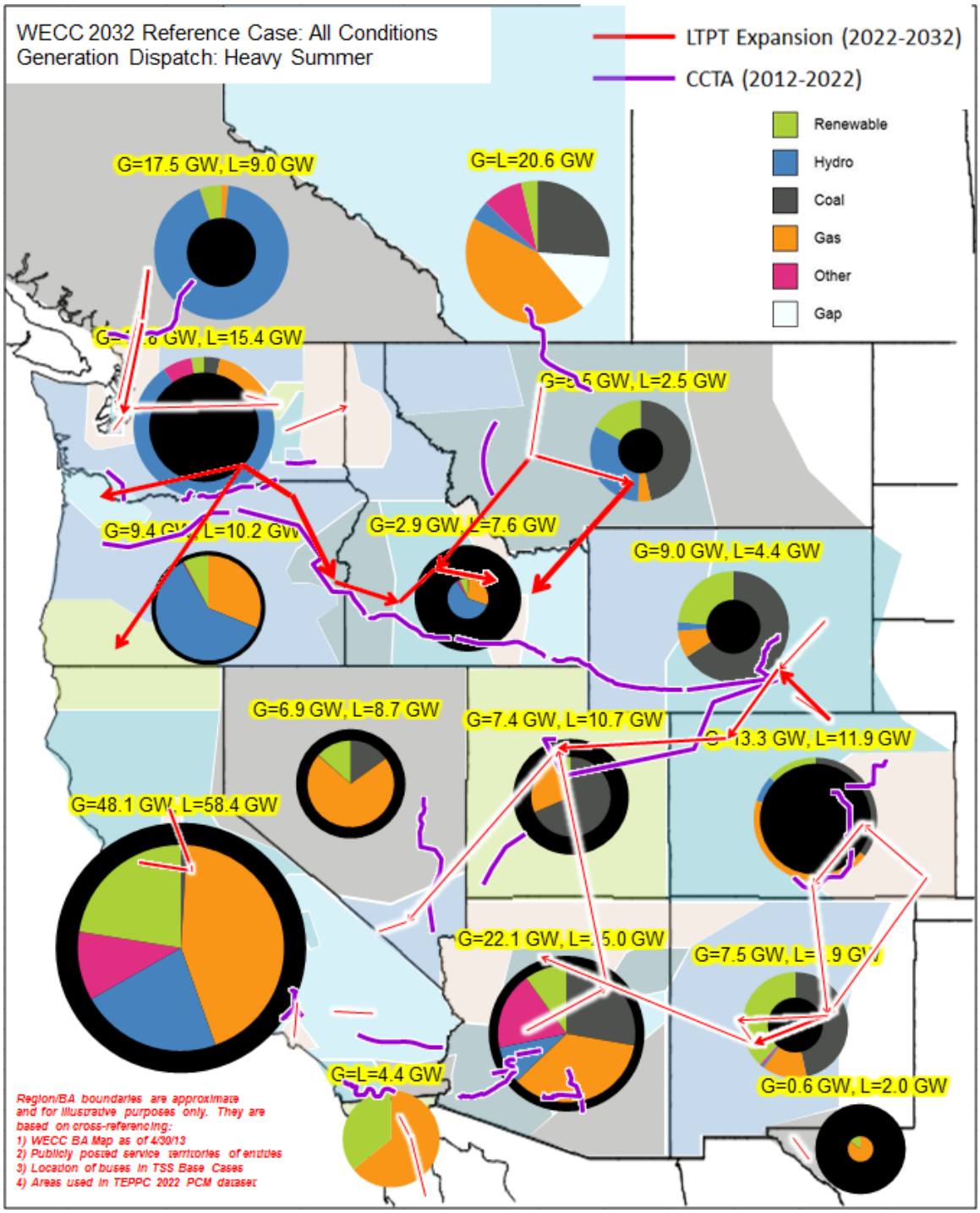

Fig. 7.22. WECC 2032 reference case line utilization – Heavy Summer

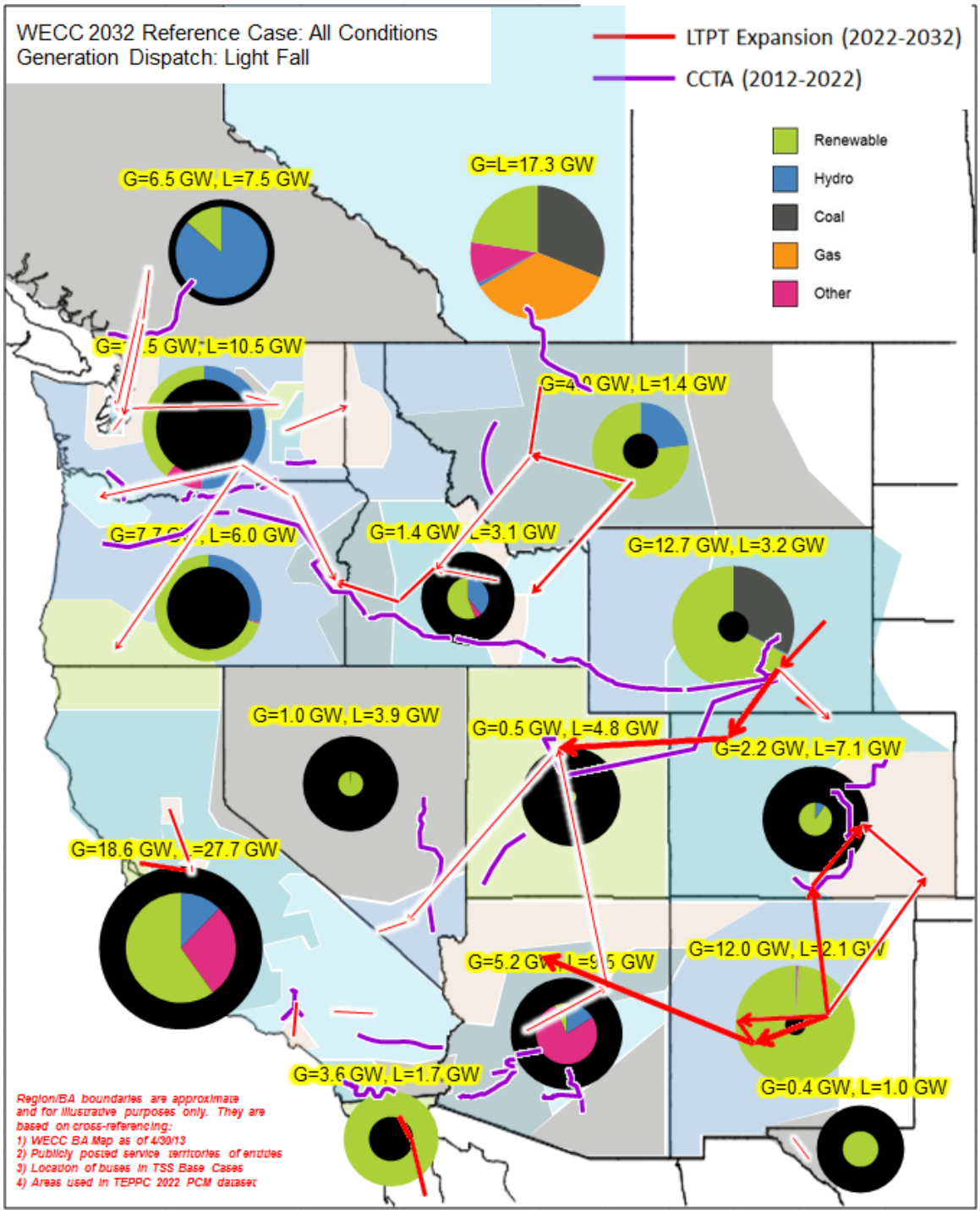

Fig. 7.23. WECC 2032 reference case line utilization – Light Fall

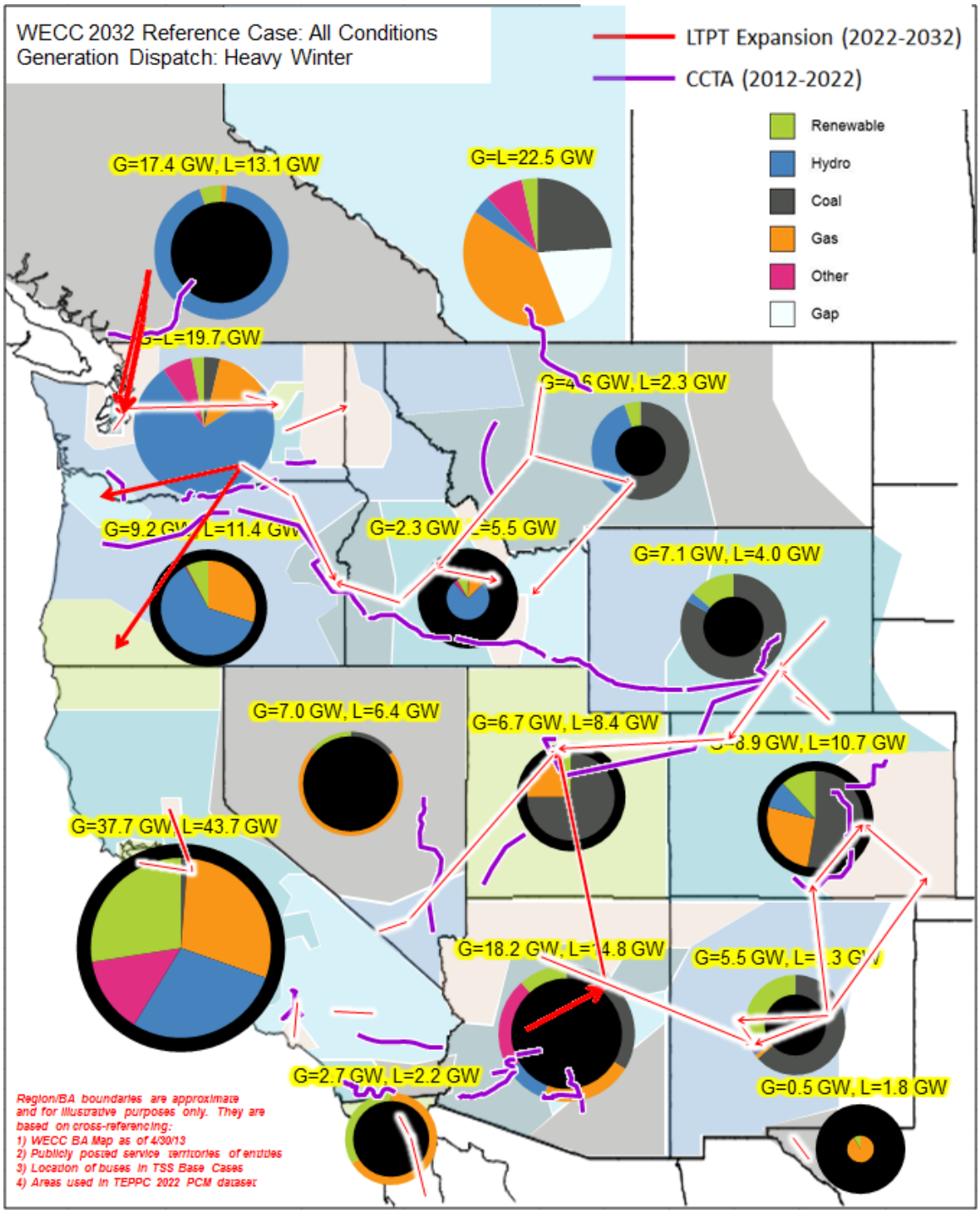

Fig. 7.24. WECC 2032 reference case line utilization – Heavy Winter

By examining Fig. 7.21 – 7.24, one can observe that in the north, lines are selected to connect British Columbia (BC), Washington, Oregon, Idaho and Montana. This is

to utilize the ample hydro resources in BC as well as the wind in Montana. In the south, lines are built to connect Nevada, Arizona, New Mexico, Utah, Colorado and Wyoming to utilize the solar in the desert areas and the wind in Wyoming. Notice that only a few in-state transmission lines are selected in California. The rest of the power will be imported from Arizona and the COI through the existing transmission facilities.

7.7 Summary

This chapter addresses the uncertainty modeling techniques in the TEP model. A two-stage stochastic TEP model is proposed. Algorithms using the *L*-shaped method and the PH are developed for solving the TEP model. The *K*-means algorithm is used to cluster the large number of scenarios in the second-stage.

The performance of the *L*-shaped method is compared with and PH and form in the case studies. The results show that the *L*-shaped method is superior to DE when the problem scale is large, while PH is very slow to converge if no heuristics are imbedded in the algorithm. The results also show that by partially aggregating scenarios in the second stage, the performance of the *L*-shaped method can be improved significantly. The 118-bus example show that the *K*-means clustering algorithm is effective in reducing the number of scenario but the solution quality of the clustered problem should be closely examined to avoid potential infeasible issues. The reduced WECC case shows how the TEP algorithm developed in this chapter can be used to solve real world planning problem. The simulation results have indicated that with the increasing penetration of renewable resource, additional transmission facilities are needed in the future U.S. Western Interconnection.

Chapter 8

CONCLUSIONS AND FUTURE WORK

8.1 Summary and Main Conclusions

The TEP problem for large power systems has been investigated in this dissertation and several new TEP models are presented to facilitate the regional TEP process. The main conclusions of this dissertation can be drawn as follows:

The loads are projected to increase 14% from 2009 to 2020 and the future generation mix is expected to have a significant departure from the past due to the massive integration of renewables to fulfill state-mandated RPS requirement. In order to connect remote renewable resources to the main power grid and prevent the potential overloads and violations of the reliability criteria, additional transmission capacity is essential in the future power system.

In Chapter 3, a MILP-based TEP model that considers the active power losses in the system and the $N-1$ criterion is proposed. Simulation results show the necessity and benefit of considering losses in TEP models. Inclusion of network losses may shift the cost from operations to investment, but will eventually provide a saving in total costs.

Chapter 4 explores the possibility of applying AC-based models to the TEP problem. The results suggest that it is possible to apply the AC model to develop TEP models, however, solving MINLP-based ACTEP models is still challenging. By relaxing the binary variables, the NLP-based ACTEP model can be solved for small systems within an acceptable time range and a local optimal solution can be obtained. Using the AC model for solving large-scale TEP problems still requires more research, especially breakthroughs in the global optimization theories.

A relaxed OPF model is developed in Chapter 5 based on a Taylor series. The proposed OPF model retains the reactive power, off-nominal bus voltage magnitudes as well as network losses. A MILP-based loss model is developed to eliminate the fictitious losses and relaxations of the MILP model are investigated. It is shown that inclusion of reactive power and the off-nominal bus voltage magnitudes makes the proposed OPF model a better approximation to the full ACOPF model. In terms of loss modeling, it is proved that by including reactive power in the model, the fictitious losses can still be present even if the all the LMPs are positive. A condition is given to identify the branches in which fictitious losses may be created. Binary variables are only needed for these branches instead of all the branches in the system.

Chapter 6 extends the relaxed ACOPF model developed in Chapter 5 to TEP studies and proposes the LACTEP model. An iterative approach for considering the $N-1$ criterion during the planning process is also developed and demonstrated on the test system. The advantage of the LACTEP model is that it dispatches the generators more accurately, gives a better estimation of the line flows, and provides a realistic TEP solution that the DC-based models usually fail to do. The iterative approach to incorporate the $N-1$ reliability criterion provides a way to make the expanded system comply with the $N-1$ contingency criterion. Mathematically, this iterative approach may not yield the optimal solution, but in terms of the computational burden, this approach attains the same goal more efficiently.

Chapter 7 addresses this uncertainty modeling techniques in the TEP model. The results in this chapter clearly show that the value of using stochastic TEP model is that it

can give a more accurate estimated to the annual operating cost as compared to the deterministic model, which is usually known for giving too conservative results.

8.2 Future Work

The following are possible areas for future research:

1. Use geospatial data to select the least cost transmission corridors.

Straight lines are usually assumed in the TEP studies; however, it not realistic to have straight line in practice and it may also result in inaccurate line cost data. Algorithms for calculating the least cost transmission corridors, e.g. Dijkstra's algorithm and Google Maps algorithm should be investigated.

2. More sophisticated HVDC line modeling in the TEP model.

Right now, HVDC lines are modeled by using a fixed power source or sink. More sophisticated HVDC modeling can be investigated to consider the multilevel power flows on the lines.

3. Coordinating TEP with generation expansion planning (GEP) by properly allocation transmission investment cost.

The selection of different generation resources can greatly affect the TEP result. On the other hand, if the transmission investment costs are allocated to the newly connected generator, then it may affect the decision of the generator resource selection as well. The mutual relationship between TEP and GEP can be investigated in the future to better coordinate the two processes.

REFERENCES

[1] Western Electricity Coordinating Council (WECC), "WECC 10-year regional transmission plan summary," Sept. 2011. [Online]. Available: http://www.wecc.biz/library/StudyReport/Documents/Plan_Summary.pdf

[2] G. Latorre, R. D. Cruz, J. M. Areiza, and A. Villegas, "Classification of publications and models on transmission expansion planning," *IEEE Trans. Power Syst.*, vol. 18, no. 2, pp. 938-946, May 2003.

[3] L. L. Garver, "Transmission network estimation using linear programming," *IEEE Trans. Power Apparatus and Syst.*, vol. PAS-89, pp. 1688–1697, Sept./Oct. 1970.

[4] L. Bahiense, G. C. Oliveira, M. Pereira, and S. Granville, "A mixed integer disjunctive model for transmission network expansion," *IEEE Trans. Power Syst.*, vol. 16, no. 3, pp. 560–565, Aug. 2001.

[5] N. Alguacil, A. L. Motto, and A. J. Conejo, "Transmission expansion planning: a mixed-integer LP approach," *IEEE Trans. Power Syst.*, vol. 18, no. 3, pp. 1070 - 1077, Aug. 2003.

[6] S. de la Torre, A. J. Conejo, and J. Contreras "Transmission expansion planning in electricity markets," *IEEE Trans. Power Syst.*, vol. 23, vo. 1, pp. 238–248, Feb. 2008.

[7] L. P. Garces, A. J. Conejo, R. Garcia-Bertrand, and R. Romero, "A bilevel approach to transmission expansion planning within a market environment," *IEEE Trans. Power Syst.*, vol. 24, no. 3, pp. 1513–1522, Aug. 2009.

[8] A. Khodaei, M. Shahidehpour, and S. Kamalinia, "Transmission switching in expansion planning," *IEEE Trans. Power Syst.*, vol. 25, no. 3, pp. 1722–1733, Aug. 2010.

[9] A. Seifu, S. Salon, and G. List, "Optimization of transmission line planning including security constraints," *IEEE Trans. Power Syst.*, vol. 4, pp. 1507–1513, Oct. 1989.

[10] *NERC System performance under normal conditions*, NERC Standard TPL-001-0.1, Oct. 2008.

[11] H. Zhang, V. Vittal, G. T. Heydt, and J. Quintero, "A mixed-integer linear programming approach for multi-stage security-constrained transmission expansion planning," *IEEE Trans. Power Syst.*, vol. 27, no. 2, pp. 1125-1133, May 2012.

[12] R. P. O'Neill, E. A. Krall, K. W. Hedman, and S. S. Oren, "A model and approach for optimal power systems planning and investment," *Mathematical Programming*, to be published.

[13] K. W. Hedman, R. P. O'Neill, E. B. Fisher, and S. S. Oren, "Optimal transmission switching with contingency analysis," *IEEE Trans. Power Syst.*, vol. 24, no. 3, pp. 1577-1586, Aug. 2009.

[14] M. J. Rider, A.V. Garcia, and R. Romero, "Power system transmission network expansion planning using AC model," *IET Gener. Transm. Distrib.*, vol. 1, no. 5, pp. 731–742, Sept. 2007.

[15] H. Zhang, G. T. Heydt, V. Vittal, and H. D. Mittelmann, "Transmission expansion planning using an AC model: formulations and possible relaxations," *IEEE PES General Meeting*, July 2012.

[16] G. C. Otiveira, A. P. C. Costa, and S. Binato, "Large scale transmission network planning using optimization and heuristic techniques," *IEEE Trans. Power Syst.*, vol. 10, no. 4, pp. 1828-1834, Nov. 1995.

[17] E. L. da Silva, J. M. A. Ortiz, G. C. de Oliveira, and S. Binato, "Transmission network expansion planning under a tabu search approach," *IEEE Trans. Power Syst.*, vol. 16, no. 1, pp. 62-68, Feb. 2001.

[18] E. L. da Silva, H. A. Gil, and J. M. Areiza, "Transmission network expansion planning under an improved genetic algorithm," *IEEE Trans. Power Syst.*, vol. 15, no. 3, pp. 1168-1175, Aug. 2000.

[19] S. Binato, G. C. de Oliveira, and J. L. de Araújo, "A greedy randomized adaptive search procedure for transmission expansion planning," *IEEE Trans. Power Syst.*, vol. 16, no. 2, pp. 247-253, May 2001.

[20] R. Romero, R.A. Gallego, and A. Monticelli, "Transmission system expansion planning by simulated annealing," *IEEE Trans. Power Syst.*, vol. 11, no. 1, pp. 364-369, Feb. 1996.

[21] N. Leeprechanon, P. Limsakul, and S. Pothiya, "Optimal transmission expansion planning using ant colony optimization," *Journal of Sustainable Energy & Environment*, vol. 1. pp. 71-76, 2010.

[22] J. H. Roh, M. Shahidehpour, and L. Wu, "Market-based generation and transmission planning with uncertainties," *IEEE Trans. Power Syst.*, vol. 24, no. 3, pp. 1587-1598, Aug. 2009.

[23] P. Maghouli, S. H. Hosseini, M. O. Buygi, and M. Shahidehpour, "A scenario-based multi-objective model for multi-stage transmission expansion planning," *IEEE Trans. Power Syst.*, vol. 26, no. 1, pp. 470-478, Feb. 2011.

[24] B. G. Gorenstin, N. M. Campodonico, J. P. Costa, and M. V. F. Pereira, "Power system expansion planning under uncertainty," *IEEE Trans. Power Syst.*, vol. 8, no. 1, pp. 129-136, Feb. 1993.

[25] A. M. L. da Silva, S. M. P. Ribeiro, V. L. Arienti, R. N. Allan, and M. B. D. C. Filho "Probabilistic load flow techniques applied to power system expansion planning," *IEEE Trans. Power Syst.*, vol. 5, no. 4, pp. 1047-1053, Nov. 1990.

[26] H. Yu, C. Y. Chung, K. P. Wong, and J. H. Zhang, "A chance constrained transmission network expansion planning method with consideration of load and wind farm uncertainties," *IEEE Trans. Power Syst.*, vol. 24, no. 3, pp. 1568-1576, Aug. 2009.

[27] W. Li, and P. Choudhury, "Probabilistic transmission planning", *IEEE power and Energy Magazine*, vol. 5, no. 5, pp. 46-53, 2007.

[28] J. Choi, T. Tran, A. A. El-Keib, R. Thomas, H. Oh, and R. Billinton, "A method for transmission system expansion planning considering probabilistic reliability criteria," *IEEE Trans. Power Syst.*, vol. 20, no. 3, pp. 1606-1615, Aug. 2005.

[29] P. Sánchez-Martín, A. Ramos, and J. F. Alonso, "Probabilistic midterm transmission planning in a liberalized market," *IEEE Trans. Power Syst.*, vol. 20, no. 4, pp. 2135-2142, Nov. 2005.

[30] A. H. Escobar, R. A. Gallego, and R. Romero, "Multistage and coordinated planning of the expansion of transmission systems," *IEEE Trans. Power Syst.*, vol. 19, no. 2, pp.735-744, May 2004.

[31] A. S. D. Braga, and J. T. Saraiva, "A multiyear dynamic approach for transmission expansion planning and long-term marginal costs computation," *IEEE Trans. Power Syst.*, vol. 20, no. 3, pp. 1631-1639, Aug. 2005.

[32] M. Xie, J. Zho,g, and F. F. Wu, "Multiyear transmission expansion planning using ordinal optimization," *IEEE Trans. Power Syst.*, vol. 22, no. 4, pp. 1420-1428, Nov. 2007.

[33] M. S. Sepasian, H. Seifi, A. A. Foroud, and A. R. Hatami, "A multiyear security constrained hybrid generation-transmission expansion planning algorithm including fuel supply costs," *IEEE Trans. Power Syst.*, vol. 24, no. 3, pp. 1609-1618, Aug. 2009.

[34] G. Andersson, *Modeling and Analysis of Electric Power Systems*, ETH Zurich, Sept. 2008, [Online]. Available:
http://www.eeh.ee.ethz.ch

[35] J. Carpentier, "Optimal power flows," *Int. J. Elect. Power Energy Syst.*, vol. 1, no. 1, pp. 3–15, 1979.

[36] H. W. Dommel, and W. F. Tinney, "Optimal power flow solutions," *IEEE Trans. Power App. Syst.*, vol. PAS-87, no. 10, pp. 1866–1876, Oct. 1968.

[37] D. I. Sun, B. Ashley, B. Brewer, A. Hughes, and W. F. Tinney, "Optimal power flow by Newton approach," *IEEE Trans. Power App. Syst.*, vol. PAS-103, no. 10, pp. 2864-2880, Oct. 1984.

[38] H. Wei, H. Sasaki, J. Kubokawa, and R. Yokoyama, "An interior point nonlinear programming for optimal power flow problems with a novel data structure," *IEEE Trans. Power Syst.*, vol. 13, no. 3, Aug. 1998.

[39] W. Yan, J. Yu, D. C. Yu, and K. Bhattarai, "A new optimal reactive power flow model in rectangular form and its solution by predictor corrector primal dual interior point method," *IEEE Trans. Power Syst.*, vol. 21, no. 1, Feb. 2006.

[40] H. Wang, C. E. Murillo-Sánchez, R. D. Zimmerman, and R. J. Thomas, "Computational issues of market-based optimal power flow," *IEEE Trans. Power Syst.*, vol. 22, no. 3, pp. 1185-1193, Aug. 2007.

[41] O. Alsac, J. Bright, M. Prais, and B. Stott, "Further developments in LP-based optimal power flow," *IEEE Trans. Power Syst.*, vol. 5, no. 3, pp. 697-711, Aug. 1990.

[42] T. Overbye, X. Cheng, and Y. Sun, "A comparison of the AC and DC power flow models for LMP calculations," in *Proc. 37th Hawaii Int. Conf. Syst. Sci.*, 2004.

[43] B. Stott, J. Jardim, and O. Alsac, "DC power flow revisited," *IEEE Trans. Power Syst.*, vol. 24, no. 3, pp. 1290–1300, Aug. 2009.

[44] H. Liu, L. Tesfatsion, and A. A. Chowdhury, "Locational marginal pricing basics for restructured wholesale power markets," *IEEE PES General Meeting*, July 2009.

[45] P. Sánchez-Martín, and A. Ramos, "Modeling transmission ohmic losses in a stochastic bulk production cost model," [Online]. Available: http://www.iit.upcomillas.es/aramos/papers/losses.pdf

[46] R. Palma-Benhke, A. Philpott, A. Jofré, and M. Cortés-Carmona, "Modeling network constrained economic dispatch problems," *Optimization and Engineering*, Springer, Oct. 2012.

[47] S. S. Oren, and G. Gross, "Economic impact assessment of transmission enhancement projects," *Final PSERC Project Report*, Sept. 2009, [Online]. Available: http://www.pserc.wisc.edu/docsa/Oren_PSERC_M_14_Final_Report_2009_ES.pdf

[48] S. Binato, M. V. F. Pereira, and S. Granville, "A new benders decomposition approach to solve power transmission network design problems," *IEEE Trans. Power Syst.*, vol. 16, no. 2, pp. 235-240, May 2001.

[49] Z. Hu, H. Cheng, Z. Yan, and F. Li, "An iterative LMP calculation method considering loss distributions," *IEEE Trans. Power Syst.*, vol. 25, no. 3, pp. 1469-1477, Aug. 2010.

[50] ECE Department, Illinois Institute of Technology (IIT), IEEE 118-bus system data, [Online]. Available: http://motor.ece.iit.edu/Data/JEAS_IEEE118.doc

[51] R. Fourer, D. M. Gay, and B. W. Kernighan, *AMPL: A Modeling Language for Mathematical Programming*, 2nd edition, Florence, KY: Duxbury Press, 2002.

[52] Gurobi Optimization, "Gurobi optimizer reference manual," [Online]. Available: http://www.gurobi.com

[53] P. Belotti, *Couenne: a user's manual*. Technical report, Lehigh University, 2009. [Online]. Available: http://www.coin-or.org/Couenne

[54] P. Bonami, and J. Lee, *Bonmin user's manual*. Technical report, IBM Corporation, June 2007. [Online]. Available: https://projects.coin-or.org/Bonmin

[55] R. A. Waltz, and T. D. Plantenga, *Knitro user's manual*, Sept. 2010, [Online]. Available: http://seldon.it.northwestern.edu/sscc/knitro/Knitro70_UserManual.pdf

[56] L. Liberti, and C. Pantelides, "An exact reformulation algorithm for large nonconvex NLPs involving bilinear terms," *Journal of Global Optimization*, no. 36, pp. 161–189, April 2006.

[57] IEEE RTS Task Force, "The IEEE reliability test system-1996," *IEEE Trans. Power Syst.*, vol. 14, no. 3, pp. 1010-1020, Aug. 1999.

[58] B. Stott, J. Jardim, and O. Alsac, "DC power flow revisited," *IEEE Trans. Power Syst.*, vol. 24, no. 3, pp. 1290–1300, Aug. 2009.

[59] C. Coffrin, and P. V. Hentenryck, "A Linear-programming approximation of AC power flows," June 2012, [Online]. Available: http://arxiv.org/abs/1206.3614

[60] X. Bai, H. Wei, K. Fujisawa, and Y. Wang, "Semidefinite programming for optimal power flow problems," *Intl J. of Electrical Power & Energy Systems*, vol. 30, no. 6-7, pp. 383–392, July-Sept. 2008.

[61] J. Lavaei, and S. Low, "Zero duality gap in optimal power flow," *IEEE Trans. Power Syst.*, vol. 27, no. 1, pp. 92–107, Feb. 2012.

[62] M. Farivar, and S. Low, "Branch flow model: relaxations and convexification," Nov. 2012, [Online]. Available: http://arxiv.org/pdf/1204.4865.pdf

[63] D. T. Phan, "Lagrangian duality and branch-and-bound algorithms for optimal power flow," *Operations Research*, vol. 60, no. 2, pp. 275–285, March-April 2012.

[64] A. Gopalakrishnan, A. U. Raghunathan, D. Nikovski, and L. T. Biegler, "Global optimization of optimal power flow using a branch & bound algorithm," Nov. 2012, [Online]. Available: http://numero.cheme.cmu.edu/uploads/globalOptBBOPF_v6(1).pdf

[65] B. Lesieutre, D. Molzahn, A. Borden, and C. L. DeMarco, "Examining the limits of the application of semidefinite programming to power flow problems," *in Proc. of the Allerton Conf. on Comm., Ctrl. and Computing*, Sept. 2011.

[66] R. D. Zimmerman, C. E. Murillo-Sánchez, and R. J. Thomas, "Matpower: steady-state operations, planning and analysis tools for power systems research and education," *IEEE Trans. Power Syst.*, vol. 26, no. 1, pp. 12-19, Feb. 2011.

[67] U.S. Energy Information Administration, "Electric power annual 2009," April 2011, [Online]. Available: http://www.eia.gov/electricity/annual

[68] T. Mason, T. Curry, and D. Wilson, "Capital costs for transmission and substations: recommendations for WECC transmission expansion planning," Oct. 2012, [Online]. Available: https://www.wecc.biz/committees/BOD/TEPPC/12110102/Lists/Minutes/1/BV_WECC_TransCostReport_Final.pdf

[69] WECC, WECC 10-year regional transmission plan: 2020 hourly loads, [Online]. Available: http://www.wecc.biz/LIBRARY/STUDYREPORT/Wiki%20Pages/Home.aspx

[70] J. R. Birge, and F. Louveaux, *Introduction to Stochastic Programming, 2nd edition.* New York: Springer Verlag, 2010.

[71] X. Zhu, "Discrete two-stage stochastic mixed-integer programs with applications to airline fleet assignment and workforce planning problems," Ph.D. dissertation, Department of Industry and System Engineering, Virginia Polytechnic Institute and State University, Blacksburg, Virginia, 2006.

[72] R. T. Rockafellar, and R. J-B. Wets, "Scenarios and policy aggregation in optimization under uncertainty," *Mathematics of Operations Research*, 1991, pp. 119–147.

[73] S. Trukhanov, L. Ntaimo, and A. Schaefer, "Adaptive multicut aggregation for two-stage stochastic linear programs with recourse," *European Journal of Operational Research*, v. 206, pp. 395–406, Feb. 2010.

[74] M. Matteucci, "A tutorial on clustering algorithms: k-means clustering," [Online]. Available: http://home.deib.polimi.it/matteucc/Clustering/tutorial_html/kmeans.html

[75] D. Arthur, and S. Vassilvitskii. "K-means++: the advantages of careful seeding," *Proceedings of the 18th annual ACM-SIAM symposium on Discrete algorithms*, Society for Industrial and Applied Mathematics, 2007.

APPENDIX A

IEEE 24-BUS SYSTEM DATA

Generator Data								
No.	**Bus**	Q^{max}	Q^{min}	P^{max}	P^{min}	c_g	b_g	a_g
1	1	10	0	20	16.0	400.7	130.0	0.00
2	1	10	0	20	16.0	400.7	130.0	0.00
3	1	30	-25	76	15.2	212.3	16.1	0.01
4	1	30	-25	76	15.2	212.3	16.1	0.01
5	2	10	0	20	16.0	400.7	130.0	0.00
6	2	10	0	20	16.0	400.7	130.0	0.00
7	2	30	-25	76	15.2	212.3	16.1	0.01
8	2	30	-25	76	15.2	212.3	16.1	0.01
9	7	60	0	100	25.0	781.5	43.7	0.05
10	7	60	0	100	25.0	781.5	43.7	0.05
11	7	60	0	100	25.0	781.5	43.7	0.05
12	13	80	0	197	69.0	832.8	48.6	0.01
13	13	80	0	197	69.0	832.8	48.6	0.01
14	13	80	0	197	69.0	832.8	48.6	0.01
15	14	200	-50	0	0.0	0.0	0.0	0.00
16	15	6	0	12	2.4	86.4	56.6	0.33
17	15	6	0	12	2.4	86.4	56.6	0.33
18	15	6	0	12	2.4	86.4	56.6	0.33
19	15	6	0	12	2.4	86.4	56.6	0.33
20	15	6	0	12	2.4	86.4	56.6	0.33
21	15	80	-50	155	54.3	382.2	12.4	0.01
22	16	80	-50	155	54.3	382.2	12.4	0.01
23	18	200	-50	400	100.0	395.4	4.4	0.00
24	21	200	-50	400	100.0	395.4	4.4	0.00
25	22	16	-10	50	10.0	0.0	0.0	0.00
26	22	16	-10	50	10.0	0.0	0.0	0.00
27	22	16	-10	50	10.0	0.0	0.0	0.00
28	22	16	-10	50	10.0	0.0	0.0	0.00
29	22	16	-10	50	10.0	0.0	0.0	0.00
30	22	16	-10	50	10.0	0.0	0.0	0.00
31	23	80	-50	155	54.3	382.2	12.4	0.01
32	23	80	-50	155	54.3	382.2	12.4	0.01
33	23	150	-25	350	140.0	665.1	11.8	0.00

Branch Data (100 MW base)								
No.	**From**	**To**	r_k	x_k	b_k	t_k	S^{max}(MW)	c_k
1	1	2	0.0026	0.0139	0.4611	0	175	3
2	1	3	0.0546	0.2112	0.0572	0	175	55
3	1	5	0.0218	0.0845	0.0229	0	175	22
4	2	4	0.0328	0.1267	0.0343	0	175	33
5	2	6	0.0497	0.192	0.052	0	175	50
6	3	9	0.0308	0.119	0.0322	0	175	31
7	3	24	0.0023	0.0839	0	1.03	400	20
8	4	9	0.0268	0.1037	0.0281	0	175	27
9	5	10	0.0228	0.0883	0.0239	0	175	23
10	6	10	0.0139	0.0605	2.459	0	175	16
11	7	8	0.0159	0.0614	0.0166	0	175	16
12	8	9	0.0427	0.1651	0.0447	0	175	43

13	8	10	0.0427	0.1651	0.0447	0	175	43
14	9	11	0.0023	0.0839	0	1.03	400	20
15	9	12	0.0023	0.0839	0	1.03	400	20
16	10	11	0.0023	0.0839	0	1.02	400	20
17	10	12	0.0023	0.0839	0	1.02	400	20
18	11	13	0.0061	0.0476	0.0999	0	500	33
19	11	14	0.0054	0.0418	0.0879	0	500	29
20	12	13	0.0061	0.0476	0.0999	0	500	33
21	12	23	0.0124	0.0966	0.203	0	500	67
22	13	23	0.0111	0.0865	0.1818	0	500	60
23	14	16	0.005	0.0389	0.0818	0	500	27
24	15	16	0.0022	0.0173	0.0364	0	500	12
25	15	21	0.0063	0.049	0.103	0	500	34
26	15	21	0.0063	0.049	0.103	0	500	34
27	15	24	0.0067	0.0519	0.1091	0	500	36
28	16	17	0.0033	0.0259	0.0545	0	500	18
29	16	19	0.003	0.0231	0.0485	0	500	16
30	17	18	0.0018	0.0144	0.0303	0	500	10
31	17	22	0.0135	0.1053	0.2212	0	500	73
32	18	21	0.0033	0.0259	0.0545	0	500	18
33	18	21	0.0033	0.0259	0.0545	0	500	18
34	19	20	0.0051	0.0396	0.0833	0	500	27.5
35	19	20	0.0051	0.0396	0.0833	0	500	27.5
36	20	23	0.0028	0.0216	0.0455	0	500	15
37	20	23	0.0028	0.0216	0.0455	0	500	15
38	21	22	0.0087	0.0678	0.1424	0	500	47

Load Data			
No.	**Bus**	$\boldsymbol{PD_d}$ (MW)	$\boldsymbol{QD_d}$ (MVAr)
1	1	108	22
2	2	97	20
3	3	180	37
4	4	74	15
5	5	71	14
6	6	136	28
7	7	125	25
8	8	171	35
9	9	175	36
10	10	195	40
11	13	265	54
12	14	194	39
13	15	317	64
14	16	100	20
15	18	333	68
16	19	181	37
17	20	128	26

APPENDIX B

IEEE 118-BUS SYSTEM DATA

Generator Data										
No.	**Bus**	P^{max}	P^{gen}	P^{min}	Q^{max}	Q^{gen}	Q^{min}	c_q	b_q	a_q
1	4	30	5	5	300	161.91	-300	32	26	0.07
2	6	30	5	5	50	50	-13	32	26	0.07
3	8	30	5	5	300	-69.88	-300	32	26	0.07
4	10	500	330.54	150	200	-146.88	-147	7	13	0.01
5	12	300	300	100	120	120	-35	7	13	0.01
6	15	30	10	10	30	30	-10	32	26	0.07
7	18	100	100	25	50	50	-16	10	18	0.01
8	19	30	5	5	24	24	-8	32	26	0.07
9	24	30	5	5	300	26.05	-300	32	26	0.07
10	25	300	288.45	100	140	-22.76	-47	7	13	0.01
11	26	350	350	100	1000	-33.48	-1000	33	11	0
12	27	30	8	8	300	74.72	-300	32	26	0.07
13	31	30	8	8	300	69.25	-300	32	26	0.07
14	32	100	100	25	42	42	-14	10	18	0.01
15	34	30	8	8	24	24	-8	32	26	0.07
16	36	100	10	25	24	24	-8	10	18	0.01
17	40	30	8	8	300	99.93	-300	32	26	0.07
18	42	30	8	8	300	54.16	-300	32	26	0.07
19	46	100	93.63	25	100	37.99	-100	10	18	0.01
20	49	250	250	50	210	133.11	-85	28	12	0
21	54	250	250	50	300	109.27	-300	28	12	0
22	55	100	94	25	23	23	-8	10	18	0.01
23	56	100	94.63	25	15	15	-8	10	18	0.01
24	59	200	200	50	180	180	-60	39	13	0
25	61	200	200	50	300	0.14	-100	39	13	0
26	62	100	71.68	25	20	20	-20	10	18	0.01
27	65	420	420	100	200	-33.12	-67	64	8	0.01
28	66	420	420	100	200	-12.02	-67	64	8	0.01
29	69	300	664.93	80	9999	12.63	-9999	7	13	0.01
30	70	80	53.1	30	32	32	-10	74	15	0.05
31	72	30	10	10	100	0.17	-100	32	26	0.07
32	73	30	5	5	100	22.47	-100	32	26	0.07
33	74	20	5	5	9	9	-6	18	38	0.03
34	76	100	100	25	23	23	-8	10	18	0.01
35	77	100	75.8	25	70	70	-20	10	18	0.01
36	80	500	294.65	150	280	172.15	-165	7	13	0.01
37	82	100	59.22	25	9900	133.14	-9900	10	18	0.01
38	85	30	10	10	23	23	-8	32	26	0.07
39	87	650	229.36	100	1000	61.69	-100	33	11	0
40	89	500	217.61	50	300	53.89	-210	7	13	0.01
41	90	20	8	8	300	70.65	-300	18	38	0.03
42	91	50	20	20	100	6.14	-100	59	23	0.01
43	92	300	226.87	100	9	9	-3	7	13	0.01
44	99	300	217.81	100	100	-35.13	-100	7	13	0.01
45	100	300	248.3	100	155	118.27	-50	7	13	0.01
46	103	20	8	8	40	40	-15	18	38	0.03
47	104	100	45.05	25	23	23	-8	10	18	0.01
48	105	100	50.78	25	23	23	-8	10	18	0.01
49	107	20	8	8	200	26.42	-200	18	38	0.03

50	110	50	25	25	23	23	-8	59	23	0.01
51	111	100	34.34	25	1000	8.64	-100	10	18	0.01
52	112	100	43.33	25	1000	28.26	-100	10	18	0.01
53	113	100	99.72	25	200	42.57	-100	10	18	0.01
54	116	50	25	25	1000	-190.63	-1000	59	23	0.01

Line Data (100 MW base)								
No.	**From**	**To**	r_k	x_k	b_k	S^{max}**(MW)**	t_k	c_k
1	1	2	0.0303	0.0999	0.0254	115	0	18
2	1	3	0.0129	0.0424	0.01082	115	0	7.6
3	4	5	0.00176	0.00798	0.0021	400	0	1.8
4	3	5	0.0241	0.108	0.0284	115	0	16.2
5	5	6	0.0119	0.054	0.01426	115	0	9.7
6	6	7	0.00459	0.0208	0.0055	115	0	4.7
7	8	9	0.00244	0.0305	1.162	400	0	5.5
8	8	5	0	0.0267	0	400	0.985	6
9	9	10	0.00258	0.0322	1.23	400	0	5.8
10	4	11	0.0209	0.0688	0.01748	115	0	12.4
11	5	11	0.0203	0.0682	0.01738	115	0	12.3
12	11	12	0.00595	0.0196	0.00502	115	0	4.4
13	2	12	0.0187	0.0616	0.01572	115	0	11.1
14	3	12	0.0484	0.16	0.0406	115	0	24
15	7	12	0.00862	0.034	0.00874	115	0	6.1
16	11	13	0.02225	0.0731	0.01876	115	0	13.2
17	12	14	0.0215	0.0707	0.01816	115	0	12.7
18	13	15	0.0744	0.2444	0.06268	115	0	36.7
19	14	15	0.0595	0.195	0.0502	115	0	29.3
20	12	16	0.0212	0.0834	0.0214	115	0	15
21	15	17	0.0132	0.0437	0.0444	400	0	7.9
22	16	17	0.0454	0.1801	0.0466	115	0	27
23	17	18	0.0123	0.0505	0.01298	115	0	9.1
24	18	19	0.01119	0.0493	0.01142	115	0	8.9
25	19	20	0.0252	0.117	0.0298	115	0	17.6
26	15	19	0.012	0.0394	0.0101	115	0	7.1
27	20	21	0.0183	0.0849	0.0216	115	0	15.3
28	21	22	0.0209	0.097	0.0246	115	0	17.5
29	22	23	0.0342	0.159	0.0404	115	0	23.9
30	23	24	0.0135	0.0492	0.0498	115	0	8.9
31	23	25	0.0156	0.08	0.0864	400	0	14.4
32	26	25	0	0.0382	0	400	0.96	6.9
33	25	27	0.0318	0.163	0.1764	400	0	24.5
34	27	28	0.01913	0.0855	0.0216	115	0	15.4
35	28	29	0.0237	0.0943	0.0238	115	0	17
36	30	17	0	0.0388	0	400	0.96	7
37	8	30	0.00431	0.0504	0.514	115	0	9.1
38	26	30	0.00799	0.086	0.908	400	0	15.5
39	17	31	0.0474	0.1563	0.0399	115	0	23.4
40	29	31	0.0108	0.0331	0.0083	115	0	6
41	23	32	0.0317	0.1153	0.1173	115	0	17.3
42	31	32	0.0298	0.0985	0.0251	115	0	17.7

43	27	32	0.0229	0.0755	0.01926	115	0	13.6
44	15	33	0.038	0.1244	0.03194	115	0	18.7
45	19	34	0.0752	0.247	0.0632	115	0	37.1
46	35	36	0.00224	0.0102	0.00268	115	0	2.3
47	35	37	0.011	0.0497	0.01318	115	0	8.9
48	33	37	0.0415	0.142	0.0366	115	0	21.3
49	34	36	0.00871	0.0268	0.00568	115	0	6
50	34	37	0.00256	0.0094	0.00984	400	0	2.1
51	38	37	0	0.0375	0	400	0.935	6.8
52	37	39	0.0321	0.106	0.027	115	0	15.9
53	37	40	0.0593	0.168	0.042	115	0	25.2
54	30	38	0.00464	0.054	0.422	115	0	9.7
55	39	40	0.0184	0.0605	0.01552	115	0	10.9
56	40	41	0.0145	0.0487	0.01222	115	0	8.8
57	40	42	0.0555	0.183	0.0466	115	0	27.5
58	41	42	0.041	0.135	0.0344	115	0	20.3
59	43	44	0.0608	0.2454	0.06068	115	0	36.8
60	34	43	0.0413	0.1681	0.04226	115	0	25.2
61	44	45	0.0224	0.0901	0.0224	115	0	16.2
62	45	46	0.04	0.1356	0.0332	115	0	20.3
63	46	47	0.038	0.127	0.0316	115	0	19.1
64	46	48	0.0601	0.189	0.0472	115	0	28.4
65	47	49	0.0191	0.0625	0.01604	115	0	11.3
66	42	49	0.0715	0.323	0.086	115	0	48.5
67	42	49	0.0715	0.323	0.086	115	0	48.5
68	45	49	0.0684	0.186	0.0444	115	0	27.9
69	48	49	0.0179	0.0505	0.01258	115	0	9.1
70	49	50	0.0267	0.0752	0.01874	115	0	13.5
71	49	51	0.0486	0.137	0.0342	115	0	20.6
72	51	52	0.0203	0.0588	0.01396	115	0	10.6
73	52	53	0.0405	0.1635	0.04058	115	0	24.5
74	53	54	0.0263	0.122	0.031	115	0	18.3
75	49	54	0.073	0.289	0.0738	115	0	43.4
76	49	54	0.0869	0.291	0.073	115	0	43.7
77	54	55	0.0169	0.0707	0.0202	115	0	12.7
78	54	56	0.00275	0.00955	0.00732	115	0	2.1
79	55	56	0.00488	0.0151	0.00374	115	0	3.4
80	56	57	0.0343	0.0966	0.0242	115	0	17.4
81	50	57	0.0474	0.134	0.0332	115	0	20.1
82	56	58	0.0343	0.0966	0.0242	115	0	17.4
83	51	58	0.0255	0.0719	0.01788	115	0	12.9
84	54	59	0.0503	0.2293	0.0598	115	0	34.4
85	56	59	0.0825	0.251	0.0569	115	0	37.7
86	56	59	0.0803	0.239	0.0536	115	0	35.9
87	55	59	0.04739	0.2158	0.05646	115	0	32.4
88	59	60	0.0317	0.145	0.0376	115	0	21.8
89	59	61	0.0328	0.15	0.0388	115	0	22.5
90	60	61	0.00264	0.0135	0.01456	400	0	3
91	60	62	0.0123	0.0561	0.01468	115	0	10.1
92	61	62	0.00824	0.0376	0.0098	115	0	6.8
93	63	59	0	0.0386	0	400	0.96	6.9

94	63	64	0.00172	0.02	0.216	400	0	4.5
95	64	61	0	0.0268	0	400	0.985	6
96	38	65	0.00901	0.0986	1.046	400	0	17.7
97	64	65	0.00269	0.0302	0.38	400	0	5.4
98	49	66	0.018	0.0919	0.0248	400	0	16.5
99	49	66	0.018	0.0919	0.0248	400	0	16.5
100	62	66	0.0482	0.218	0.0578	115	0	32.7
101	62	67	0.0258	0.117	0.031	115	0	17.6
102	65	66	0	0.037	0	400	0.935	6.7
103	66	67	0.0224	0.1015	0.02682	115	0	15.2
104	65	68	0.00138	0.016	0.638	400	0	3.6
105	47	69	0.0844	0.2778	0.07092	115	0	41.7
106	49	69	0.0985	0.324	0.0828	115	0	48.6
107	68	69	0	0.037	0	400	0.935	6.7
108	69	70	0.03	0.127	0.122	400	0	19.1
109	24	70	0.00221	0.4115	0.10198	115	0	61.7
110	70	71	0.00882	0.0355	0.00878	115	0	6.4
111	24	72	0.0488	0.196	0.0488	115	0	29.4
112	71	72	0.0446	0.18	0.04444	115	0	27
113	71	73	0.00866	0.0454	0.01178	115	0	8.2
114	70	74	0.0401	0.1323	0.03368	115	0	19.8
115	70	75	0.0428	0.141	0.036	115	0	21.2
116	69	75	0.0405	0.122	0.124	400	0	18.3
117	74	75	0.0123	0.0406	0.01034	115	0	7.3
118	76	77	0.0444	0.148	0.0368	115	0	22.2
119	69	77	0.0309	0.101	0.1038	115	0	15.2
120	75	77	0.0601	0.1999	0.04978	115	0	30
121	77	78	0.00376	0.0124	0.01264	115	0	2.8
122	78	79	0.00546	0.0244	0.00648	115	0	5.5
123	77	80	0.017	0.0485	0.0472	400	0	8.7
124	77	80	0.0294	0.105	0.0228	400	0	15.8
125	79	80	0.0156	0.0704	0.0187	115	0	12.7
126	68	81	0.00175	0.0202	0.808	400	0	4.5
127	81	80	0	0.037	0	400	0.935	6.7
128	77	82	0.0298	0.0853	0.08174	115	0	15.4
129	82	83	0.0112	0.03665	0.03796	115	0	6.6
130	83	84	0.0625	0.132	0.0258	115	0	19.8
131	83	85	0.043	0.148	0.0348	115	0	22.2
132	84	85	0.0302	0.0641	0.01234	115	0	11.5
133	85	86	0.035	0.123	0.0276	400	0	18.5
134	86	87	0.02828	0.2074	0.0445	400	0	31.1
135	85	88	0.02	0.102	0.0276	115	0	15.3
136	85	89	0.0239	0.173	0.047	115	0	26
137	88	89	0.0139	0.0712	0.01934	400	0	12.8
138	89	90	0.0518	0.188	0.0528	400	0	28.2
139	89	90	0.0238	0.0997	0.106	400	0	17.9
140	90	91	0.0254	0.0836	0.0214	115	0	15
141	89	92	0.0099	0.0505	0.0548	400	0	9.1
142	89	92	0.0393	0.1581	0.0414	400	0	23.7
143	91	92	0.0387	0.1272	0.03268	115	0	19.1
144	92	93	0.0258	0.0848	0.0218	115	0	15.3

145	92	94	0.0481	0.158	0.0406	115	0	23.7
146	93	94	0.0223	0.0732	0.01876	115	0	13.2
147	94	95	0.0132	0.0434	0.0111	115	0	7.8
148	80	96	0.0356	0.182	0.0494	115	0	27.3
149	82	96	0.0162	0.053	0.0544	115	0	9.5
150	94	96	0.0269	0.0869	0.023	115	0	15.6
151	80	97	0.0183	0.0934	0.0254	115	0	16.8
152	80	98	0.0238	0.108	0.0286	115	0	16.2
153	80	99	0.0454	0.206	0.0546	115	0	30.9
154	92	100	0.0648	0.295	0.0472	115	0	44.3
155	94	100	0.0178	0.058	0.0604	115	0	10.4
156	95	96	0.0171	0.0547	0.01474	115	0	9.8
157	96	97	0.0173	0.0885	0.024	115	0	15.9
158	98	100	0.0397	0.179	0.0476	115	0	26.9
159	99	100	0.018	0.0813	0.0216	115	0	14.6
160	100	101	0.0277	0.1262	0.0328	115	0	18.9
161	92	102	0.0123	0.0559	0.01464	115	0	10.1
162	101	102	0.0246	0.112	0.0294	115	0	16.8
163	100	103	0.016	0.0525	0.0536	400	0	9.5
164	100	104	0.0451	0.204	0.0541	115	0	30.6
165	103	104	0.0466	0.1584	0.0407	115	0	23.8
166	103	105	0.0535	0.1625	0.0408	115	0	24.4
167	100	106	0.0605	0.229	0.062	115	0	34.4
168	104	105	0.00994	0.0378	0.00986	115	0	6.8
169	105	106	0.014	0.0547	0.01434	115	0	9.8
170	105	107	0.053	0.183	0.0472	115	0	27.5
171	105	108	0.0261	0.0703	0.01844	115	0	12.7
172	106	107	0.053	0.183	0.0472	115	0	27.5
173	108	109	0.0105	0.0288	0.0076	115	0	6.5
174	103	110	0.03906	0.1813	0.0461	115	0	27.2
175	109	110	0.0278	0.0762	0.0202	115	0	13.7
176	110	111	0.022	0.0755	0.02	115	0	13.6
177	110	112	0.0247	0.064	0.062	115	0	11.5
178	17	113	0.00913	0.0301	0.00768	115	0	5.4
179	32	113	0.0615	0.203	0.0518	400	0	30.5
180	32	114	0.0135	0.0612	0.01628	115	0	11
181	27	115	0.0164	0.0741	0.01972	115	0	13.3
182	114	115	0.0023	0.0104	0.00276	115	0	2.3
183	68	116	0.00034	0.00405	0.164	400	0	0.9
184	12	117	0.0329	0.14	0.0358	115	0	21
185	75	118	0.0145	0.0481	0.01198	115	0	8.7
186	76	118	0.0164	0.0544	0.01356	115	0	9.8

Load Data			
No.	**Bus**	PD_d (MW)	QD_d (MVAr)
1	1	87	46
2	2	34	15
3	3	67	17
4	4	51	20
5	6	89	38
6	7	32	3
7	11	119	39
8	12	80	17
9	13	58	27
10	14	24	2
11	15	154	51
12	16	43	17
13	17	19	5
14	18	102	58
15	19	77	43
16	20	31	5
17	21	24	14
18	22	17	9
19	23	12	5
20	27	106	22
21	28	29	12
22	29	41	7
23	31	73	46
24	32	101	39
25	33	39	15
26	34	101	44
27	35	56	15
28	36	53	29
29	39	46	19
30	40	34	39
31	41	63	17
32	42	63	39
33	43	31	12
34	44	27	14
35	45	90	38
36	46	48	17
37	47	58	0
38	48	34	19
39	49	148	51
40	50	29	7
41	51	29	14
42	52	31	9
43	53	39	19
44	54	193	55
45	55	107	38
46	56	143	31
47	57	20	5
48	58	20	5
49	59	473	193

50	60	133	5
51	62	131	24
52	66	67	31
53	67	48	12
54	70	113	34
55	74	116	46
56	75	80	19
57	76	116	61
58	77	104	48
59	78	121	44
60	79	67	55
61	80	222	44
62	82	92	46
63	83	34	17
64	84	19	12
65	85	41	26
66	86	36	17
67	88	82	17
68	90	133	72
69	92	111	17
70	93	20	12
71	94	51	27
72	95	72	53
73	96	65	26
74	97	26	15
75	98	58	14
76	100	63	31
77	101	38	26
78	102	9	5
79	103	39	27
80	104	65	43
81	105	53	44
82	106	73	27
83	107	48	20
84	108	3	2
85	109	14	5
86	110	67	51
87	112	43	22
88	114	14	5
89	115	38	12
90	117	34	14
91	118	56	26

APPENDIX C

SUBROUTINE OF A MATLAB BASED TEP PROGRAM

```
%% number of buses
nb = length(bus(:,1));
%% number of branches & candidate lines
nl = length(branch(:,1));
nlz = sum(branch(:,12)==0);
%% number of generators
ng = length(gen(:,1));
%% number of loads
nd = length(load(:,1));
%% system swing bus
swbus = find(bus(:,2)==0);
%% suseptance
gl =  zeros(nl,1);
bl = -1./branch(:,5);
%% variable initialization
nvar = nb+nl+ng+nlz;
nc = nl+3*nlz;
dimNodBal = zeros(nb,nvar);
dimDCFlow = zeros(nl+nlz,nvar);  % number of bus angle contraints
dimLnCap  = zeros(2*nlz,nvar);  % number of line capacity limit
dimPLoad  = zeros(nb,1);
M = 5;
tic
for b = 1 : nb

    indg = find(b == gen(:,2));
    if isempty(indg) == 0
        for i = 1:length(indg)
            dimNodBal(b,nb+nl+indg(i)) = 1;
        end
    end

    indd = find(b == load(:,2));
    if isempty(indd) == 0
        for i = 1:length(indd)
            dimPLoad(b) = dimPLoad(b) + load(indd(i),3);
        end
    end
end

for k = 1 : (nl+nlz)
    if k <= (nl-nlz)
        dimDCFlow(k,branch(k,2)) = +1;
        dimDCFlow(k,branch(k,3)) = -1;
        dimDCFlow(k,nb+k) = 1./(bl(k)*Sbase);

        dimNodBal(branch(k,2),nb+k) = -1;
        dimNodBal(branch(k,3),nb+k) = +1;

    elseif (k > (nl-nlz))&&(k <= nl)
        dimDCFlow(k,branch(k,2)) = +1;
        dimDCFlow(k,branch(k,3)) = -1;
        dimDCFlow(k,nb+k) = 1./(bl(k)*Sbase);
        dimDCFlow(k,nb+ng+nlz+k) = M;
```

```
        dimNodBal(branch(k,2),nb+k) = -1;
        dimNodBal(branch(k,3),nb+k) = +1;

        dimLnCap(k-(nl-nlz),nb+k) = 1;
        dimLnCap(k-(nl-nlz),nb+ng+nlz+k) = -branch(k,9);
    else
        dimDCFlow(k,branch(k-nlz,2)) = -1;
        dimDCFlow(k,branch(k-nlz,3)) = +1;
        dimDCFlow(k,nb-nlz+k) = -1./(bl(k-nlz)*Sbase);
        dimDCFlow(k,nb+ng+k) = M;

        dimLnCap(k-(nl-nlz),nb-nlz+k) = -1;
        dimLnCap(k-(nl-nlz),nb+ng+k) = -branch(k-nlz,9);
    end
end

toc
dimNodBal = sparse(dimNodBal);
dimDCFlow = sparse(dimDCFlow);
dimLnCap  = sparse(dimLnCap);

clear model;
%model.Q      = sparse(1:nvar, 1:nvar, [zeros(nb+nl,1); gen(:,14)]);
model.A      = [dimNodBal; dimDCFlow; dimLnCap];
%model.obj    = [zeros(nb+nl,1); gen(:,13);branch(nl-nlz+1:nl,11)];
model.obj    = [zeros(nb+nl+ng,1); branch(nl-nlz+1:nl,11)];
%model.objcon = sum(gen(:,12));
model.rhs    = [dimPLoad; zeros(nl-nlz,1); M*ones(2*nlz,1); ze-
ros(2*nlz,1)];
model.lb     = [-inf(swbus-1,1);0;-inf(nb-swbus,1);-branch(:,9);
gen(:,6); -inf(nlz,1)];
model.ub     = [ inf(swbus-1,1);0; inf(nb-swbus,1); branch(:,9);
gen(:,5);  inf(nlz,1)];
model.sense  = [repmat('=',nb+nl-nlz,1); repmat('<', 4*nlz,1)];
model.vtype  = [repmat('C',nb+nl+ng,1); repmat('B',nlz,1)];
model.modelsense = 'min';

result = gurobi(model);
result.x(1:nb) = result.x(1:nb)/pi*180;
if strcmp(result.status, 'OPTIMAL')
  fprintf('Optimal objective: %e\n', result.objval);
  adl = find(result.x(nb+nl+ng+1:nvar) == 1);
  fprintf('The following %2d lines need to be built:\n', length(adl));
  fprintf('FromBus   ToBus\n');
  for i = 1: length(adl)
      fprintf('%5d%8d\n', branch(nl-nlz+adl(i),2),branch(nl-
nlz+adl(i),3));
  end

  fprintf('Elapsed time: %e\n', result.runtime);
else
  fprintf('Optimization returned status: %s\n', result.status);
end
```

```
%%%%%%%%%%%%%%%%%%%%%%%%%%%%%%%%%%%%%%%%%%%%%%%%%%%%%%%%%%%%%%%%%%%%%%%%%%%%
```

Sample data file: IEEE 24-bus system

```
%% system MVA base
Sbase = 100;

%% bus data
%   bus_i   type    Gs  Bs  area    zone    Vm  Va  baseKV  Vmax
Vmin
bus = [
1   2   0   0   1   1   0   138 1   1.05    0.95;
2   2   0   0   1   1   0   138 1   1.05    0.95;
3   1   0   0   1   1   0   138 1   1.05    0.95;
4   1   0   0   1   1   0   138 1   1.05    0.95;
5   1   0   0   1   1   0   138 1   1.05    0.95;
6   1   0   -100    2   1   0   138 1   1.05    0.95;
7   2   0   0   2   1   0   138 1   1.05    0.95;
8   1   0   0   2   1   0   138 1   1.05    0.95;
9   1   0   0   1   1   0   138 1   1.05    0.95;
10  1   0   0   2   1   0   138 1   1.05    0.95;
11  1   0   0   3   1   0   230 1   1.05    0.95;
12  1   0   0   3   1   0   230 1   1.05    0.95;
13  0   0   0   3   1   0   230 1   1.05    0.95;
14  2   0   0   3   1   0   230 1   1.05    0.95;
15  2   0   0   4   1   0   230 1   1.05    0.95;
16  2   0   0   4   1   0   230 1   1.05    0.95;
17  1   0   0   4   1   0   230 1   1.05    0.95;
18  2   0   0   4   1   0   230 1   1.05    0.95;
19  1   0   0   3   1   0   230 1   1.05    0.95;
20  1   0   0   3   1   0   230 1   1.05    0.95;
21  2   0   0   4   1   0   230 1   1.05    0.95;
22  2   0   0   4   1   0   230 1   1.05    0.95;
23  2   0   0   3   1   0   230 1   1.05    0.95;
24  1   0   0   4   1   0   230 1   1.05    0.95;
];

%% branch data
%   i_branch    fbus    tbus    rl  xl  gc  bc  tap rateA   rateB
cost    status  no_cont
branch = [
1   1   2   0.0026  0.0139  0   0.4611  0   175 175 0   1   1;
2   1   3   0.0546  0.2112  0   0.0572  0   175 175 0   1   1;
3   1   5   0.0218  0.0845  0   0.0229  0   175 175 0   1   1;
4   2   4   0.0328  0.1267  0   0.0343  0   175 175 0   1   1;
5   2   6   0.0497  0.192   0   0.052   0   175 175 0   1   1;
6   3   9   0.0308  0.119   0   0.0322  0   175 175 0   1   1;
7   3   24  0.0023  0.0839  0   0   1.03    100 400 0   1   1;
8   4   9   0.0268  0.1037  0   0.0281  0   175 175 0   1   1;
9   5   10  0.0228  0.0883  0   0.0239  0   175 175 0   1   1;
10  6   10  0.0139  0.0605  0   2.459   0   175 175 0   1   1;
11  7   8   0.0159  0.0614  0   0.0166  0   175 175 0   1   1;
12  8   9   0.0427  0.1651  0   0.0447  0   175 175 0   1   1;
13  8   10  0.0427  0.1651  0   0.0447  0   175 175 0   1   1;
14  9   11  0.0023  0.0839  0   0   1.03    100 400 0   1   1;
```

```
15  9   12  0.0023  0.0839  0   0   1.03    100 400 0   1   1;
16  10  11  0.0023  0.0839  0   0   1.02    100 400 0   1   1;
17  10  12  0.0023  0.0839  0   0   1.02    100 400 0   1   1;
18  11  13  0.0061  0.0476  0   0.0999  0   100 500 0   1   1;
19  11  14  0.0054  0.0418  0   0.0879  0   100 500 0   1   1;
20  12  13  0.0061  0.0476  0   0.0999  0   100 500 0   1   1;
21  12  23  0.0124  0.0966  0   0.203   0   100 500 0   1   1;
22  13  23  0.0111  0.0865  0   0.1818  0   100 500 0   1   1;
23  14  16  0.005   0.0389  0   0.0818  0   100 500 0   1   1;
24  15  16  0.0022  0.0173  0   0.0364  0   100 500 0   1   1;
25  15  21  0.0063  0.049   0   0.103   0   100 500 0   1   1;
26  15  21  0.0063  0.049   0   0.103   0   100 500 0   1   1;
27  15  24  0.0067  0.0519  0   0.1091  0   100 500 0   1   1;
28  16  17  0.0033  0.0259  0   0.0545  0   100 500 0   1   1;
29  16  19  0.003   0.0231  0   0.0485  0   100 500 0   1   1;
30  17  18  0.0018  0.0144  0   0.0303  0   100 500 0   1   1;
31  17  22  0.0135  0.1053  0   0.2212  0   100 500 0   1   1;
32  18  21  0.0033  0.0259  0   0.0545  0   100 500 0   1   1;
33  18  21  0.0033  0.0259  0   0.0545  0   100 500 0   1   1;
34  19  20  0.0051  0.0396  0   0.0833  0   100 500 0   1   1;
35  19  20  0.0051  0.0396  0   0.0833  0   100 500 0   1   1;
36  20  23  0.0028  0.0216  0   0.0455  0   100 500 0   1   1;
37  20  23  0.0028  0.0216  0   0.0455  0   100 500 0   1   1;
38  21  22  0.0087  0.0678  0   0.1424  0   100 500 0   1   1;
39  1   2   0.0026  0.0139  0   0.4611  0   175 175 3   0   1;
40  1   3   0.0546  0.2112  0   0.0572  0   175 175 55  0   1;
41  1   5   0.0218  0.0845  0   0.0229  0   176 176 22  0   1;
42  1   8   0.0348  0.1344  0   0   0   500 500 35  0   1;
43  2   4   0.0328  0.1267  0   0.0343  0   175 175 33  0   1;
44  2   6   0.0497  0.192   0   0.052   0   175 175 50  0   1;
45  2   8   0.0328  0.1267  0   0   0   500 500 33  0   1;
46  3   9   0.0308  0.119   0   0.0322  0   175 175 31  0   1;
47  3   24  0.0023  0.0839  0   0   1.03    400 400 50  0   1;
48  4   9   0.0268  0.1037  0   0.0281  0   175 175 27  0   1;
49  5   10  0.0228  0.0883  0   0.0239  0   175 175 23  0   1;
50  6   7   0.0497  0.192   0   0   0   175 175 50  0   1;
51  6   10  0.0139  0.0605  0   2.459   0   175 175 16  0   1;
52  7   8   0.0159  0.0614  0   0.0166  0   175 175 16  0   1;
53  8   9   0.0427  0.1651  0   0.0447  0   175 175 43  0   1;
54  8   10  0.0427  0.1651  0   0.0447  0   175 175 43  0   1;
55  9   11  0.0023  0.0839  0   0   1.03    400 400 50  0   1;
56  9   12  0.0023  0.0839  0   0   1.03    400 400 50  0   1;
57  10  11  0.0023  0.0839  0   0   1.02    400 400 50  0   1;
58  10  12  0.0023  0.0839  0   0   1.02    400 400 50  0   1;
59  11  13  0.0061  0.0476  0   0.0999  0   500 500 66  0   1;
60  11  14  0.0054  0.0418  0   0.0879  0   500 500 58  0   1;
61  12  13  0.0061  0.0476  0   0.0999  0   500 500 66  0   1;
62  12  23  0.0124  0.0966  0   0.203   0   500 500 134 0   1;
63  13  14  0.0057  0.0447  0   0.1818  0   500 500 62  0   1;
64  13  23  0.0111  0.0865  0   0.0818  0   500 500 120 0   1;
65  14  16  0.005   0.0389  0   0.0364  0   500 500 54  0   1;
66  14  23  0.008   0.062   0   0.103   0   500 500 86  0   1;
67  15  16  0.0022  0.0173  0   0.103   0   500 500 24  0   1;
68  15  21  0.0063  0.049   0   0.1091  0   500 500 68  0   1;
69  15  24  0.0067  0.0519  0   0.0545  0   500 500 72  0   1;
70  16  17  0.0033  0.0259  0   0.0485  0   500 500 36  0   1;
```

```
71  16  19  0.003   0.0231  0   0.0303  0   500 500 32  0   1;
72  16  23  0.0105  0.0822  0   0.2212  0   500 500 114 0   1;
73  17  18  0.0018  0.0144  0   0.0545  0   500 500 20  0   1;
74  17  22  0.0135  0.1053  0   0.0545  0   500 500 146 0   1;
75  18  21  0.0033  0.0259  0   0.0833  0   500 500 36  0   1;
76  19  20  0.0051  0.0396  0   0.0833  0   500 500 55  0   1;
77  19  23  0.0078  0.0606  0   0.0455  0   500 500 84  0   1;
78  20  23  0.0028  0.0216  0   0.0455  0   500 500 30  0   1;
79  21  22  0.0087  0.0678  0   0.1424  0   500 500 94  0   1;
];

%% Generator data
%   i_gen   bus Pg  Qg  Pmax    Pmin    Qmax    Qmin    Vg  mBase
Gtype   gma gmb gmc ramp_10 ramp_30 status  no_cont
gen = [
1   1   10  0   20  16  10  0   1.035   100 1   400.6849    130 0
9999    9999    1   1;  %   U20
2   1   10  0   20  16  10  0   1.035   100 1   400.6849    130 0
9999    9999    1   1;  %   U20
3   1   76  0   76  15.2    30  -25 1.035   100 1   212.3076    16.0811
0.014142    9999    9999    1   1;  %   U76
4   1   76  0   76  15.2    30  -25 1.035   100 1   212.3076    16.0811
0.014142    9999    9999    1   1;  %   U76
5   2   10  0   20  16  10  0   1.035   100 1   400.6849    130 0
9999    9999    1   1;  %   U20
6   2   10  0   20  16  10  0   1.035   100 1   400.6849    130 0
9999    9999    1   1;  %   U20
7   2   76  0   76  15.2    30  -25 1.035   100 1   212.3076    16.0811
0.014142    9999    9999    1   1;  %   U76
8   2   76  0   76  15.2    30  -25 1.035   100 1   212.3076    16.0811
0.014142    9999    9999    1   1;  %   U76
9   7   80  0   100 25  60  0   1.025   100 1   781.521 43.6615
0.052672    9999    9999    1   1;  %   U100
10  7   80  0   100 25  60  0   1.025   100 1   781.521 43.6615
0.052672    9999    9999    1   1;  %   U100
11  7   80  0   100 25  60  0   1.025   100 1   781.521 43.6615
0.052672    9999    9999    1   1;  %   U100
12  13  95.1    0   197 69  80  0   1.02    100 1   832.7575    48.5804
0.00717 9999    9999    1   1;  %   U197
13  13  95.1    0   197 69  80  0   1.02    100 1   832.7575    48.5804
0.00717 9999    9999    1   1;  %   U197
14  13  95.1    0   197 69  80  0   1.02    100 1   832.7575    48.5804
0.00717 9999    9999    1   1;  %   U197
15  14  0   35.3    0   0   200 -50 0.98    100 1   0   0   0   9999
9999    1   1;  %   SynCond
16  15  12  0   12  2.4 6   0   1.014   100 1   86.3852 56.564
0.328412    9999    9999    1   1;  %   U12
17  15  12  0   12  2.4 6   0   1.014   100 1   86.3852 56.564
0.328412    9999    9999    1   1;  %   U12
18  15  12  0   12  2.4 6   0   1.014   100 1   86.3852 56.564
0.328412    9999    9999    1   1;  %   U12
19  15  12  0   12  2.4 6   0   1.014   100 1   86.3852 56.564
0.328412    9999    9999    1   1;  %   U12
20  15  12  0   12  2.4 6   0   1.014   100 1   86.3852 56.564
0.328412    9999    9999    1   1;  %   U12
```

```
21  15  155 0   155 54.3    80  -50 1.014   100 1   382.2391    12.3883
0.008342    9999    9999    1   1;  %   U155
22  16  155 0   155 54.3    80  -50 1.017   100 1   382.2391    12.3883
0.008342    9999    9999    1   1;  %   U155
23  18  400 0   400 100 200 -50 1.05    100 1   395.3749    4.4231
0.000213    9999    9999    1   1;  %   U400
24  21  400 0   400 100 200 -50 1.05    100 1   395.3749    4.4231
0.000213    9999    9999    1   1;  %   U400
25  22  50  0   50  10  16  -10 1.05    100 1   0.001   0.001   0
9999    9999    1   1;  %   U50
26  22  50  0   50  10  16  -10 1.05    100 1   0.001   0.001   0
9999    9999    1   1;  %   U50
27  22  50  0   50  10  16  -10 1.05    100 1   0.001   0.001   0
9999    9999    1   1;  %   U50
28  22  50  0   50  10  16  -10 1.05    100 1   0.001   0.001   0
9999    9999    1   1;  %   U50
29  22  50  0   50  10  16  -10 1.05    100 1   0.001   0.001   0
9999    9999    1   1;  %   U50
30  22  50  0   50  10  16  -10 1.05    100 1   0.001   0.001   0
9999    9999    1   1;  %   U50
31  23  155 0   155 54.3    80  -50 1.05    100 1   382.2391    12.3883
0.008342    9999    9999    1   1;  %   U155
32  23  155 0   155 54.3    80  -50 1.05    100 1   382.2391    12.3883
0.008342    9999    9999    1   1;  %   U155
33  23  350 0   350 140 150 -25 1.05    100 1   665.1094    11.8495
0.004895    9999    9999    1   1;  %   U350
];

%% load data
%   i_load  bus pload   qload
load = [
  1       1       108   22;
  2       2       97    20;
  3       3       180   37;
  4       4       74    15;
  5       5       71    14;
  6       6       136   28;
  7       7       125   25;
  8       8       171   35;
  9       9       175   36;
 10      10       195   40;
 11      13       265   54;
 12      14       194   39;
 13      15       317   64;
 14      16       100   20;
 15      18       333   68;
 16      19       181   37;
 17      20       128   26;
];
```